Scuola Normale Superiore di Pisa

Tesi di perfezionamento in Neurobiologia

2011-2014

Cell dynamics during killifish embryos development and diapause

CANDIDATO

Luca Dolfi

RELATORE

Prof. Alessandro Cellerino

Contents

Abstract 4

1. Introduction 6

1.1 The model *taxon* 6

1.1.1 Killifishes 6

1.1.2 Annualism 7

1.1.3 Embryogenesis and development 8

1.1.4 Diapause 11

1.1.5 *Nothobranchius furzeri* 13

1.2 Transgenesis 15

1.2.1 Basis of trasgenesis 15

1.2.2 Transgenesis in *Nothobranchius* 16

1.3 Cell cycle 18

1.3.1 General mechanics 18

1.3.2 FUCCI 19

Aims 22

2. Results 23

2.1 Developmental differences 23

2.1.1 Non-annual killifishes development description 26

2.1.2 Annual killifishes development description 29

2.1.3 Cleavage rate differences 30

2.2 Exploring cell dynamics during development 33

2.2.1 Segmentation 33

2.2.2 FUCCI transgenic fish. 35

2.2.3 FUCCI red F2 fish description. 37

2.2.4 FUCCI green F2 fish description. 40

2.2.5 Fin cut FUCCI green adult validation. 45

2.3 F3 double FUCCI fish time lapse. 47

2.3.1 Epiboly 48

2.3.2 Early dispersed phase (Wourms stages 19-20) and diapause I. 51

2.3.3 Release from diapause I. 53

2.3.4 Late dispersed phase (Wourms stage 20). 55

2.3.5 Reaggregation (Wourms stages 21-26). 56

2.3.6 Somitogenesis (Wourms stages 29-33+). 60

2.3.7 Diapause II 64

2.3.8 Release from diapause II 65

2.3.9 DCE development past diapause II (Wourms stages 33+). 68
2.3.10 Development of not-DCE 68
2.4 Molecular analysis of diapause 71
2.4.1 MicroRNAs differential analysis 71
2.4.2 MiR-430 expression in *N. furzeri* 75
3. Discussion 78
3.1 Early development in annual and non-annual killifishes 78
3.2 FUCCI transgenesis in *N. furzeri*. 79
3.3 Diapause I 79
3.4 Release from dipause I 81
3.5 Diapause II 82
3.6 Diapause molecular factors. 83
4. Material and methods 86
4.1 Fish maintenance 86
4.1.1 Fish husbandry 86
4.1.2 Fish feeding 86
4.2 Breeding 87
4.3 Eggs collection 87
4.4 Eggs husbandry 88
4.5 Transgenic eggs husbandry 89
4.6 Transgenic embryos screening 89
4.7 Transgenic lines generation 90
4.7.1 FUCCI plasmids construction 90
4.7.2 Tol2 RNA synthesis 91
4.7.3 **Eggs injection** 91
4.8 FUCCI synthetic RNA 91
4.9 Mir-430 reporter RNA 92
4.10 Microscopy 92
4.10.1 Samples preparation 92
4.10.2 Brightfield acquisitions 93
4.10.3 Brightfield videos and images processing 93
4.10.4 Confocal acquisitions 93
4.10.5 Fluorescence images processing 94
4.10.6 Imaris analysis 94
4.11 Graphs productions 95
4.12 Sequencing 95

4.12.1 Samples collection 95
4.12.2 RNA extraction 96
4.12.3 Sequencing 96
4.13 Fin cut experiment 96
4.14 Mir-430 sensor experiment 97
4.14.1 Sensor injection 97
4.14.2 Sensor image acquisition 97
4.14.3 Sensor graph production 97
References 98

Abstract

Annual killifishes inhabit temporary ponds and their embryos survive the dry season encased in the mud by entering diapause, a process that arrests embryonic development in response to hostile conditions. During diapause oxygen consumption is suppressed and the cell cycle arrested, however the key factors responsible for these effects are largely unknown. Killifish developmental stages were described in the 70s in several species, mainly by direct microscopic observation. There is however lack of a precise description of cells dynamics during the whole developmental process. Annual killifishes are present within three clades distributed in Africa (one East and one West of the Dahomey gap) and South America. Within each of these phylogenetic clades, a non-annual clade is sister taxon to a annual clade and therefore represent an example of convergent evolution. Transgenesis is possible in at least one among the killifishes annual species, *Nothobranchius furzeri*.

Early cleavage of teleost embryos is characterized by a very fast cell cycle (15-30 minutes) and lack of G1 and G2 phases. In this work I used time lapse brightfield microscopy to investigate cells division's kinetics during the first developmental stages of annual- and non-annual species belonging to the three different phylogenetic clades. Annual killifishes of all three clades had cleavage times significantly longer when compared to their non-annual sister taxa (average 35 min vs. average 75 min), showing, for the first time, that cell cycle rate during cleavage, a trait thought to be rather evolutionary conserved can undergo convergent evolutionary change in response to variations in life-history.

Furthermore, using FUCCI fluorescent imaging of the cell cycle after microinjection in the annual species *Nothobranchius furzeri*, I demonstrated that the first 5 division are synchronous, do not show a G1 phase, and cell cycle synchronization is lost after the 5th cleavage division.

I generated FUCCI *N. furzeri* trangenic fish and finely characterized through time-lapse imaging cell cycle progression during all developmental steps: epiboly, dispersed phase, diapause I, reaggregation, somitogenesis and diapause II. I discovered that dispersed phase is divided in two steps and that diapause I arrest happens at the transition between them. In addition, I showed that the reactivation of cell cycle upon release from diapause I and II release is synchronous and very fast (hours).

Finally, I compared the microRNA profile of several species (annual and non annual) in diapause II or at the equivalent morphological stage and I identified some miRNAs that are differentially

expressed. Among these the miR-430 cluster is a particularly interesting candidate since it plays a key role during early development of zebrafish embryos.

1. Introduction

1.1 The model *taxon*

1.1.1 Killifishes

Killifish are small oviparous (egg-laying) fish that belong to the order of *Cyprinodontiformes*. Altogether, there are about 1270 different species of killifish, divided in 7 families according to fishbase, including Aplocheilidae, Cyprinodontidae, Fundulidae, Nothobranchiidae, Profundulidae, Rivulidae and Valenciidae [1].

Killifishes are mainly distributed in three regions of the world: South America, middle-west Africa (west of Dahomey gap) and middle-east Africa (east of Dahomey gap) and families that live in the same geographical area belong to a mophyletic group [2].

Killifishes usually colonize environments like permanent streams, rivers and lakes, but some species adapted to survive in extreme enviroments like ephemeral pond of water. These species are called annual while the species that lives in permanent water environments are called non annual [3]

Early studies suggest the existence of four events of loss and re-gain of an ancestral annual trait [2], [4], [5] while more recent studies suggests that it repeatedly evolved, at least three times in Africa and three times in South America [6]. In either of the two scenarios, an annual clade has always a sister non-annual clade that is phylogenetically closer than any other annual clade (Figure 1.1).

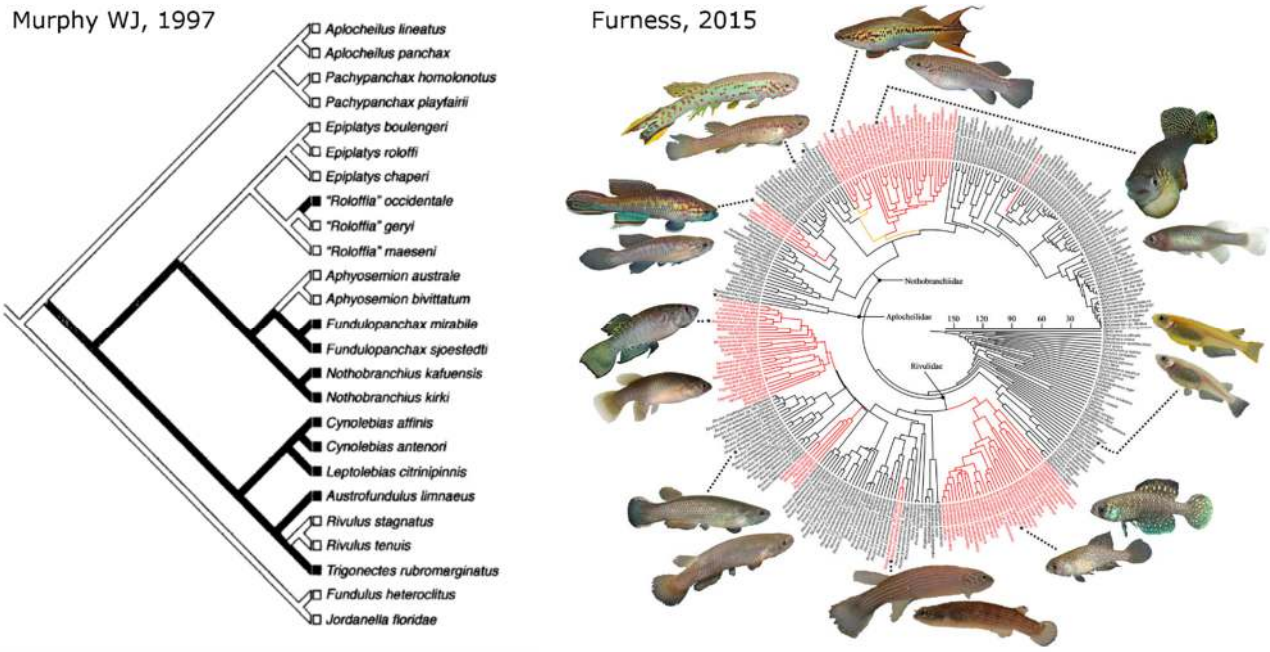

Figure 1.1: ***Distribution of annualism onto the proposed molecular phylogeny.*** *Left, the cladogram belongs to Murphy and Collier molecular analysis* [2] *based on cytochrome b, 12 s rRNA and 16 s rRNA genes. Black branches represent annual lineages, while white branches indicate non-annual lineages. Right, the tree has been done by Furness et al. using supermatrix tree construction methods on seven mitochondrial and two nuclear genes from GenBank* [6]. *Species highlighted in red have embryos capable of undergoing diapause II, while those in black do not.*

1.1.2 Annualism

Annual killifishes inhabit ephemeral bodies of water that fill during the monsoon season and disappear by evaporation after its end. Annual killifishes are present in Africa and South America and are adapted to alternating wet and dry seasons [2], [7]–[11] (Figure 1.2).

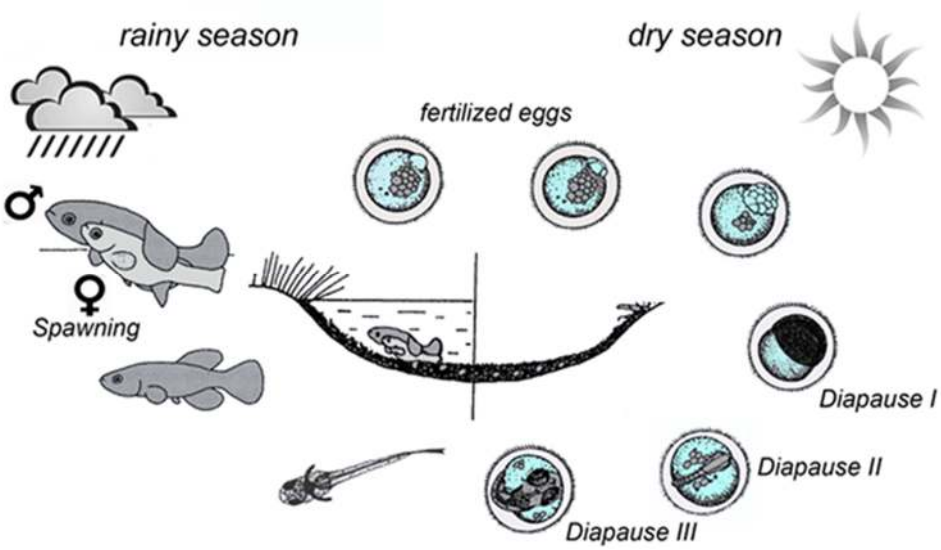

Figure 1.2: ***Annual killifishes life cycle.*** *Fertilized eggs are layed in the mud during the rainy season. Their development arrests in Diapause I II or III in response to negative environmental condition due to the dry season, not hatching and preserving the species. As rainy season starts again embryos complete their development and hatch. The figure has been modified from aqualog.de.*

For surviving in such an extreme environment, annual killifishes (regardless of the species) evolved some peculiar and distinctive traits, that mainly concern embryonic development, grow rates and lifespan.

Growth rates of annual killifishes are extraordinary high [8], not only for cyprinodontiformes but for vertebrates in general. The largest body of studies on this aspect has been conducted in the african annual killifish *Nothobranchius furzeri*, that shows exceptional growing rates after hatching, reaching its maximum size in less than 10 weeks[9]. Annual killifish evolved this very fast growth rate in order to reach sexual maturity and reproduce before their environment dryes out, becoming fertile in less than three weeks [8].

With each breeding event, annual fish can lay in the mud up to hundreds of eggs every day [8]. All adult fish die when their habitat dries out and survival of the population is ensured by desiccation-resistant eggs that enter into diapause and remain encased in the dry mud until the next rainy season [2], [7]–[12].

Diapause is a common feature of insect species from temperate climates and seasonal life cycle and fresh-water crustaceans from ephemeral habitats such as *Artemia* [13]–[15]. In vertebrates evolved in annual killifishes species and in over 130 species of mammals, including mouse, mustelid carnivores and some species of marsupialis, that are three of the most studied mammals models [16]. It consists in a suspension of development at precise developmental stages and its trigger can greatly vary among the species. In insects is mainly triggered in response to onset of direct hostile enviromental conditions or changes of the photoperiod predicting the proximity of the winter season [13]. In mammals it instead happens as an obligatory developmental stage or in response to maternal signals like hormonal changes, that indicates adverse environmental conditions outside the uterus [16].

1.1.3 Embryogenesis and development

Killifishes embryos developmental stages are broadly similar to any other teleost fish embryo. Embryos proceed through the phases of early meroblastic discoidal cells cleavages (segmentation), late cell cleavages, epiboly, dispersed phase, diapause I (optional), reaggregation, axis formation, somitogenesis, diapause II (optional), organogenesis and diapause III (optional). Among these

phases only dispersed phase, reaggregation and diapauses are peculiar of some of killifishes species (mainly, but not only, annual species), while all the other steps are common to all teleost fishes [3], [17], [18].

In the killifish *Fundulus heteroclitus* [19], it is well described that during the cleavage phase cell divisions are synchronized so that 2, 4, 8, 16 and 32 cells arise in succession. This pattern is broadly conserved in teleost species, and cell cycle during cleavage is extremely fast (in the order of 15 to 30 minutes) in typical model teleosts such as *Danio rerio* [20], *Oryzia latipes* [21], *Gasterosteus aculeatus* [22] and also *Xenopus laevis* [23]. During cleavage, there is no transcription of the embryonic genome but only translation of maternal transcripts and the cell cycle lacks the G_1 and G_2 phases, thus proceeding directly from S- to M-phase [24], [25].

Not so much is known about the activation of zygotic transcription. Recent studies revealed that in medaka and also in zebrafish the first signs of transcription from the zygotic genome are observed around the sixth division [26], [27] and are defined as pre-MBT transcription. This is considerably earlier than the tenth division, as originally reported for *D. rerio* in correspondence to the mid blastula transition [20], and is in line with recent results obtained in *O. latipes,* where the desynchronization is observed between the fifth and the sixth division [26]. It is therefore possible that in annual fish as well, the activation of the very first zygotic genes corresponds to the first signs of asynchrony.

Epiboly in *Fundulus heteroclitus* [19] is very similar or identical to *Danio rerio* [20], *Oryzia latipes* [21], *Gasterosteus aculeatus* [22], and cells generated at the animal pole migrate over the yolk surface until the complete envelopment.

As it happens for zebrafish, two layers of cells migrate during epiboly: the yolk syncytial layer and the blastomeres layer [17], [28]. The YSL is a transient extra-embryonic syncytial tissue that forms during early cleavage stages and persists until larval stages. During gastrulation, the YSL undergoes highly dynamic movements, which are tightly coordinated with the movements of the overlying blastomeres cells layer, and has critical functions in cell fate specification and morphogenesis of the early germ layers [28], the blastomeres cells instead are the cells that will form the embryos primordial axis [17].

Due to the dispersed phase that happens after the end of epiboly, axis formation in killifishes occurs at a different time compared to other teleost species like medaka or zebrafish. These two species in fact start to form the axis already before the epiboly is completed [20], [21] while killifishes first

completely envelop the yolk with cells, then disperse the blastomeres, and finally reaggregate them to form the primordial axis [17], [19].

The morphogenetic events that occur during somitogenesis and organogenesis in killifish are broadly similar to those shaping embryos of other teleost fish, with the obvious exception of diapause II arrest phase, that was never described in other fish like medaka or zebrafish. The somite formation dynamics are characterized by a progressive increase in the somites number together with the formation of the precursors of some of the main organs of an embryo, like eyes, heart, brain and liver [12], [29].

During somitogenesis two different developmental pathways have been described for annual killifishes, in relation to their commitment to go or not in diapause II [30], [31]. The commitment to enter diapause II is made during the previous developmental stages (already at the 24 somites stage or even earlier) and is irreversible [31]. This decision will lead embryos that will stop or not on diapause II to follow two different developmental ways, assuming a different morphology during somitogenesis. Embryos that will enter diapause II develop evolving their primordial axis mainly increasing its lenght and not growing radially. As a result, once arrested in diapause II, at the stage of 30-36 somites, these embryos present with a long and thin axis and head. Embryos that will not enter diapause II instead homogeneously develop growing both over the antero-posterior and the radial axis during somitogenesis, resulting broad at 30-36 somites (Figure 1.3). At this stage these embryos have indeed an axis and a head that are considerably wider compared to embryos entered in diapause II. In addition the head and some of its structures like the eyes primordia are way bigger and more defined than in diapausing embryos. These dynamics were demonstrated for Austrofundulus limnaeus [31] and for *Nothobranchius furzeri* [30], a south american and african annual species, respectively, and are thought to be a common feature among annual killifishes species. Due to this, diapause II has recently been defined as an alternative developmental pathway more than as a developmental stage itself, which affect a large part of embryos morphogenesis, shaping in a different way embryonal axis during almost all the somitogenesis.

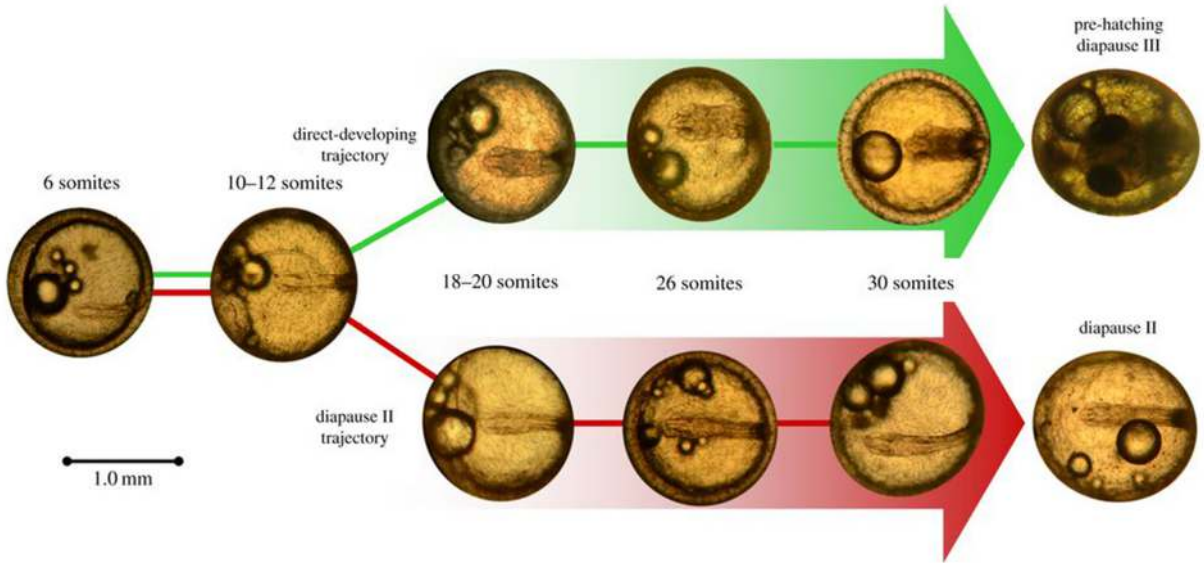

Figure 1.3: ***Nothobranchius furzeri differential developmental pathways****. Nothobranchius furzeri and annual killifishes in general develop in a different way accordingly to their decision to stop or not in diapause 2. Diapause 2 is entered around the 30-somite stage, yet morphological divergence in the head region is readily apparent well before this stage is reached. Figure design modified from original* [30].

1.1.4 Diapause

The early development of annual fish is conserved in the different annual genera Callopanchax, Nematolebias, Rachovia, Nothobranchius, Austrofundulus, Cynolebias [3], [17], [30], [32] and is characterized by three possible points of developmental arrest, termed diapause I, II and III [3]. Diapause I occurs early in development, after epiboly ends and before the somite embryo has formed, during a dispersed cell phase, which is unique to annual killifish [3]. Although embryos have been induced to enter this state through low temperatures or hypoxia [3], [18], [33], embryos reared under standard laboratory conditions rarely undergo diapause I [30]. Diapause II occurs after the formation of the embryonic axis, in embryos possessing from 30 to 36 pairs of somites, and several organ systems are recognizable [3], [18]. Lastly, diapause III occurs when the embryo is fully developed and precedes hatching.

The major point of developmental arrest occurs during diapause II (DII). DII is a facultative stage: it can be skipped when embryos are incubated at high temperature [8], [30], [31], [34], [35],but lower temperature, darkness, dehydration or anoxia (all conditions occurring in natural habitats) induce DII [10], [33], [36]. The duration of DII is highly variable and the embryos can remain in this stage for several months [11], [34] or even years (A. Cellerino, unpublished).

As a result of arrest at one or more of these three stages, embryos can extend greatly their developmental time, allowing them to overcome the dry season, when adult fish have perished.

Embryos, even of the same clutch, routinely follow different developmental trajectories arresting or not in diapause I, II, or III [17], [31] that makes their individual developmental time very different and unpredictable. This is supposed to represent a bet hedging strategy, to cope with the fact that environmental conditions are only partially predictable. The rain season can vary in its timing and amount of pluvial input, up to the point that in some particularly dry seasons the habitats may not be filled for sufficient amount of time to sustain killifish reproduction while in other seasons they may fill multiple times. Such a bet hatching strategy is well known for seed banks in the soil [37], [38]. Multiple phases of developmental arrest, that can last a variable amount of time, generate therefore diversity in the developmental stage of embryos, so that embryos of the same clutch can be shifted in any phase of the development. Among the whole pool of embryos a subgroup will be always ready to hatch in response to any sudden environmental change, giving the species an extremely high chance to survive in its extreme environment [38].

The physiological and molecular mechanisms of diapause were studied in detail in the South-American species, *Austrofundulus limnaeus*. Diapause II is characterized by drastic depression of protein synthesis, oxygen consumption and of mitochondrial respiration associated with G_1 arrest of the cell-cycle [11], [39]–[41]. These basic mechanisms seem to be conserved in also in African annual genus *Nothobranchius* [6], [30], [38], [42].

Diapause in annual killifish is also associated with major metabolic remodeling, where several pathways involved in energy production are modulated in order to minimize the embryo's aerobic metabolism and production of reactive oxygen species allowing quiescence. During diapause, oxygen consumption is suppressed and the cell cycle arrested [11], [41]. In some habitats of annual killifish the duration of the temporary pools is only a few months [43], and therefore the animals spend the largest fraction of their life in diapause.

Studies in the tapeworm Caenorabditis elegans have drawn a connection between diapause and aging. C. elegans can enter a stage of dormancy called dauer when the environmental conditions are unfavorable. Some genetic mutations that influence dauer formation also modulate longevity. In particular, the daf-2 mutation that affects an ortholog of the IGF/insulin receptor, increases lifespan over two-fold. Strikingly, the influence of the IGF/insulin pathway on longevity is conserved also in vertebrates and humans [44], [45]. In addition, the gene expression profile in the dauer larvae stage show high similarities to the expression profile of long-lived adult mutants [46]. Also small non-coding RNAs are embedded in the genetic network that links diapause and longevity, as exemplified by miR-71. This microRNA is a longevity gene and an aging biomarker in C. elegans and is also essential for diapause [47]–[50].

1.1.5 *Nothobranchius furzeri*

One of the most studied annual killifishes is the african species *Nothobranchius furzeri*. This species of killifish, as many african annual killifishes, is small (typically <8 cm), with marked sexual dimorphism and dichromatism. Due to its reduced dimensions, large tollerance of water parameter and ease of alimentation with commercially-available foods, captive care of this species is relatively easy and convenient (though time-consuming), and studies requiring a large number of individuals (in the order of hundreds) have been performed in several laboratories [9], [51], [52]

Nothobranchius fish have a short maximum natural lifespan (<12 months) due to annual desiccation of the pools they inhabit. Notably, this short lifespan is also retained in captivity, varying between 3 and 18 months [52]–[54] and depends on the humidity of habitat of origin, suggesting that duration of the pools in the wild drives evolution of aging in natural populations [43] (Figure 1.4).

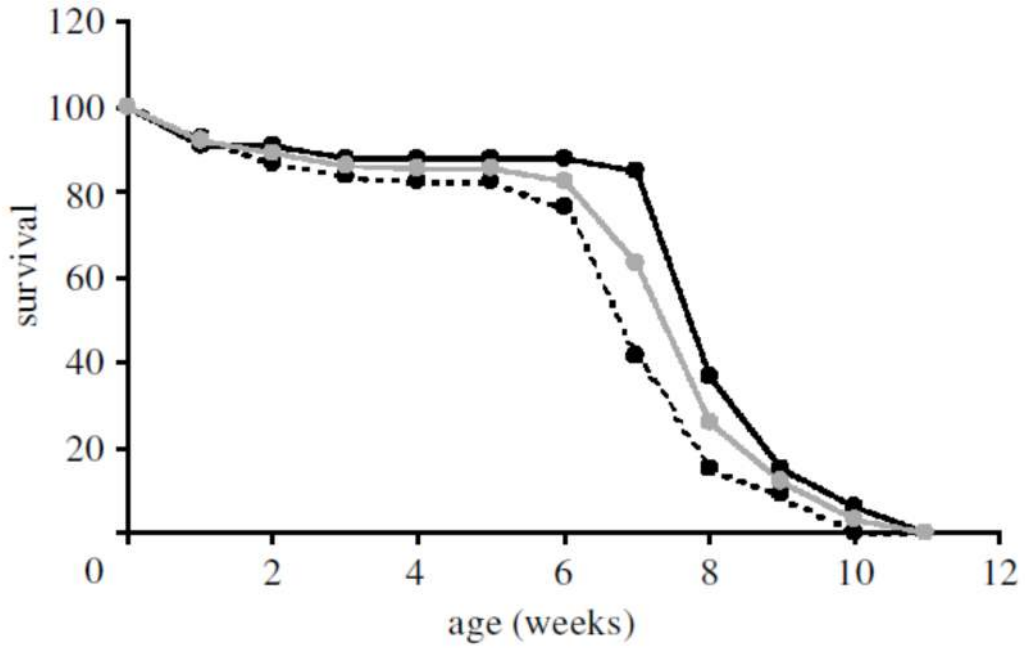

Figure 1.4: Survival trajectory of Nothobranchius furzeri in the laboratory. Survival is expressed as a percentage of maximum survival. The 25°C curve (dashed line) plots the survival rate of 68 fishes kept at a constant temperature of 25°C. The 'Var' curve (black line) plots the survival rate of 33 fishes kept at room temperature during the months June–August in Canossa, Italy. Tot (grey line) is the average of the two curve [52].

Nothobranchius extremely short lifespan and aging phenotype has made this *taxon* a laboratory model for in research for the study of age related diseases and age mechanics. Over the years, many

aspects of their aging phenotype were charachterized [53], [54], such as behavioural impairmentes [55]–[57], histopathological lesions [58] and disruption of the circadian rhythms [54]. In addition, telomere erosion [59]–[61], reduced mitochondrial numbers and function [62], accumulation of lipofuscin [56], [61], [63], [64], increased apoptosis [58], [63] and dramatic reduction of stem cell activity [65] were described in aged fishes. Finally, genome-wide analysis of transcript regulation revealed similarities in gene expression during aging between *N. furzeri* and humans both at the level of microRNAs and protein-coding transcripts [66], [67]. The *Nothobranchius* life cycle is entirely adapted to the ephemeral and unpredictable conditions of their habitat. As the other annual killifishes described above, fish hatch when the pool is filled with water, grow rapidly and become sexually mature within a few weeks [8], [37]. After reaching sexual maturity, they reproduce daily, also in laboratory conditions [8], [68], that means that every day a lot of eggs are available for observation or manipulation. Nowadays embryos can be routinely genetically manipulated in order to generate transgenic lines with a gene insertion [35] or deletion [69].

Diapause and early development in *N. furzeri* have been characterized over years, with studies that investigated specifically cleavage and early cell movements in *Nothobranchius* as well as the effects of some environmental variables on diapause [42], [70]–[72].

Nothobranchius furzeri developmental stages and diapause dynamics reflect entirely the stages and the dynamics described above for Austrofundulus [12] or any other annual killifish.

1.2 Transgenesis

1.2.1 Basis of trasgenesis

Transgenesis is used in a wide variety of research applications ranging from the study of gene expression to the creation of animal models of human diseases. Transgenic tools enabled in vivo labeling and detailed observation of specific cell types using fluorescent reporters and thereby complement mutagenesis by facilitating targeted genetic screens [73], [74].

In fish, many of the transgenesis techniques were developed in zebrafish, due to its high fecundity, ease of egg manipulation, developmental speed and the transparency of the zebrafish embryos [20].

Transgenic zebrafish were first generated by microinjection of naked DNA [75]. In this technique, a plasmid DNA is linearized with a restriction enzyme, purified, and then microinjected into the cytoplasm of one-cell stage embryos. On average, a small percentage of the injected fish (< 10%) transmit the transgene to the next generation. These transgenes tend to form tandem arrays or concatamers at the integration site, which in some cases may lead to variegated expression or silencing in the subsequent generation. Thus, while numerous transgenic fish have been generated with this technique [76]–[78], the germline transmission frequency and the reliability of transgene expression have been low. Pseudotyped retroviral vectors have also been successfully used for transgenesis in zebrafish, particularly for genome-wide insertional mutagenesis [79], [80] and enhancer trapping [81]. However, the retroviral vectors can only carry inserts of small sizes and their application in the laboratory is labor intensive.

To further improve the rate and ease of transgenesis in zebrafish and to create vectors that are useful for genetic analyses in this model vertebrate, were optimized transposable elements [82]–[85]. Among them, the *Tol2* transposable element from the medaka fish appears to have the highest rate of genomic integration in the germ lineage and is now widely used as a genetic tool (reviewed in [86], [87]).

Tol2 is an active DNA transposable element capable of catalyzing transposition upon recognition of a target sequence. The Tol2 transposition system used for transgenesis consists of two elements: an RNA encoding the Tol2 transposase and a plasmid containing a nonautonomous Tol2 transposon (i.e. not encoding the transposase) surrounding the gene of interest [87]–[89]. The transposase recognizes the target Tol2 sequence in the plasmid, excises the gene of interest, and integrates it into the host's genome [88], [90], thus allowing efficient and stable transgenesis.

In addition, a vector containing the minimal DNA sequences required for *Tol2* transposition has been described, making preparation of new transgene constructs relatively easy [91], [92].

Many *Tol2* vectors have been reported to date, including vectors that facilitate the rapid construction of promoter- or protein-GFP fusions through the Gateway technology [93]–[95]. These vectors can be used for expression of any foreign genes in embryos by transient and stable transgenic approaches. Furthermore, *Tol2* gene and enhancer trap vectors have been developed for gene expression studies and mutagenesis [96]–[98]. *Tol2* -mediated transgenesis is a highly efficient method to create stable transgenic fish since 50–70% of injected fish transmit genomic insertions of the injected *Tol2* construct to the next generation [92], [96]**.** Insertion, however, remains mosaic.

Tol2 transposon was also developed as a system to efficiently generate transgenic animals in other fish model systems, including stickleback and cichlids [99] or commercially relevant fishes species such as salmon, trout, and tilapia [100], [101]

1.2.2 Transgenesis in *Nothobranchius*

In the year 2011, Valenzano et al. Tested the efficiency of the *Tol2* system in N. furzeri and reported a good efficiency of transgene insertion in the germline [35] (Figure 1.5). Early embryonic development is much slower in *N. furzeri* as compared to zebrafish, with cell cycle speeds in the order of almost two hours as opposed to 15 minutes (see Results). This may facilitate early integration of the transgene and germline transmission. The slow embryonic development of *N. furzeri* might increase the chances of early embryo integration and, therefore, robust germline transmission as compared with other model systems. Indeed, the frequency of GFP-positive F1 offspring from a cross between GFP-positive P0 parents and wild-type fish was reported to be about 30% in *N. furzeri* [35]. These results were replicated by Hartmann & Englert and Allard et al. [102]

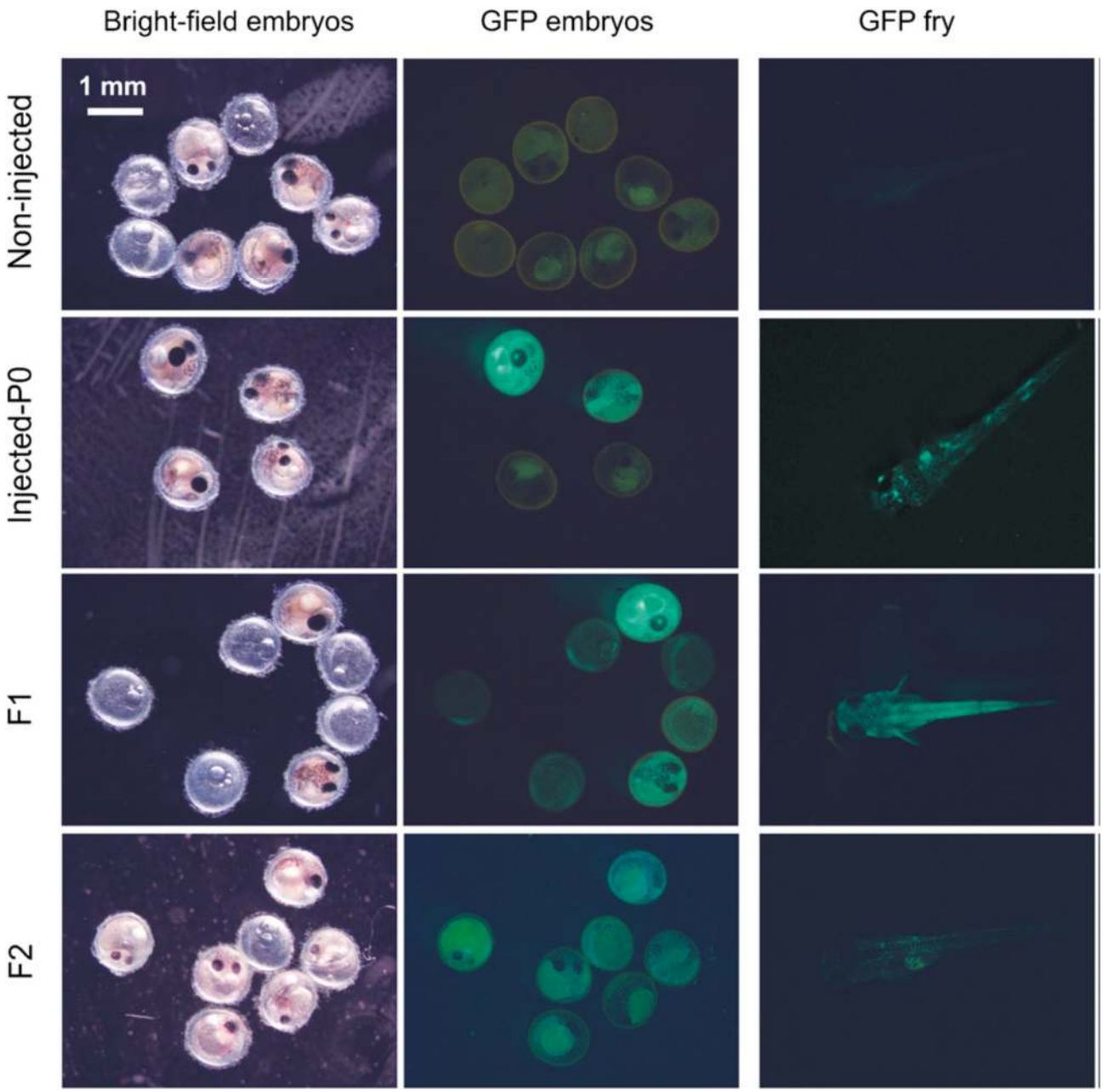

*Figure 1.5:**Nothobranchius furzeri transgenic fish**. Expression of GFP in pCska-gfp Tol2 transgenic N. furzeri. GFP expression in live noninjected (top row), injected P0fish (second row), and the F1 (third row),and F2 (bottom row) progeny of GFP positive N. furzeri.* [35]

1.3 Cell cycle

1.3.1 General mechanics

Cell cycle is an ubiquitous, complex process involved in the growth and proliferation of cells, organismal development, regulation of DNA damage repair, tissue hyperplasia and response to injury and diseases such as cancer. The cell cycle involves numerous regulatory proteins that direct the cell through a specific sequence of events culminating in mitosis and the production of two daughter cells. Central to this process are the cyclin-dependent kinases (cdks) and the cyclin proteins that regulate the cell's progression through the stage of the cell cycle referred to as G1, S, G2 and m phases [103].

The cell cycle can be morphologically subdivided into interphase and stages of M (mitotic) phase, which include prophase, metaphase, anaphase, and telophase [104]. Interphases encompasses G1, S, and G2 [103]. The G1 and G2 phases of the cycle represented the "gaps" in the cell cycle that occur between the two obvious landmarks, DNA synthesis and mitosis. In the first gap, G1 phase, the cell is preparing for DNA synthesis. S phase cells are synthetizing DNA and therefore have aneuploid DNA content between 2N and 4N. The G2 phase is the second gap in the cell cycle during which the cell prepares for mitosis or M phase. G0 cells are not actively cycling [103].

The timely execution of each stage of the cell cycle is intimately linked to key developmental processes such as differentiation and organogenesis. On the other hand, failure to precisely regulate cell-cycle progression leads to various diseases such as cancer [105], [106]. To ensure that events such as S phase and mitosis proceed both in an orderly fashion and with high fidelity, cells have developed a series of checkpoints that act as quality control centers at each stage of the cell cycle. These checkpoints, which govern the transitions between G1/S and G2/M, are designed to monitor cellular parameters such as genomic integrity and cell size throughout the division cycle [107], [108].

If a cell fails to meet minimal requirements at any point during the process, regulatory factors prevent the onset of the next phase until the task at hand has been completed [107]. For many years, it has been difficult to precisely track cell-cycle progression in a live, multicellular context. This is because most of the techniques currently used to monitor the cell cycle—such as BrdU incorporation or immunostaining of cell-cycle markers—require cell fixation prior to analysis. As a consequence, these methods do not permit the dynamic behaviors of cycling cells to be visualized in real time.

1.3.2 FUCCI

In the 2008 Sakaue-Sawano and colleagues designed a fluorescent reporter to track cell-cycle progression with high spatiotemporal resolution in a multicellular contex [109] that provided a molecular tool to easily distinguishing between cells engaged in different stages of the cell cycle with minimal perturbation to the system under study, allowing the dynamic behavior of cycling cells to be monitored in real-time.

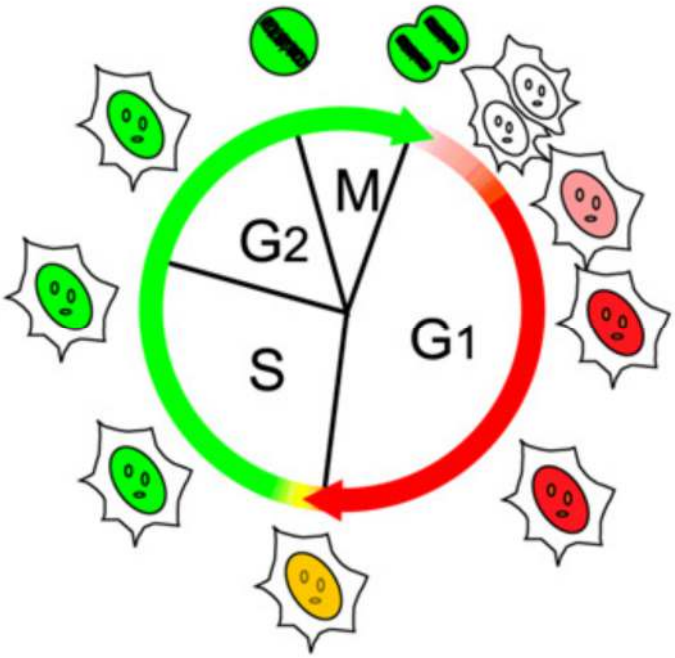

Figure 1.6: ***Cell cycle visialization with FUCCI reporters****. Cells that brings FUCCI reporters emit green fluorescence during S G2 and M phases, red fluorescence during G1 and G0 phases and are colorless at the interface between M and G1/G0 phase.*

This method, termed fluorescent ubiquitination-based cell-cycle indicator (FUCCI), exploits cell-cycle-dependent proteolysis of the ubiquitination oscillators, Cdt1 and Geminin, to specifically mark the G1/S transition in living cells [109], [110].

By fusing the red- and green-emitting fluorescent proteins monomeric Kuzabira Orange 2 (mKO2) and monomeric Azami Green (mAG) to the sequences of Cdt1 and Geminin respectively that carry the ubiquitination sites, is possible to achieve striking contrast between various stages of the division cycle (Figure 1.6). Specifically, the nuclei of cells in G1 phase (and G0) appear red, because the mAG-Gemin fusion protein is preferentially degraded, while those of cells in S/G2/M appear green because the mKO2-Cdt1 fusion protein is preferentially degraded. During the

transition from G1 to S phase, cell nuclei turn yellow, clearly marking cells that have initiated DNA replication [109], [110].

The dramatic color changes exhibited by Fucci are based upon the reciprocal activities of the ubiquitin E3 ligase complexes APC^{Cdh1} and SCF^{Skp2} [111].

The APC^{Cdh1} and SCF^{Skp2} complexes are E3 ligase activities that mark a variety of proteins with Ub in a cell cycle-dependent manner [111]. Because the SCF^{Skp2} complex is a direct substrate of the APC^{Cdh1} complex but also functions as a feedback inhibitor of APC^{Cdh1} [112], [113], these two ligase activities oscillate reciprocally during the cell cycle. The APC^{Cdh1} complex is active in the late M and G1 phases, while the SCF^{Skp2} complex is active in the S and G2 phases. Two direct substrates of the APC^{Cdh1} and SCF^{Skp2} complexes, Geminin and Cdt1, are involved in ‘‘licensing’’ of replication origins [114]. This carefully regulated process ensures that replication occurs only once in a cell cycle. In higher eukaryotes, proteolysis and Geminin-mediated inhibition of the licensing factor Cdt1 are essential for preventing re-replication.

Consequently, the APC^{Cdh1} and SCF^{Skp2} substrates Geminin and Cdt1 are specifically degraded during G1 and S/G2/M, respectively [115].

Even if these proteins function as effective G1 and S/G2/M markers, geminin, but not Cdt1, is interchangeable between mammals and fish in terms of ubiquitin-mediated degradation [116]. In the 2009 Sugiyama et al. generated DNA constructs using the zebrafish homologs of Cdt1 (zCdt1) and geminin (zGem), characterized them using cultured fish cells, constructed transgenic zebrafish lines and observed the correct dynamic patterns of cell-cycle progression in several parts of the embryo, including the retina and notochord [116] (Figure 1.7).

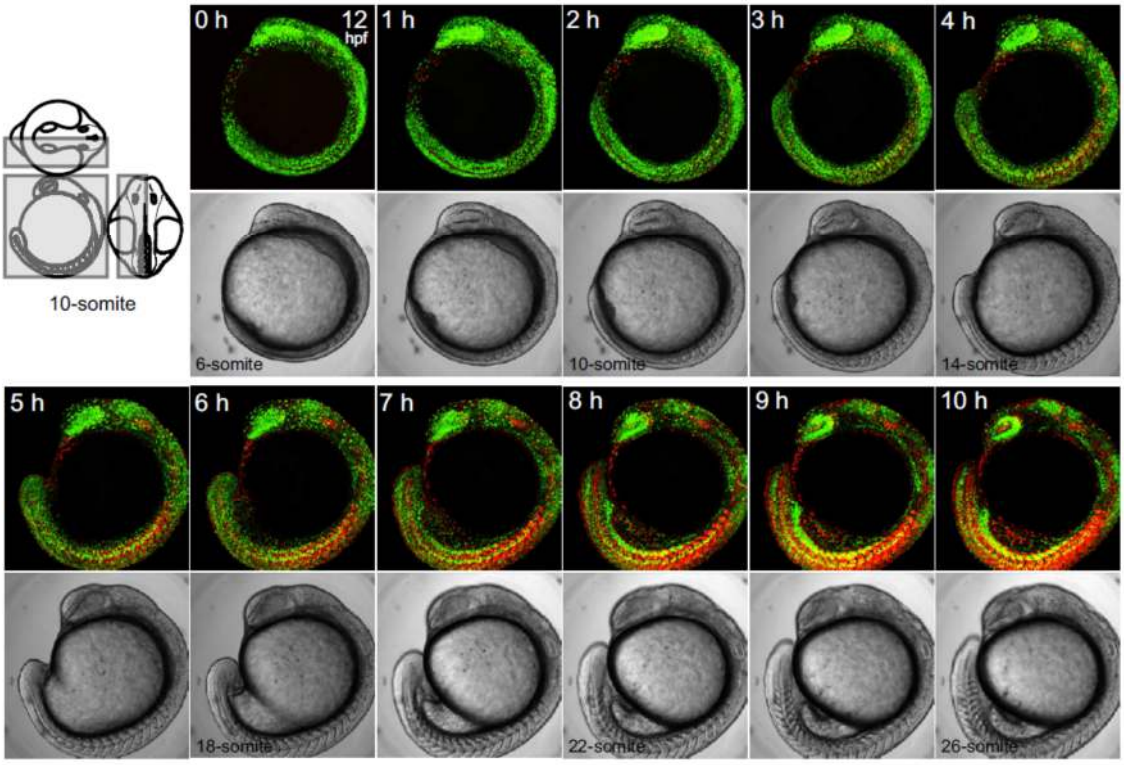

Figure 1.7: ***Time-lapse imaging of a FUCCI transgenic zebrafish embryo during segmentation****. Green and red cells populate specific embryonic regions during development. First steps of segmentation are characterized by a predominance of green cells, and red cells increase in number, populating the somites, as development proceeds. Due to z-stacking, green and orange signals at different z-positions merge to generate yellow signal. Note that zebrafish FUCCI reporters does not yield yellow fluorescence at the G1/S transition, whereas the original FUCCI in mammalian cells does* [116].

Summarizing, FUCCI technology offers a powerful in-vivo tool for studying the cell cycle in mammals and fishes, because cell nuclei color changes in a fast and reliable way as cell cycle proceeds.

This technique is particularly powerful when used in combination with traditional confocal laser scanner microscopy [117] or new generation microscopy, such as selective plane illumination microscopy [118] and digital scanned laser light sheet fluorescence microscopy [119], that have been developed for high-speed in vivo observation of embryonic development at subcellular resolution.

Aims

Annual killifishes are some of the most stiking fishes living on our planet, because of their adaptation to extreme environments, that led to the evolution of extreme growth rates ,extraordinary fast aging, peculiar embryonic development and the evolution of diapause.

Unfortunately, our knowledge of annual killifish biology is very limited and many observations were made by amateurs that raise these fishes as an hobby rather than by professional scientists. For this reason, even basic aspects of embryonic development and diapause mechanics are unknown.

The objective of my thesis was to shed some light on the processes that characterize the cell cycle of annual and non annual killifishes during embryonic development and in the diapause phase both from a macroscopic and molecular point of view.

I therefore set three main aims:

1) To describe the development of non annual kilifishes embryos (that lacks from the literature entirely) and compare it with the known development of annual killifishes [3], [17], [18], evidencing any possible difference in morphogentic processes.

2) To test the applicability of FUCCI technology [116] to killifish species to describe cellular dynamics during early development and diapause phases, in order to define the cell cycle profile for embryos arrested in diapause, committed to enter in diapause, committed to escape diapause and releasing from diapause.

3) To identify some of the molecular factors involved in the diapause control, in particular microRNAs.

2. Results

2.1 Developmental differences

The first set of experiments aimed at describing the early developmental dynamics of a taxonomically representative collection of killifishes species covering all continents where killifishes are distributed:. South America, west Africa and east Africa (Figure 2.1)

Eggs or adults of 12 killifishes species were obtained and raised under laboratory conditions. At least one annual and one non-annual species were chosen for each of the three geographical clades. From South America, we chose the annual species *Rachovia brevis* and the related non-annual species *Rivulus cylindraceus.* From Africa, west of Dahomey gap, the annual species *Callopanchax occidentalis* and the non-annual species *Scriptaphyosemion guignardi* and *Epiplatys dageti monroviae.* From Africa, east of Dahomey gap, the annual species *Nothobranchius furzeri, N. guentheri, N. korthausae* and *N. melanospilus* and the non-annual species *Aphyosemion australe* and *A. striatum.*

As outgroup, we chose the closest outgroup *taxon* to all annual killifishes *Aplocheilus lineatus, as based on the phylogeny reported by Murphy and Collier* [2]. *However, more recently two studies of molecular phylogeny indicate that Aplocheilus is sister taxon to the African killifishes* [30]. *These studies were published after my work was completed. According to these views, an outgroup for all killifishes would be Fundulus, for which a detailed description of embryonic development is available* [19].

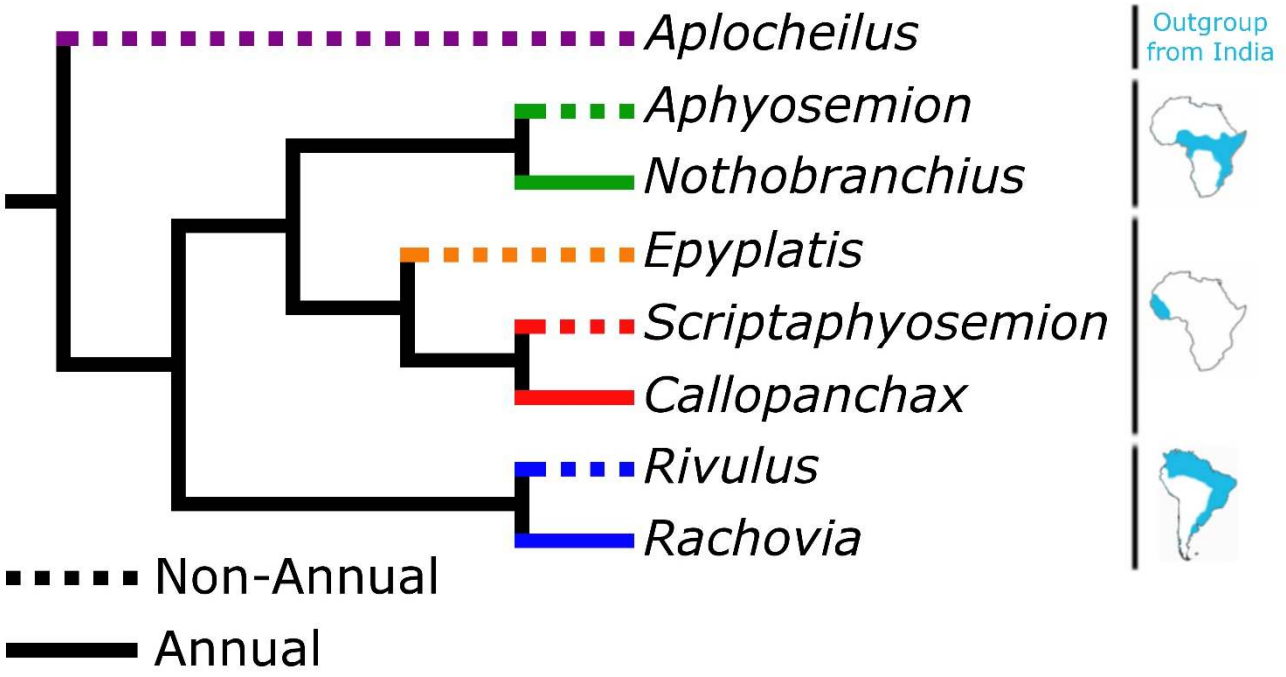

Figure 2.1: ***Phylogram of the species used for the experiments.*** *Dashed lines indicate non-annual species, solid lines annual species and color codes for the three evolutionary lineages. The geographic distribution of each lineage is show on the right. The phylogram is derived from the original Murphy and Collier molecular phylogram* [2] *based on cytochrome b, 12 s rRNA and 16 s rRNA genes.*

To document embryonic development, we used live imaging and fertilized embryos were imaged for hours up to days, every few minutes (2 to 5 minutes, depending on the species), with a brightfield microscope. For most of the species analyzed, it was possible to image the development up to some days after the end of epiboly and in some cases also the formation of the embryonic axis and the process of somitogenesis (Figure 2.2).

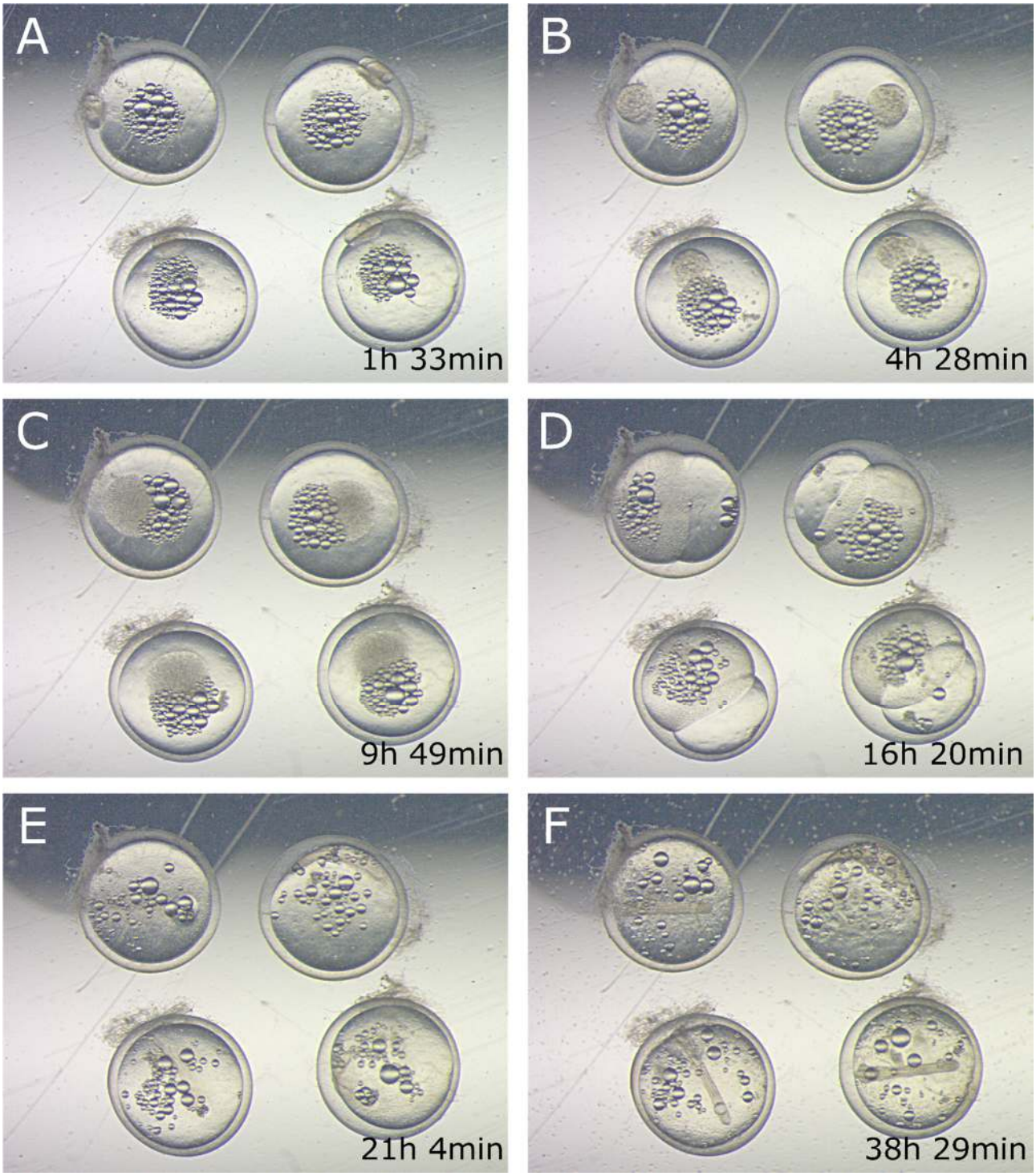

Figure 2.2: ***Killifish embryo time lapse example.*** *Figures show Aplocheilus lineatus embryos raw acquisitions, in some of the critical developmental steps: segmentation (A), asynchronous cell divisions (B,C) epiboly (D), axis formation (E) axis grow (F). Time at which each stage occurs is shown.*

2.1.1 Non-annual killifishes development description

Non-annual killifishes have an early development that is very similar to the one described for other fish model organism, like *Fundulus* [19], zebrafish [20] or medaka [21].

For the first hours, the cells divide synchonously, rapidly and at regular time intervals of less than 30 minutes (Figure 2.3).

After this phase of synchronous divisions (that on average spans the first 6 cleavages), asynchronous division starts and each cell or cells group divides independently, with a pace that depends on its position within the embryo.

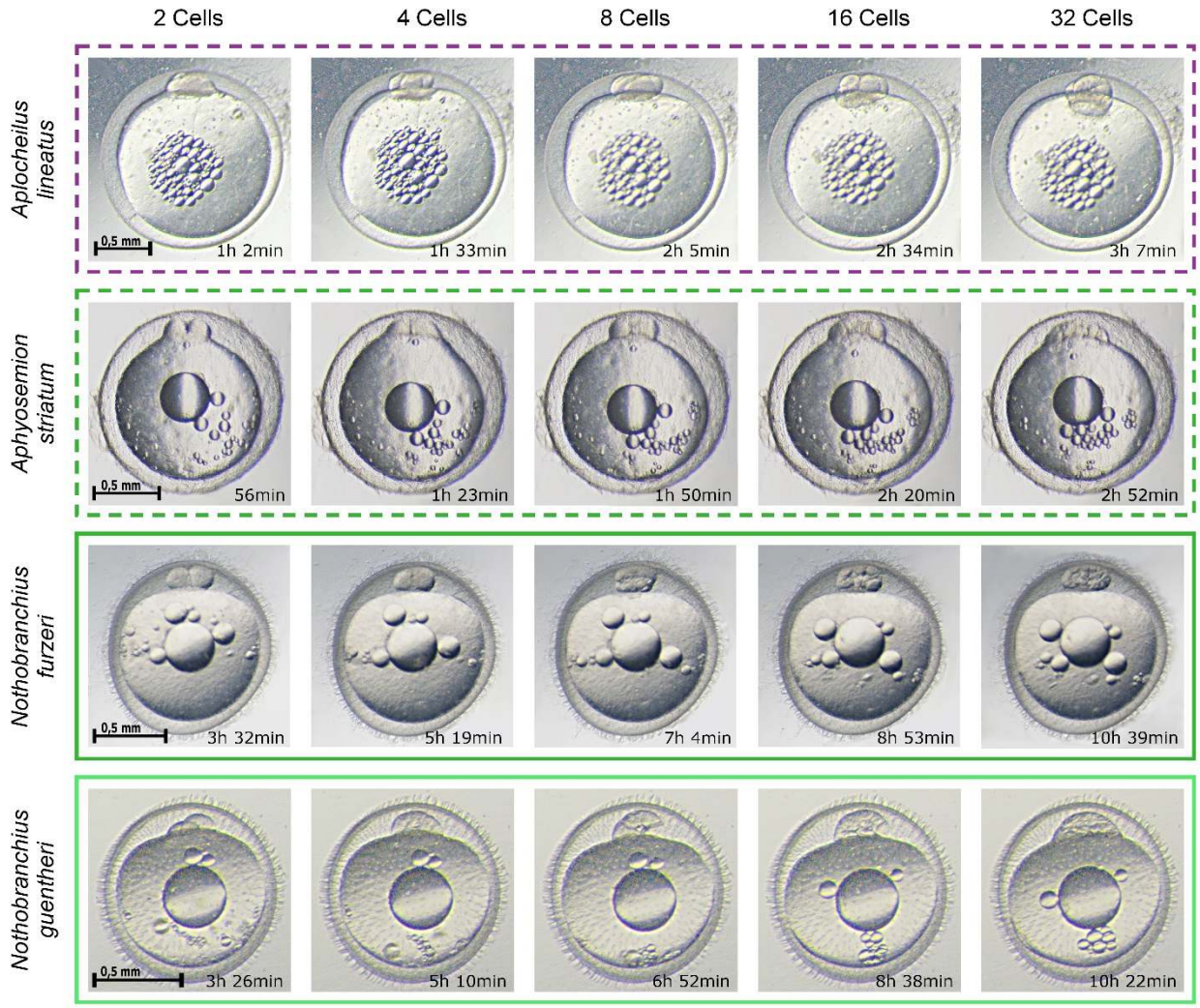

Figure 2.3: ***Early cleavage time-lapse.*** *Non-annual species (dashed boxes) are compared with annual species (solid boxes) by brightfield time lapse imaging. Early cleavage stages are shown for each species and the average time at which they occur is indicated. There is a large difference in early cell division rates between annual and non-annual species.*

When a critical number of cells is reached (this number cannot be assessed by simple brightfield microscopy due to overlaid cell masses) the epiboly starts and cells begin to migrate over the yolk surface toward the opposite part of the embryo (Figure 2.4 D).

Two layers of migrating cells can be recognized. The first layer that migrate is a thin and almost transparent layer of cells and is composed by the yolk syncytial layer (YSL) cells, that contact directly the yolk surface (Figure 2.4 D,E).

The other layer of cells is composed by the epiblast cells, that migrate in the same direction of YSL cells, moving on top of them, and not contacting the yolk directly. These cells appear to be much smaller and their borders are well-defined compared to the YSL cells that form a syncitium.

Once epiboly is completed, or in some species, even before this process ends, the embryonic axis starts to appear, as a thicker and oval aggregation of cells (Figure 2.4 H).

Some species, like *Aplocheilus* and *Epiplatys*, shows a pecocius formation of the primordial axis, that precedes the completion of epiboly, as it happens in other teleost fishes like zebrafish [20]. Other species, belonging to *Aphyosemion* or *Scriptaphyosemion* genera shows instead a delayed formation of the axis. These fishes after epiboly is completed have a phase similar to annual fishes dispersed phase (Figure 2.5), where epiblast cells migrates over the YSL for minutes or hours, without reaggregating to form the axis.

The embryonic axis extends over time, generating slowly the several embryo structures like the somites, the head, the eyes, the fins and all the other organs (Figure 2.4 I-M).

All these structures slowly evolve, growing and shaping in a continuous developmental process, forming finally a fry ready to hatch (Figure 2.4 N). All the developmental process, from the fertilized cell to the fry, regardless to the species of killifish, excluding diapauses arrests, usually takes an average time of 22 days at 26°C.

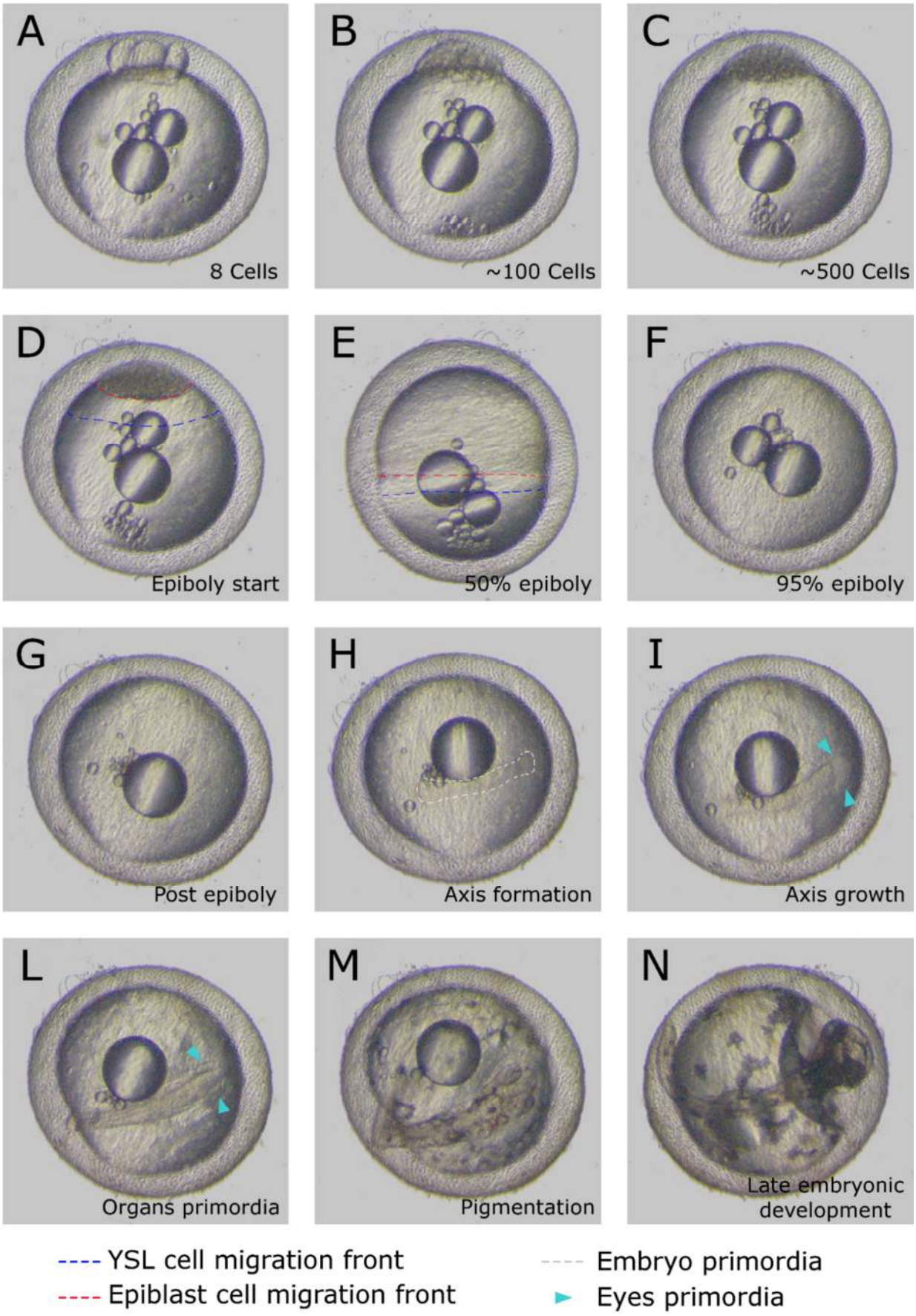

*Figure 2.4: **Killifish developmental table.** Aphyosemion striatum (non annual) complete embryonic development. The developmental steps shown are common to annual and non annual killifishes.*

2.1.2 Annual killifishes development description

Development of annual killifishes (Movie S1) shares various similarities with the development of non-annual species, but presents some major differences.

In the first place, as treated in the introduction, annual killifish can stop their development in diapause, but the arrest of the development itself is not the only peculiar feature since alternative developmental pathways are taken in embryos that enter or skip diapause.

Diapause I is a phase where an embryo can arrest after epiboly ends, when the YSL and the epiblast cells have already completely enveloped all the yolk surface (Figure 2.5). Annual embryos epiboly dynamics are slightly different from non-annual ones, because epiblast cells are smaller in number and are dispersed (Figure 2.5 B, arrows). In annual embryos, indeed, epiblast cells never contact closely each other, as it is the case in the majority of non annual species . The number of epiblast cells that migrate over the YSL greatly varies among the observed non annual species. Cell density is reduced in *Scriptaphyosemion* (Figure 2.5 A) and in *Aphyosemion* while is very high in *Epiplatys* and *Rivulus*, so much that is impossible to distinguish one cell from each other with brightfield microscopy. Non annual species that have a lower epiblast cells density during epiboly have as well an higher propension to not immediately form embryonic axis after epiboly and to spend some hours in a dispersed-phase like stage. Annual species always have spread and clearly detectable epiblast cells, as well as they always have a dispersed phase that lasts for several days (figure 2.5 B).

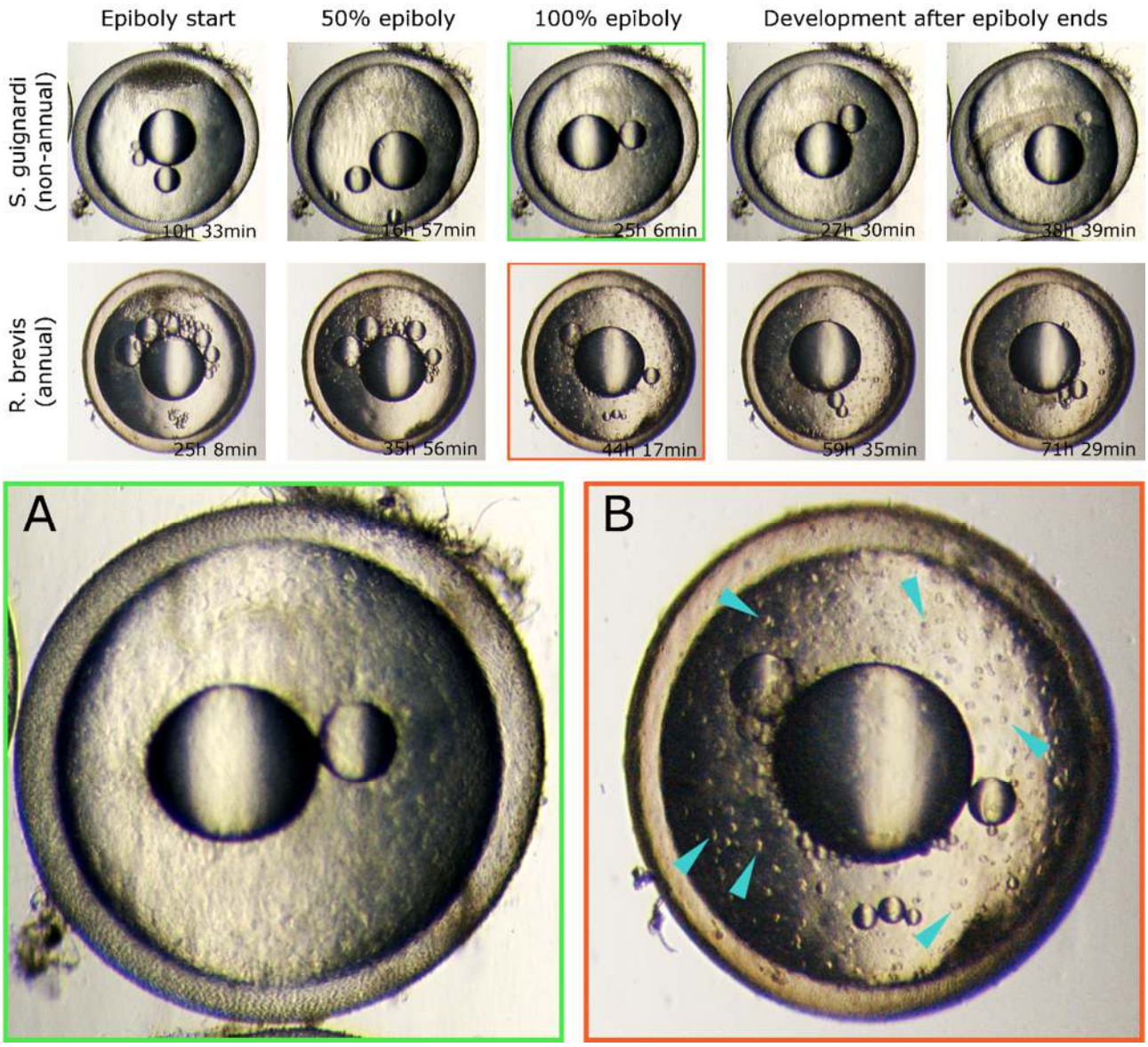

Figure 2.5: ***Differential development after epiboly in non annual and annual killifishes****. A Scriptaphyosemion guignardi (non annual) and a Rachovia brevis (annual) embryos are compared during and after epiboly. Epiboly proceeds the same in both species, with YSL and epiblast cells enveloping the yolk. In S. guignardi epiblast cells' density is higher (A) while in R. brevis they are more discrete and spread (B, arrows). Few hours after epiboly ends S. guignardi forms the embryonic axis, while R. brevis begins the dispersed phase or stops in the diapause 1 phase. The embryonic axis in R. brevis willstart to form much later.*

Once epiboly is over, annual killifishes epiblast cells continue to randomly migrate over the yolk surface for an undefined amount of time (usually days) before reaggregating to form the embryonic axis. This phase has been described as the dispersed phase, is peculiar of annual species and is obligatory. During this phase, an arrest in diapause I can happen.

2.1.3 Cleavage rate differences

The main result obtained from brightfield time lapse analysis is a large-scale difference in segmentation timings between annual and non-annual species (Figure 2.6).

Converting the image sequences into videos, it was possible to evaluate the pace of cell divisions for each species, in order to precisely quantify this difference (Movie S2).

Figure 2.6: ***Early cleavage time-lapse.*** *Non-annual species (dashed boxes) are compared with annual species (solid boxes) by brightfield time-lapse imaging. Early cleavage stages are shown for each species and the time at which they occur is indicated. There is a large difference in early division rate between annual and non-annual species.*

The length of the cell cycle varies dramatically between annual and non-annual species (Figure 2.7, Student's t-test, P <0.001) and this difference is conserved in both the africans and the south americans killifish species. As showed in figure 2.8, where the number of cells is reported as a function of time for each of the species of our taxonomical sampling, there is a clear separation between annual and non-annual killifish early segmentation rates. Regardless of the phylogenesis or the geographic orgin of a given species, if that species is annual, it has an early cleavage rate that is slower than any other non-annual species. Precisely, the five non-annual species analyzed show an average cleavage time of 34.8 minutes (range 23.0 to 48.0), that is comparable to the outgroup *A. lineatus,* while the six annual species analyzed show an average cleavage time of 75.6 minutes (range 66.0 to 100.0). If *Fundulus* and not *Aplocheilus* is considered as outgroup, according to Furness and Moritz phylogenesis, the result of the study remains unchanged. In fact *Fundulus* has a cleavage time of 28 minutes [19], that is comparable with non annual species cleavage time.

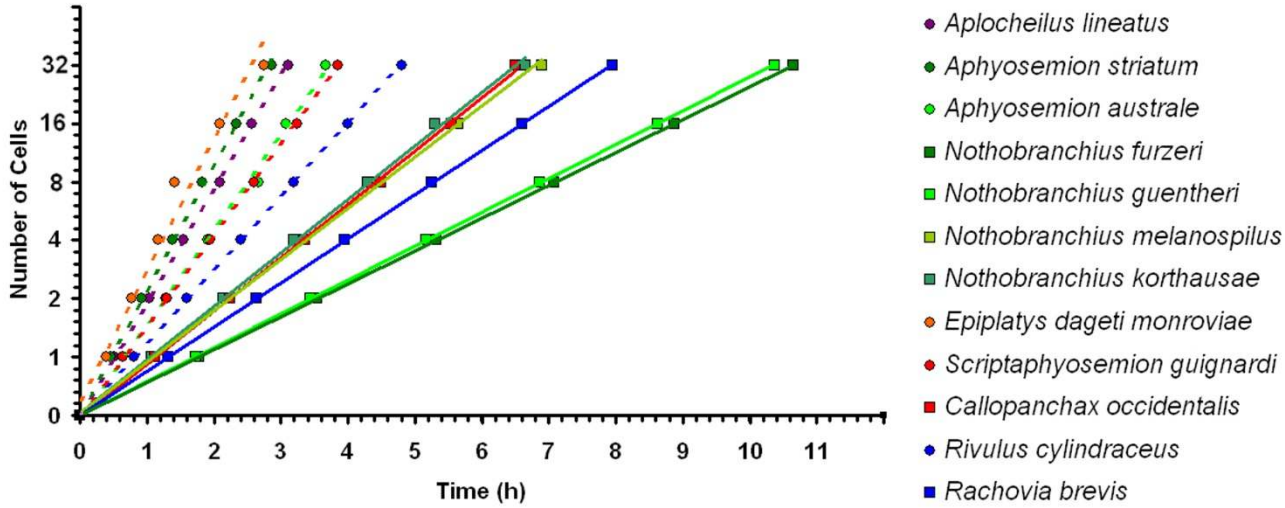

Figure 2.7: ***Difference between annual and non-annual division rate is conserved in Aplocheloidei.*** *All species followed with time-lapses videos were plotted. Developmental stages are shown on the x-axis and time at which they occur on the y-axis. Dashed lines indicate non-annual species, solid lines annual species and color codes the geographic clade. For each species only one individual embryo is plotted.*

To confirm the data, replications of the time lapses were performed for the crucial species considered for the studies: *Nothobranchius furzeri* and *N. guentheri*, as annual killifishes, their closest non-annual relative *Aphyosemion striatum,* and the closest outgroup *taxon* to all annual killifishes *Aplocheilus lineatus*.

As before, a clear separation between annual and non-annual segmentation rates is observed, with a very low variation between the replicas (Figure 2.8).

The average cells doubling time is 106.5 minutes +/-2.2 for *N. furzeri (annual)*, 103.6 minutes +/- 2.6 for *N. guentheri (annual)*, 28.2 minutes +/- 1.5 for *A. striatum (non-annual)* and 31.1 +/- 0.8 for *A. lineatus (non-annual)*.

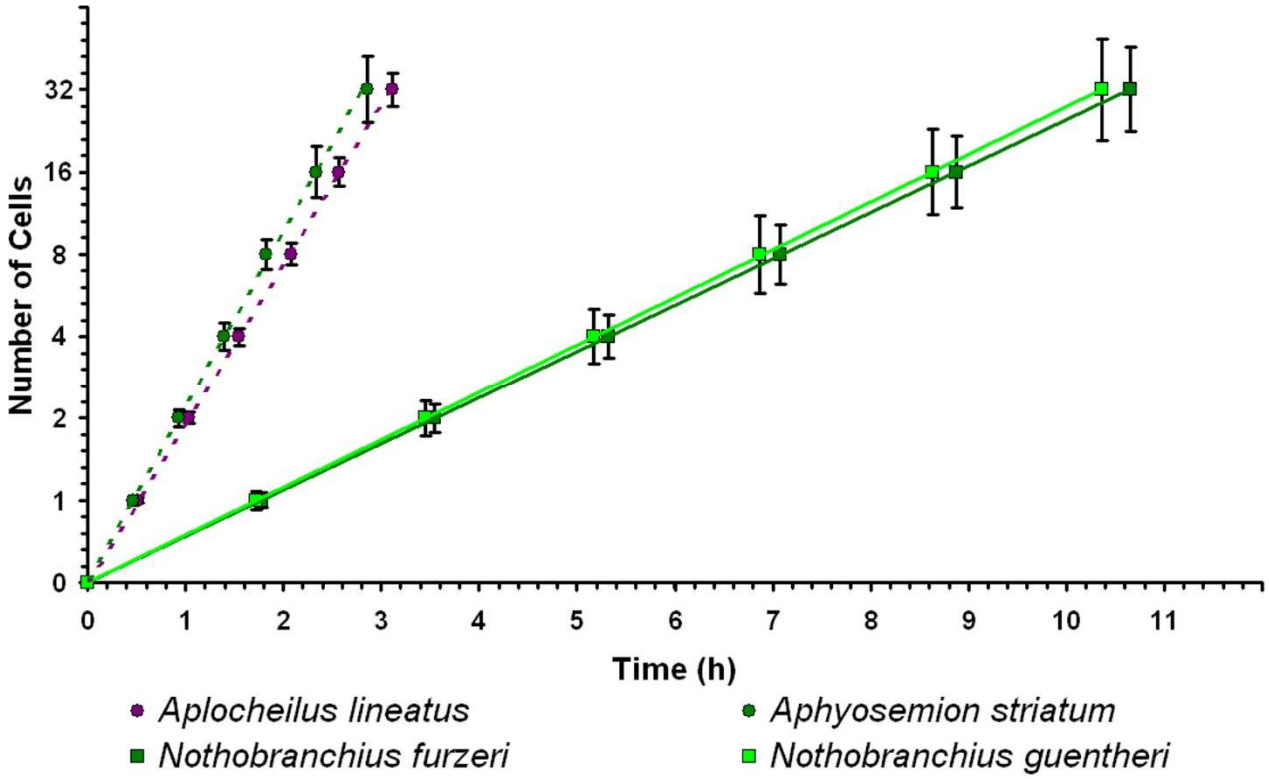

Figure 2.8: ***Early division rates greatly differ between annual and non-annual species.*** *Time-lapses videos were plotted, with developmental stages on the x-axis and time of occurrence on y-axis. Data are means of three independent experiments. Error bars represent standard deviations. Dashed lines indicates confidence intervals of the regressions. The slopes of the lines clearly show the great difference between annual and non-annual early division times.*

2.2 Exploring cell dynamics during development

2.2.1 Segmentation

The differences in segmentation rates between annual and non-annual species led to the next question concerning the mechanisms responsible for this difference .

Non annual killifishes show division rates similar to those observed in the other teleost fishes were this phenomenon was investigated, with very fast early cleavages (under 40 minutes for each division), probably due to an alternation of only an M and a S phase [24], that can be considered as a basal trait. Therefore, I focused my investigations on annual species, whose segmentation dynamics can be considered as the derived trait. In particular, I used the annual species

Nothobranchius furzeri, because it is the annual species most diffused in the scientific community, protocols for microinjections are available [35], [102] and it showed the slowest cell division rate in the segmentation phase. I assume that the basic mechanisms will be identical in the two other annual clades.

Cell cycle dynamics of *Nothobranchius furzeri* embryos were explored by FUCCI (see Introduction). In this system, a red and a green fluorescent reporters are fused to protein motives that drive degradation in the G_1 and the S phase respectively [109]. Therefore, a cell in the G_1 phase would appear red and a cell in the $S/G_2/M$ phase green, while cells at the transition between M and G1, or M and S, would show no fluorescence. This experiment therefore will indicate whether slow cell cycle is due to slower S and M phases or rather to the presence of a G1 phase.

FUCCI reporter mRNAs optimized for zebrafish [116] were microinjected in *N. furzeri* fertilized one cell stage eggs and then the embryos fluorescence was analysed in time lapse using confocal microscopy (five independent experiments). From these experiments (Figure 2.9 and Movie S3), it is clear that the first five divisions (Wourms stages 4-8) are synchronous. The red and green fluorescent reporters rise in phase after cell division (Figure 2.9 A-F), become cytoplasmic (Figure 2.9 G) and are then degraded (Figure 2.9 H) shortly before cell division. Starting from the sixth division (Wourms stage 9) (Figure 2.9 K), cells with a prevalence of red fluorescence intermingled with cells with a prevalence of green fluorescence are detectable, demonstrating desynchronization of the cell cycle and the appearance of a G_1 phase.

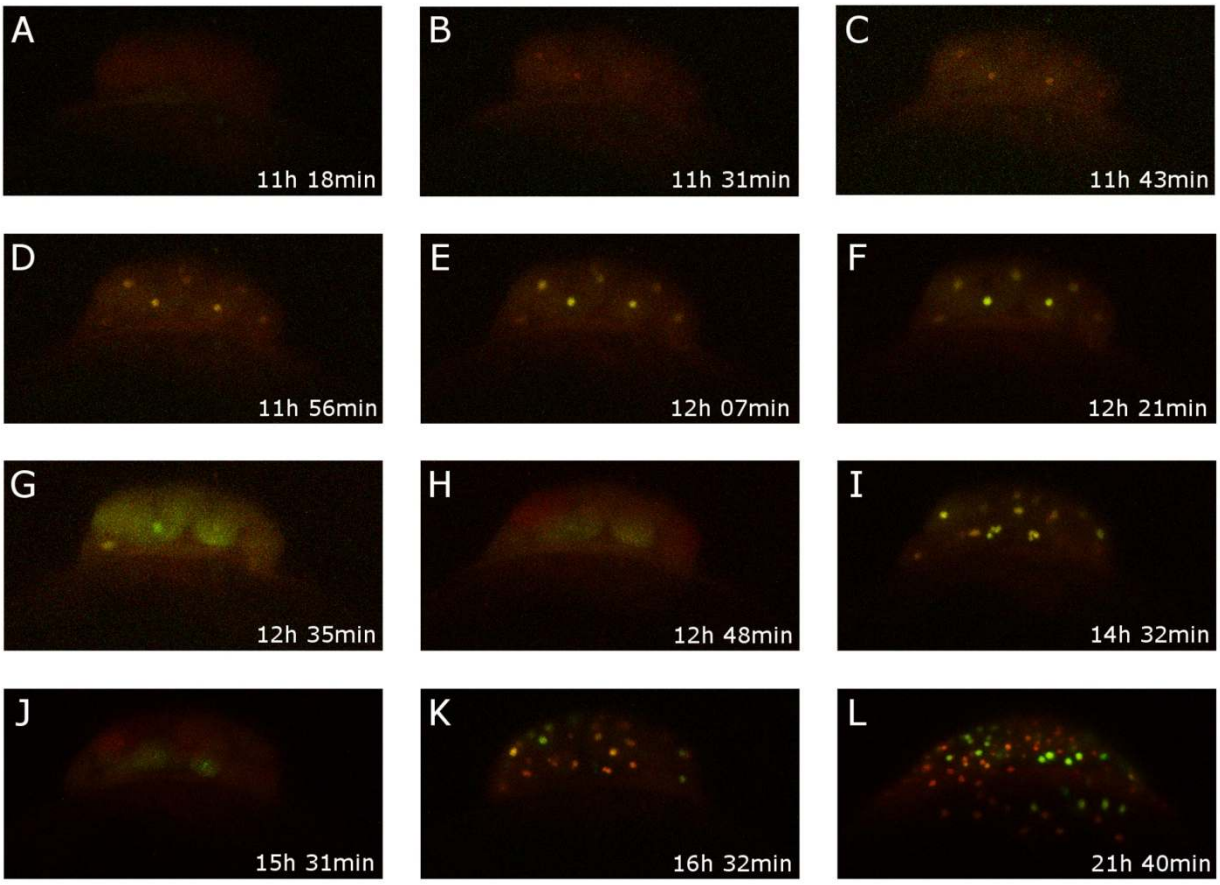

Figure 2.9: ***Cell cycle during early cleavage (Wourms stages 4-11).*** *Cell cycle progression in* Nothobranchius furzeri *was visualized by fluorescent ubiquitination-based cell cycle indicator (FUCCI). From* ***(A)*** *to* ***(H)*** *the last synchronus division (fourth) is shown, all nuclei are yellow and cells perfectly synchronized in cycling.* ***(I)*** *Represents the first division where asynchrony starts.* ***(J)*** *last synchronous dark stage.* ***(K-L)*** *later stages when cells are clearly asynchronous and cells in different phases can be recognized at the same time point.*

2.2.2 FUCCI transgenic fish.

Exogenous RNA has limited half-life and is stable just for 5-14 day once injected in a *N. furzeri* embryos. This stability greatly depends on the temperature of embryo incubation, which in turns influences developmental pace, and the time spent in the diapause I stage. In practical terms, injecting a dose of exogenous RNA that does not cause toxicity in an embryo always lead to a RNA stability that in a major part does not last longer than the dispersed phase, resulting in a weak signal and leading to a difficult or not correct microscopic analysis . So, tracking cell cycle progression and cell movements after the dispersed phase for exploring cell cycle dynamics during diapause I, somitogenesis, diapause II and organogenesis, required the generation of a transgenic line with stable expression of FUCCI reporters.

Two different *N. furzeri* transgenic lines were created, integrating FUCCI constructs in the fish genome through the TOL2 transgenesis system [87].

The first transgenic line carried the FUCCI red construct (Kusabira orange - Cdt1) under the control of the zebrafish ubiquitin promoter (Figure 2.10 B)

The second transgenic line carried the FUCCI green construct (Azami green - Geminin) under the control of the zebrafish ubiquitin promoter (Figure 2.10 A)

Zebrafish ubiquitin promoter is a 3483 base pair promoter that drives ubiquitous expression of the downstream gene in zebrafish at all developmental stages. Its activity was tested in our lab in the Nothobranchius species and the expression pattern resulted the same as for zebrafish (Figure 2.10 D).

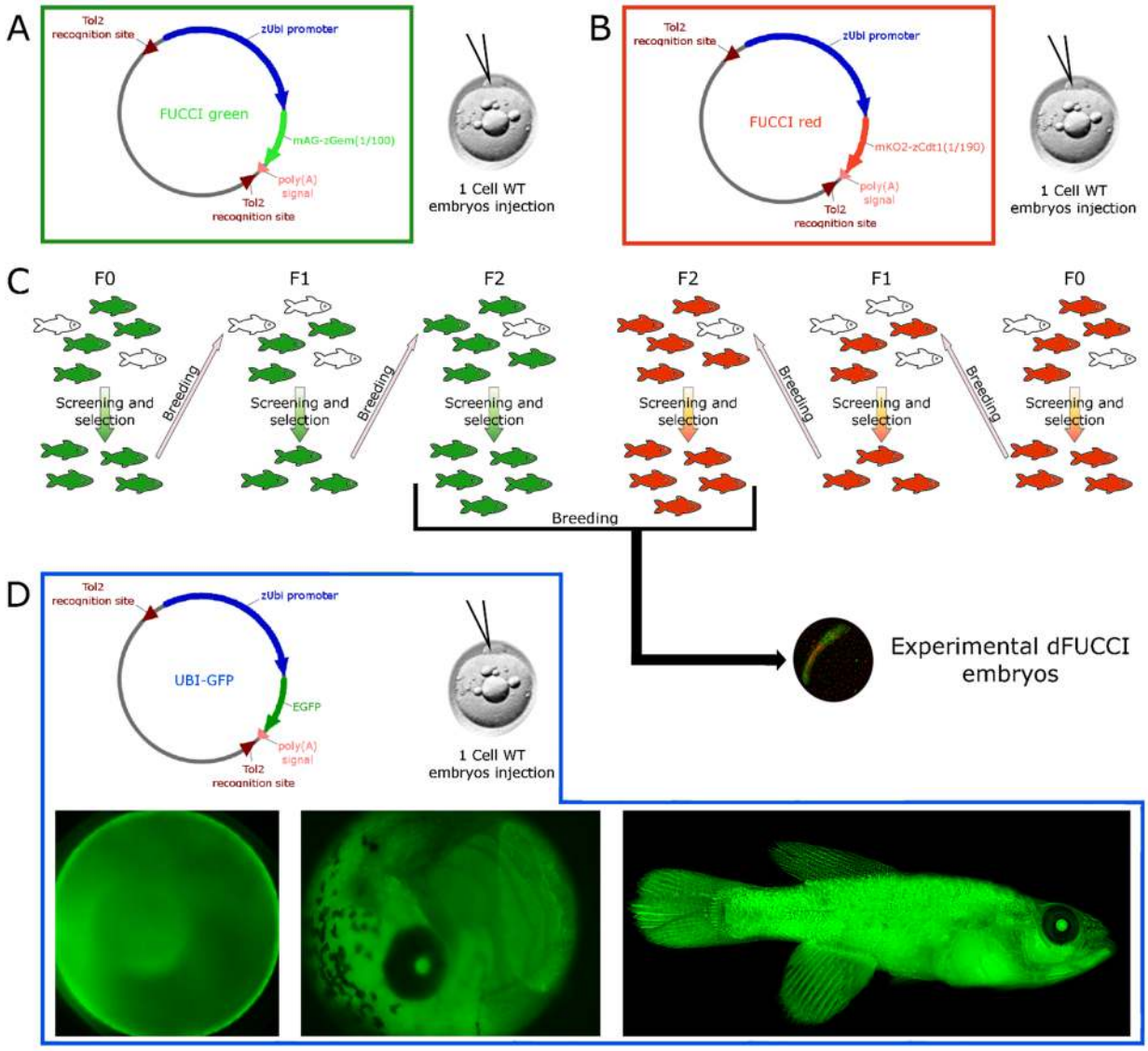

Figure 2.10: ***FUCCI transgenic lines generation****. A and B are schematic representations of FUCCI green and red constructs, respectively. FUCCI constructs were injected separately in different 1 cell stage fertilized embryos. Positive embryos were raised into adult fish, bred and screened for 3 generations (C). F2 FUCCI green fish were finally bred with F2 FUCCI red fish to generate*

double FUCCI embryos, that were used for the largest part of the experiments (C). D is a schematic representations of zUbiquitin-EGFP construct. EGFP expression in Nothobranchius embryos and adult fish is shown.

F0 transgenic fish were bred one to another for 2 generations (FUCCI red with FUCCI red and FUCCI green with FUCCI green, separately), in order to increase the number copies of FUCCI constructs in their genome, enhancing the signal. F2 transgenic fish were then used to characterize the FUCCI pattern (Figure 2.10 C).

2.2.3 FUCCI red F2 fish description.

FUCCI red was documented during the dispersed phase (Wourms stages 19-20), the somitogenesis (Wourms stage 31), in the newly hatched embryo (Wourms stage 44) and in adult fish.

FUCCI red fluorescence was nuclear. During the dispersed phase, two cell types express red fluorescence: large cells of the YSL and some other smaller cells of the epiblast (Figure 2.11). The nucleus of the YSL cells was 22-27 μm of diameter and these nuclei formed a regular array.The nuclear diameter of the epiblast cells was much smaller, in the order of 7-9 μm (Figure 2.11, arrows). The red fluorescence YSL appeared as a constant red signal that lasted for all the embryonic development, until hatch and over, while the red signal of the epiblast cells was transient, and lasted for a variable amount of hours before fading.

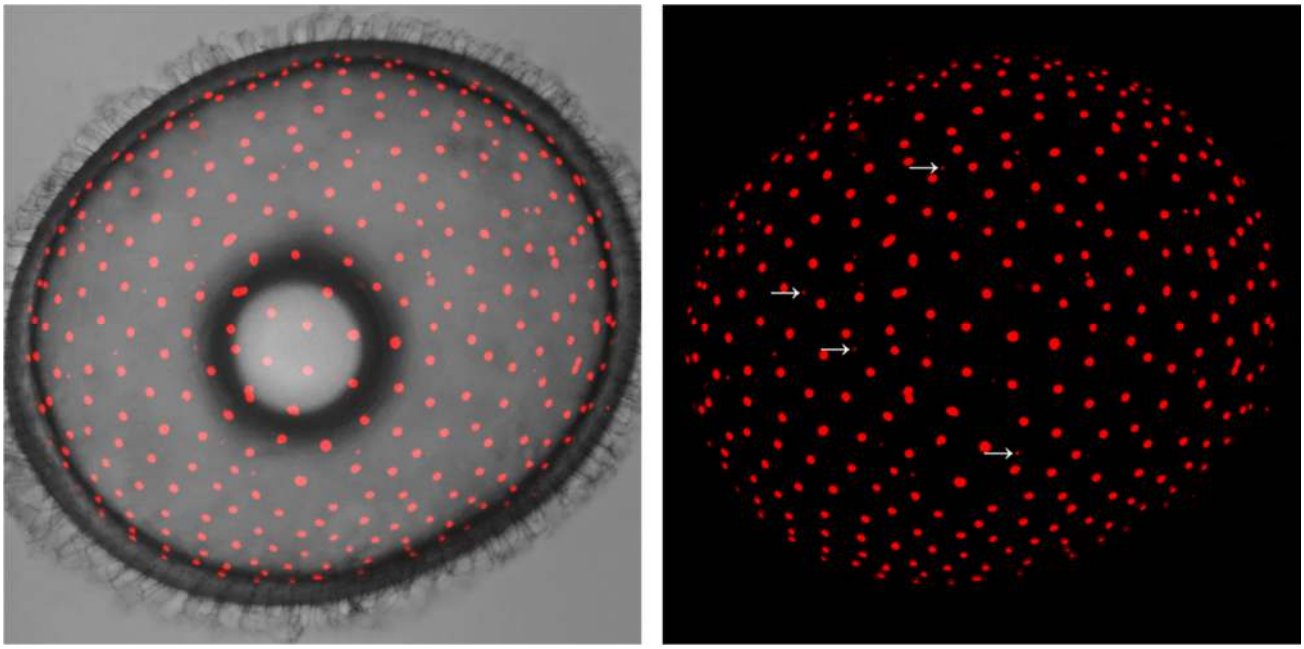

Figure 2.11: ***Dispersed phase FUCCI red embryo (Wourms stages 19-20).*** *Big red nuclei belong to the YSL (yolk syncytial layer) cells while small red nuclei (arrows) belong to epiblast cells. YSL nuclei red fluorescence never fade or cycle, so YSL cells are probably blocked in G0 phase.*

At the somitogenesis stage, the YSL pattern was unchanged and all the other red cells showed a clear patterned distribution that delinated specific regions of the embryo (Figure 2.12). In the older, more rostral, somites, the inner part of the somite showed a high concentration of red cells. In the more caudal part of the embryo, where somites were still forming, red cells were more spread and diffused. Once that the new somite pair was completely formed, they increased in numbers and retained the higher density in the inner part. These groups of somite red cells were reminiscent of the pattern previously described in zebrafish FUCCI transgenic line [116]. Just below the nothochord midline there was another narrow streak of red cells that extended from the tip of the head region to the tip of the tail. Also in the head, several regions contained red cells, but in these regions they were quite rare, spread and did not delineate specific areas.

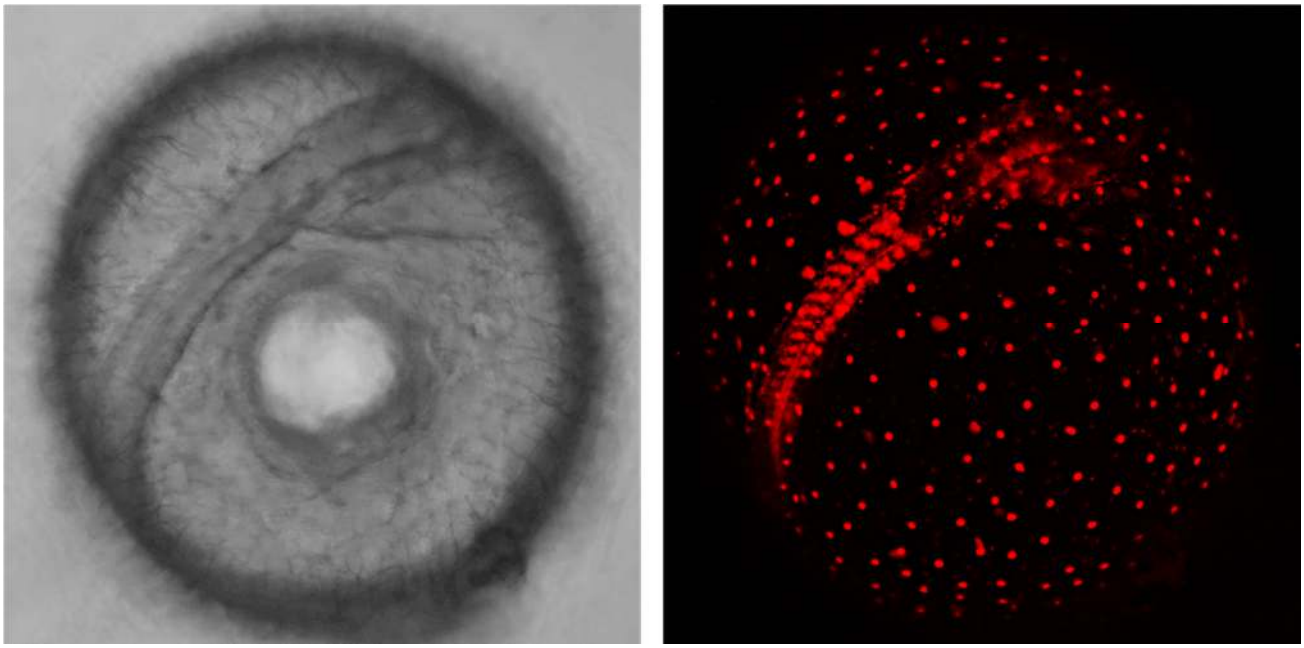

Figure 2.12: ***Mid somitogenesis FUCCI red embryo (Wourms stage 31).*** *Red aggregates of cells belonging to somites are clearly distinguishable. Red cells also populate some undefined regions of the head and a narrow streak that goes from the base of the head to the tip of the tail between the somite pairs.*

In the hatched fry, the concentration of red cells increased greatly (Figure 2.13). The lateral muscles of the trunk (d) and of the tail (e) presented a majority of red cells. In the head region, almost every part of the brain had some spread red cells or red cells aggregates (a). The lens (b) showed strong red fluorescence at this stage. This could be an artefact due to the high protein stability in this region that did not permit the correct degradation of the FUCCI reporter. What remained of the yolk, was still sorrounded by red large cells belonging to the YSL (f). As last, the pectoral fins (c) appeared to be greatly populated by red cells.

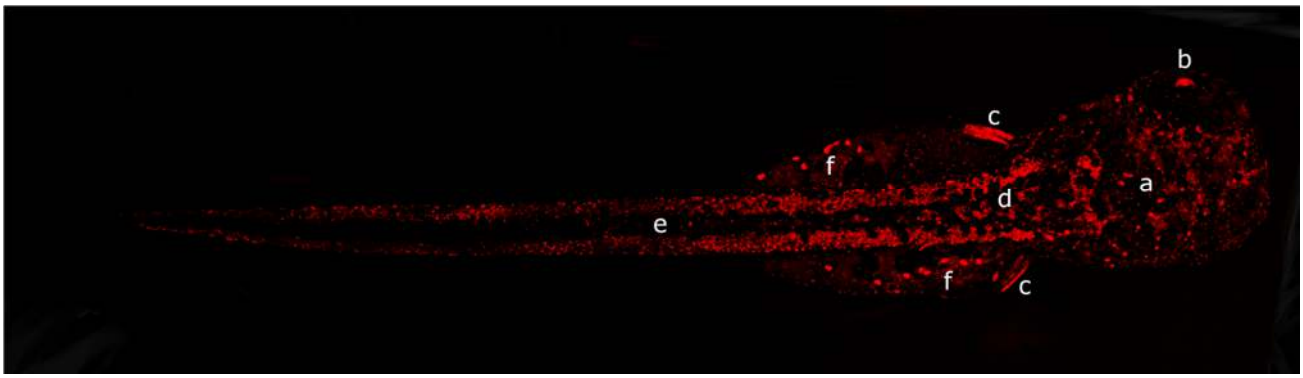

Figure 2.13: ***Hatched FUCCI red fry (Wourms stage 44).*** *Discrete regions in the embryo's body are populated by red cells at this stage: a) brain b) lens c)pectoral fins d-e) trunk dorsal and lateral muscles, f) YSL leftovers cells.*

The adult FUCCI red trasgenic fish appeared completely red under the fluorescence since many cells were in a G1 or G0 phase at this stage (Figure 2.14).

Males and females showed a pattern that could be defined identical, and also the signal intensity was comparable between different specimens.

Figure 2.14. ***Adult FUCCI red fish.*** *The majority of the cells present red at this stage, probably in G0 phase since many of them are fully differentiated. Fish look homogeneously red under the microscope and there are no striking differences between males and females specimens. The signal in the lens could be artificial, due to incorrect protein stability in this region..*

2.2.4 FUCCI green F2 fish description.

FUCCI green fish showed two different kind of fluorescence patterns, one of which was unexpected. Some specimens showed the a concentration of green fluorescent cells in the mitotically-active regions of the embryo while some other specimens showed a ubiquitous expression of green fluorescence at any developmental stage (Figure 2.15). This odd pattern was not further investigated and the embryos discared, but is probably the result of a partial integration of

the construct in the fish genome, or a mutation in the transgene sequence itself, that impairs the functionality of the geminin targeting sequence.

.

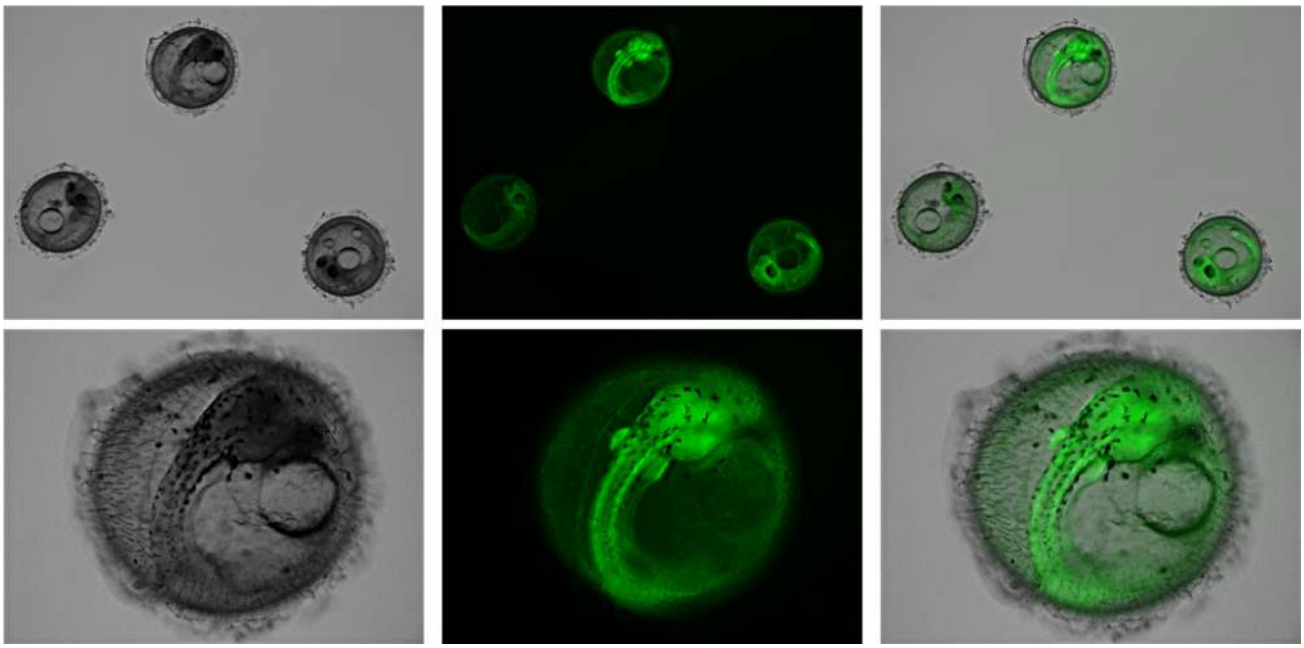

Figure 2.15. ***Unexpected FUCCI green embryos pattern.*** *Examples of embryos showing the unexpected FUCCI green pattern. In these embryos the fluorescence is ubiquitous at any developmental stage.*

The "correct" pattern of the FUCCI green F2 embryos can be described as follows:

During the dispersed phase, a variable proportion of green epiblast cells were detected (Figure 2.16). The nuclei of these cells were between 7 and 25 μm in diameter, with a higher proportion of the smaller cells. During this developmental stage, both in the case that many (Figure 2.16 B) or few (Figure 2.16 A) green cells were present, they seemed to be arranged randomly on the embryo surface. The phase of the cell cycle of these cells was for sure one among S/G2/M, but unfortunately the FUCCI system is not able to give information about exactly which one of these.

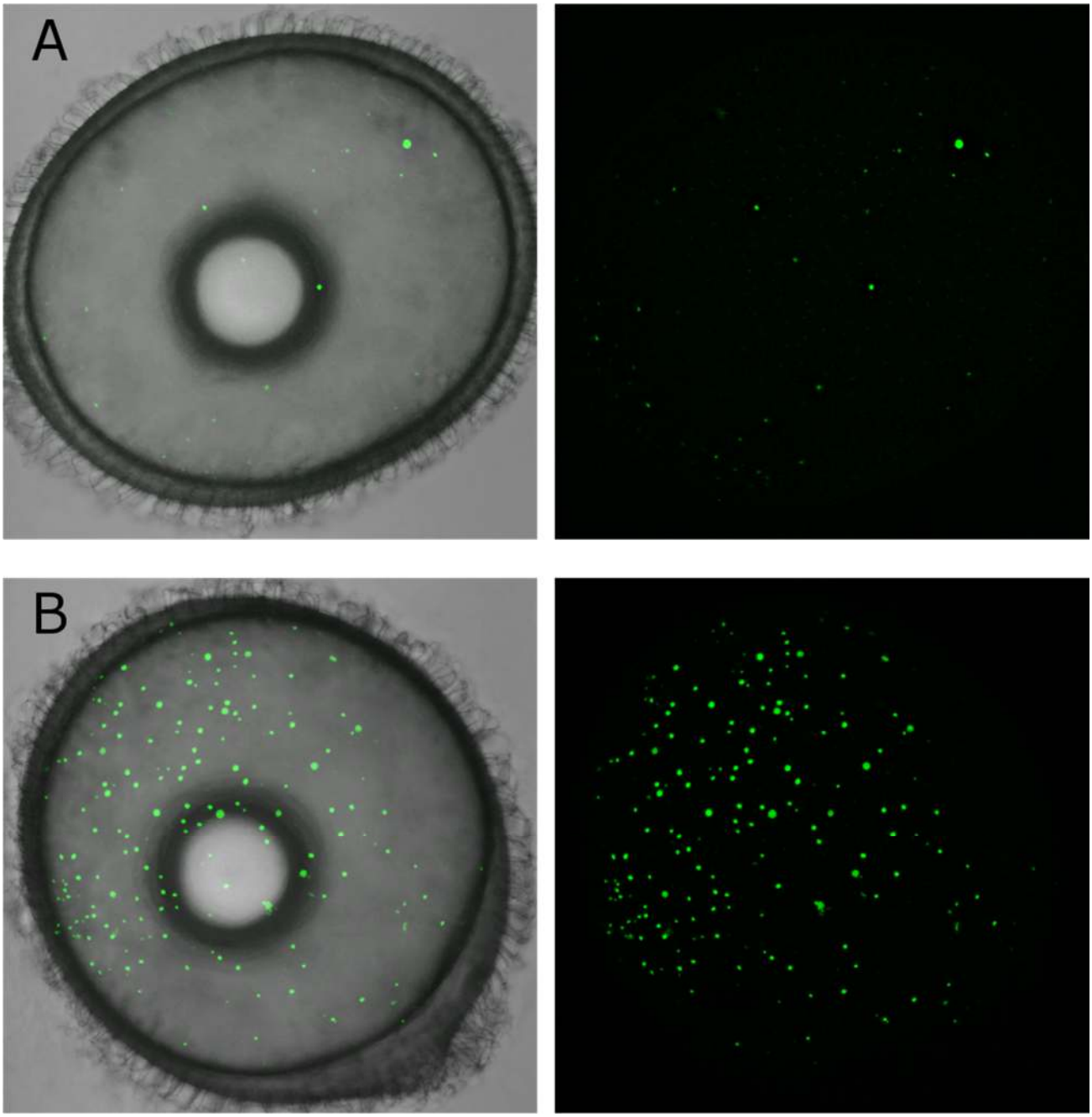

Figure 2.16: ***Dispersed phase FUCCI green embryos (Wourms stages 19-20).*** *At the dispersed phase FUCCI green embryos revealed two possible conditions of cells proliferation. A) represent the condition where only few green cells are present while B) the one where many of them can be detected. There is a simultaneous presence of big and small green nuclei at this stage, even if small nuclei are predominant.*

During active somitogenesis (in developing embryos and not in diapausing ones) proliferating green cells were spotted in every part of the developing embryo. The signal was moderately strong both in the trunk, in the tail and in the head primordia (figure 2.17). The maximum intensity of the signal, that corresponded to the maximum density of proliferating cells, was limited to a narrow region along the midline of the embryo, that went from the end of the head to the end of the tail, and that was positioned between the yolk surface and the ventral part of the developing embryo. Among the

yolk surfaces, a large number of green cells, that reminded the dispersed phase stage, were still visible, even if was not clear if these cells were actually proliferating or blocked in the G2 phase and migrating on the yolk surface.

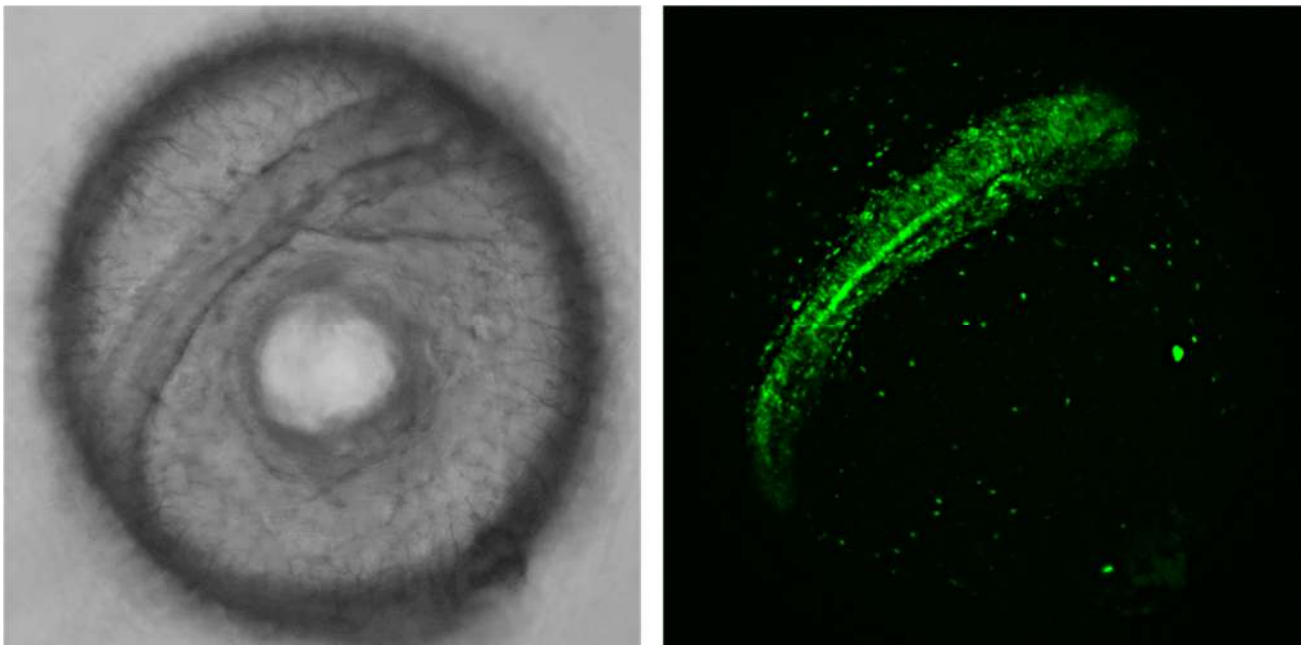

Figure 2.17: ***Mid somitogenesis FUCCI green embryo (Wourms stage 31).*** *At this stage the whole growing axis is populated by green cells. The higher density of green cells lies in a narrow streak in the middle of the forming axis, starting from the base of the head and ending in the middle part of the embryonic axis.*

In the hatched fry, the proliferative regions in the embryo were more defined (Figure 2.18). In the torso and the tail the proliferating green cells that could be detected were spread and homogeneously distributed (f). Other spread green cells, even if with a slightly increased density, could be detected in the caudal and pectoral fins (d) and at the base of the head, in the hindbrain (e). The forebrain (a) showed a totally different pattern. The proliferating cells were not widespread but formed dense aggregates on the borders of the optic tectum that corresponded to the neuronal stem cell niches [65], while no proliferating cells could be seen in the inner part, that appeared completely dark. The olfactory epithelium (b) at this stage seemed to be one of the major proliferating regions, composed by dense streaks of proliferating cells. As last, the pupils (c) shone of green fluorescence at this stage, but, as discussed for the FUCCI red trasgenic line, this could be an artefact due to the high protein stability in the lens that did not permit the correct degradation of the FUCCI construct.

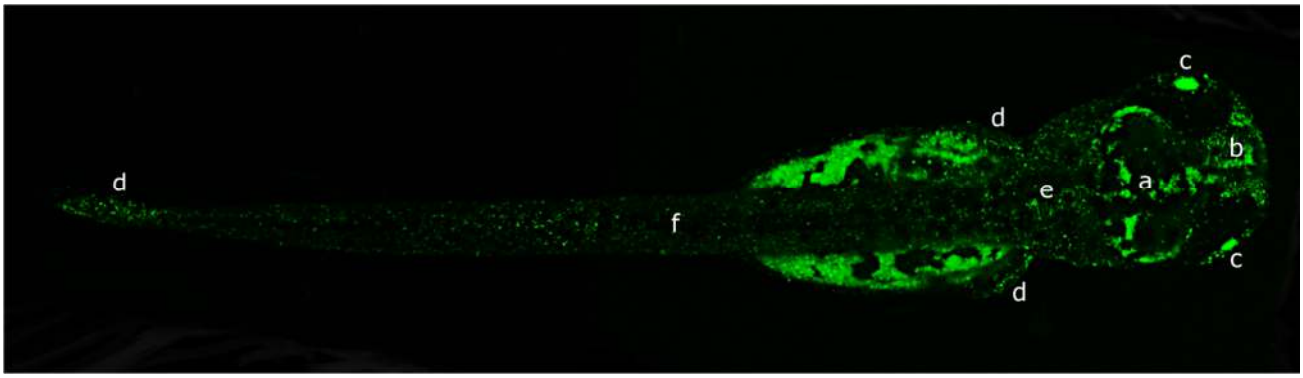

*Figure 2.18**: Hatched FUCCI green fry (Wourms stage 44).** Discrete regions are populated by green cells at this stage: a) forebrain b) olfactory nerves c) lens d) fins e) hindbrain f) torso and tail muscles.*

In adult FUCCI green specimens, no green cells could be detected under a stereomicroscope and the only green signal present at this stage was confined to the region of the eye (Figure 2.19).

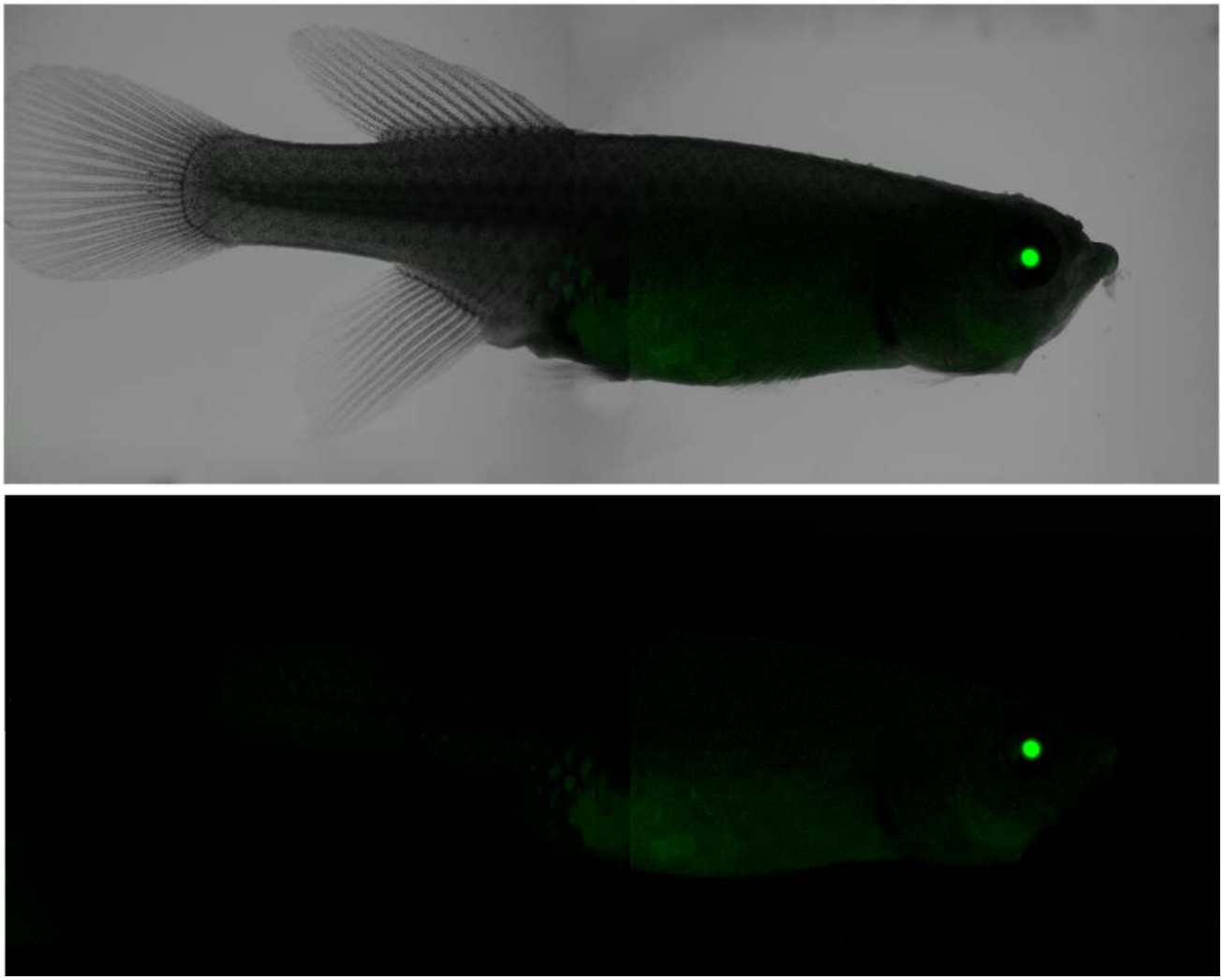

*Figure 2.19**. Adult FUCCI green fish.** The majority of the cells present colorless at this stage because prolifertion is greatly reduced at this stage, compared to embryonic stages. Green intense signal is retained in the lens but it could be an artefact due to increased protein stability in this region.*

This negative pattern was expected, since only few cells proliferate in the adult fish and only the skin surface is visible. For this reason, is understandable that no green signal was detectable with a stereomicroscope.

Concerning the signal retained in the eye, as noticed for the previous stage of hatched fry, it was probably due to a different stability of the proteins in the lens, caused by the peculiar chaperones present there that protects crystallins from degradation. These chaperones probably lead to an uncommon high stability of FUCCI in this region, and so there is the chance that azami green-geminin protein formed in the lens primordia could not be degraded as soon as the cells exited from S/G2/M phases, accumulating over time.

2.2.5 Fin cut FUCCI green adult validation.

To check if the rest of the body, that appeared not green, was still able to express the green signal in response of proliferation events, a fin cut experiment was performed (Figure 2.20).

One male and one female belonging to the F2 generation of FUCCI green were isolated and half of their caudal fin was cutted away. Another FUCCI green F2 female was left uncutted, as control.

After 24 hours and for the next 9 days the transgenic fish showed a huge amount of green cells near to the cutted region of the fin, as long as it was regrowing, indicating proliferation. So, FUCCI green marker was absolutely able to mark proliferating cells also in the adult.

In details the proliferation event showed a burst in all the region before the cutted site just after 48 hours from the cut. 72 hours after the cut was performed, the green cells clustered in a specific region just next to the cutted site, defining short and dense proliferation areas that spread single cells towards the distal part of the fin. These green proliferating regions extended as the fin grew, reducing gradually their density until the fin was totally regenerated.

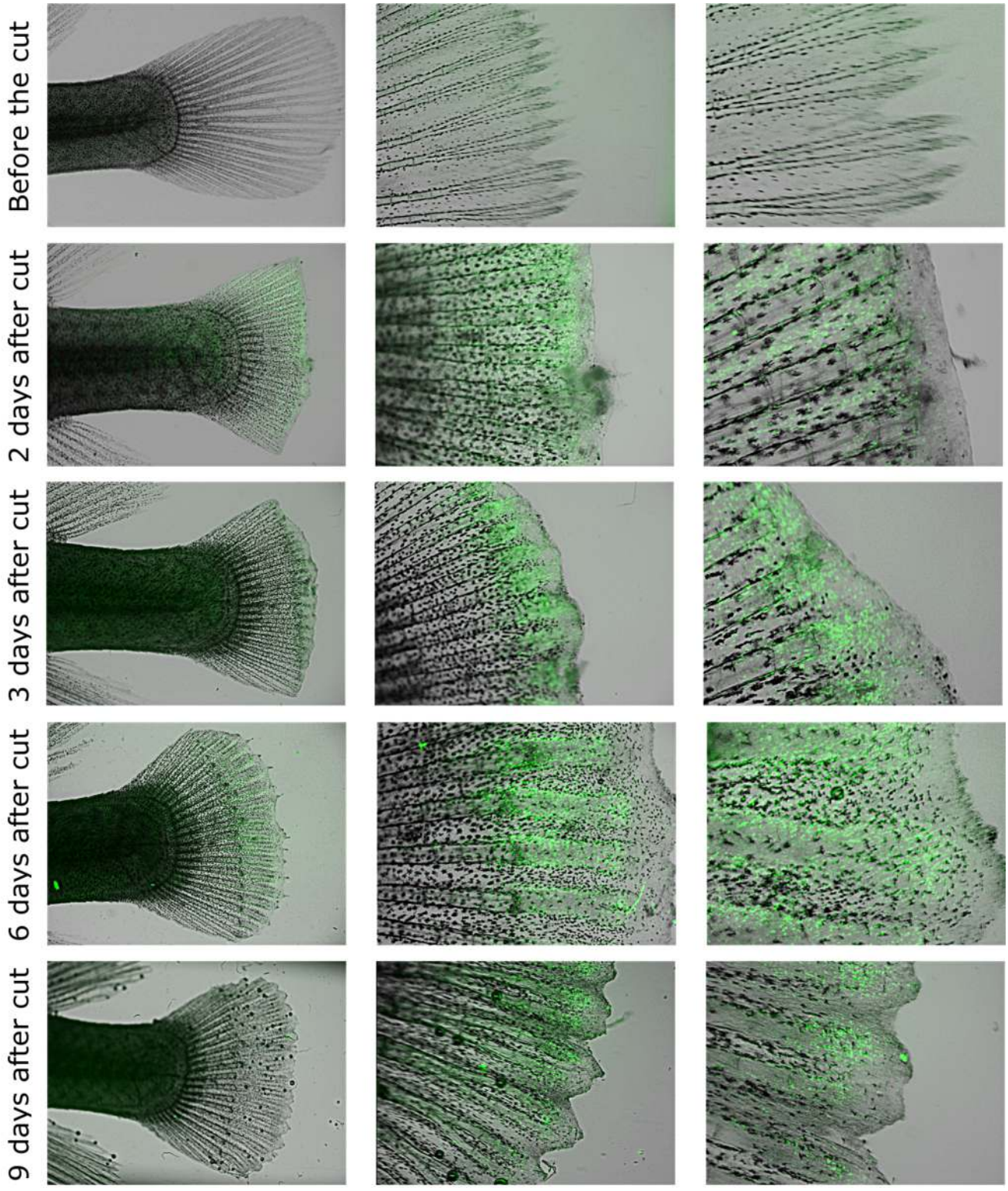

Figure 2.20. ***FUCCI green adult speciemen caudal fin cut.*** *In a normal condition there are no green cells in the caudal fin of an adult FUCCI green fish. If part of the fin is removed performing a cut, after 2 days many green cells gathers, with a density that slowly drops toward the animal body. In the following days green cells specifically localize in proximity of the injury, reducing greatly their presence in the distal part. Over time the number of green cells drops, until the fin is totally regenerated.*

2.3 F3 double FUCCI fish time lapse.

Once verified the correct pattern and functioning of both the FUCCI red and green transgenic lines, the F2 fish were crossed (FUCCI red with FUCCI green), generating double FUCCI green/red embryos, that were analyzed through confocal imaging.

Three to five embryos that showed at the stage of epiboly both the green and the red signal (indicating the inheritance of both the FUCCI red and green transgene), were acquired for periods spanning from hours to days at stages from the end of epiboly to almost the end of somitogenesis, i.e. past the stage when embryos would enter into diapause II.

The stacks of images of each time point were then processed with Imaris and analyzed through particle analysis or surface analysis, depending on the specific cases.

All experiments were performed through time lapse confocal microscopy, acquiring the same embryo or different embryos multiple times, for many hours, during different phases of their development. Unfortunately each of these experiments required a huge amount of time, since every single time lapse acquisition lasted from 8 hours to 4 days, and for this reason the amount of repetitions for each stage is small (Table 2.1). In addition some stages, like the release from diapause I, are very difficult to image, since they do not happen at a fixed developmental time, and last a relatively short amount of time (10 hours or less). I used the time lapse strategy because my main purpose was to give a complete overview about N. Furzeri development even if the compromise was to have a small number of repetitions.

The transgenes expression was activated after the MBT stage, and detection of a fluorescence signal with a confocal microscope was not possible before the stage of 70% epiboly, so any image reported here and relative to an earlier stage was obtained by synthetic RNA injection.

Embryonic Stage		Amount of embryos imaged
Dispersed Phase (WS 19-20)	Early (with few green cells)	4
	Late (with many green cells)	6
Dispersed Phase transition (from few to many green cells)		1
Reaggregation Phase (WS 21-25)		4
Extension Phase (WS 26)		4
Somitogenesis (without diapause II arrest) (WS 29-33)		6
Diapause II arrest and release		3

Table 2.1: Embryos acquisitions for each developmental stage. Table shows the number of embryos acquired at each developmental stage. From stage to stage embryos acquired could be the same, acquired progressively during its development, or different ones. WS means wourms stage.

2.3.1 Epiboly

For the first day (at 26°C) the embryos divided synchronously for the first 5 divisions and then in an asynchronous way. Proliferating cells were confined to the animal pole, the region of the embryos where the first cell was located.

At the beginning of the second day, some cells started to migrate over the yolk surface. The first cells that migrated were the cells belonging to the YSL, that anticipated the migration of the other cells by at least 6 hours. YSL cells were blocked in G1-G0 phase (red color) for all the span of subsequent development, they never divided and their nuclei appeared to be much larger as compared to the other epiblast cells (21-27 μm vs. 8-12 μm).

The start of the epiboly (Wourms stage 15) overlapped for some hours (around 13 hours) with the end of the proliferating process at the animal pole. At 40% epiboly (Wourms stages 16-17), the division process at the animal pole was completed, and only some big spread green cells, probably blocked in G2, red small cells (much smaller and less intense than the YSL ones), and big YSL red cells could be detected (Figure 2.21).

The green and the small red cells belonging to the epiblast migrated in an apparently random direction, with shorter or longer paths above the YSL cells layer. This data confirms what already shown by Lesseps et al., that studied the cell movements at this stage and after a pathways track analysis defined the movements random [120].The average speed of the epiblast cells was higher than the one of the YSL cells.

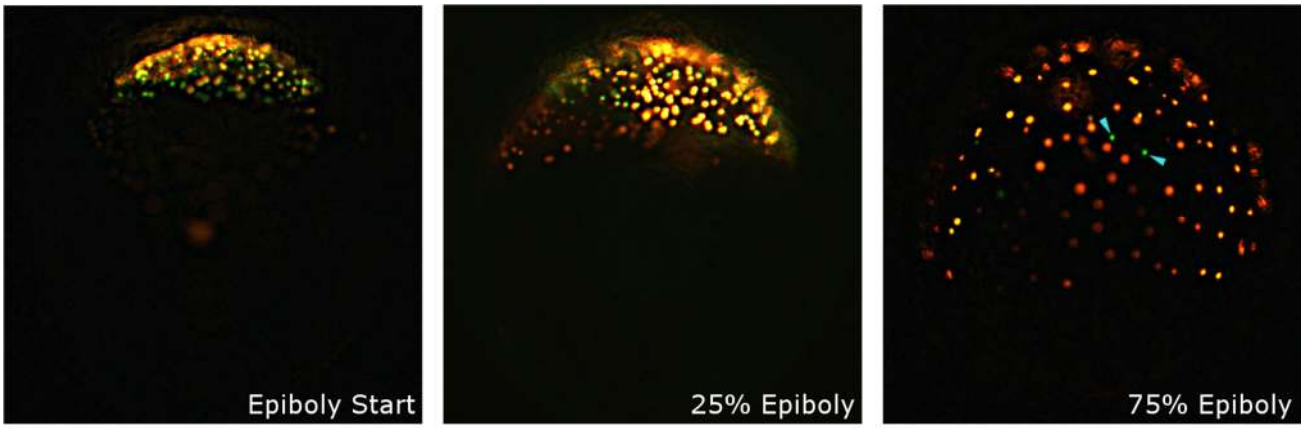

Figure 2.21: Cell cycle during epiboly (Wourms stage 14-19) and dispersed phase. *Cell cycle progression in Nothobranchius furzeri was visualized by fluorescent ubiquitination-based cell cycle indicator (FUCCI). Green cells in the S-/G2 phase, red cells are G1-phase cells. Cells divide for the first days of development at the animal pole and then just migrate in G1 onto the embryo surface during late epiboly and the dispersed cell phase. As long as epiboly proceeds green cells number progressively decrease and only few are left at the stage of 75% epiboly (arrows).*

Concerning the YSL cells, their movements over the yolk surface were slow and ordered, they moved towards a defined position (opposite to the animal pole) in a straight (curved because the surface of the yolk is a sphere) way, and they continued to move until the completion of epiboly (Wourms stages 18-19) (Movie S4), when they reached their final position in the syncitium that will be maintained during ensuing development. In the final position, the nuclei of the YSL cells distributed a very defined and regular architecture, covering entirely the yolk surface at an average distance of about 80 μm from each other. Their number was also quite stable and was estimated to be around 500 (Figure 2.22).

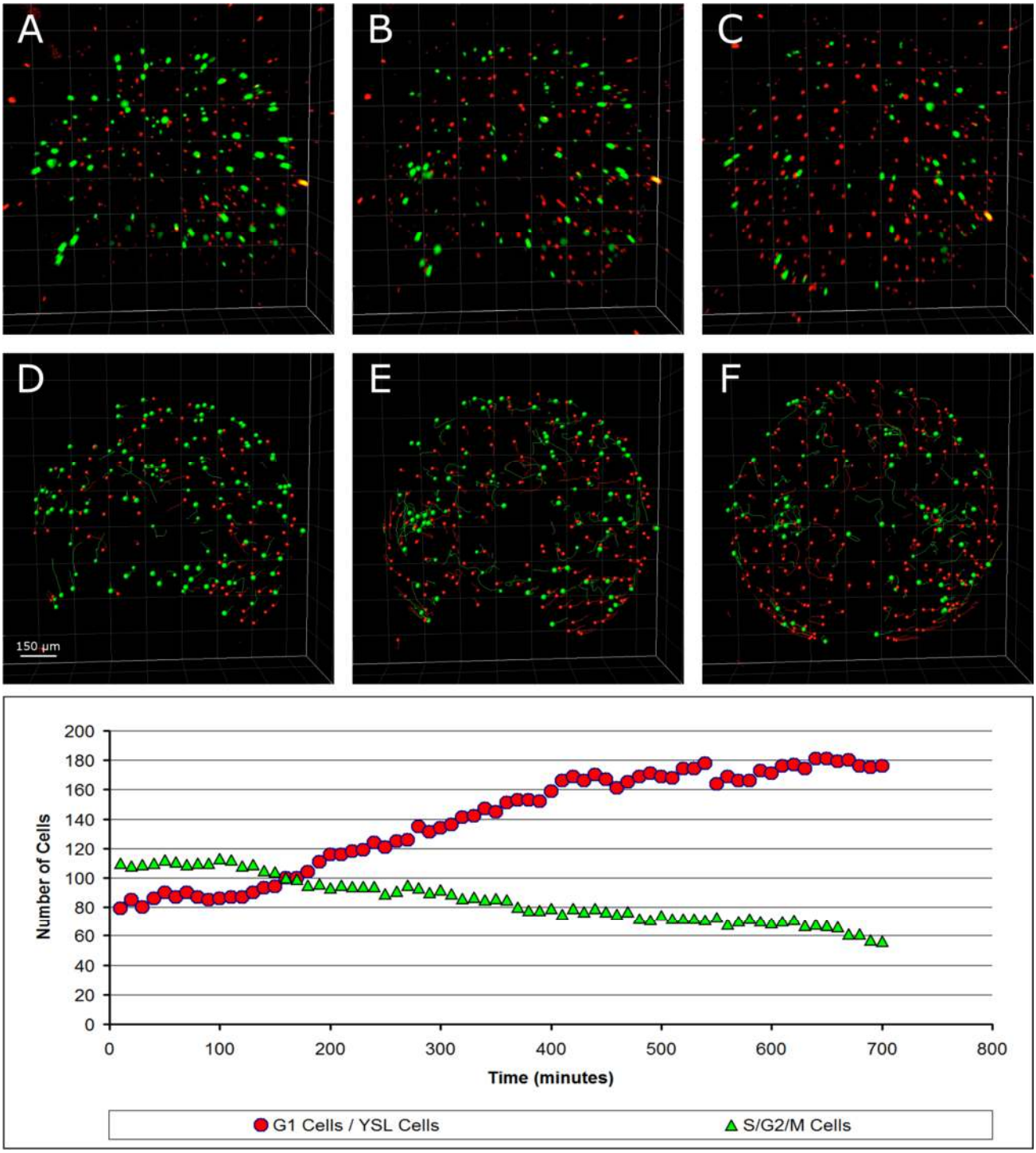

Figure 2.22. ***Cell's behaviour during epiboly (Wourms stages 18-19).*** *When epiboly occurs both green and red cells are present in double FUCCI embryos (A). As long as epiboly proceed (B, C) the number of green cells gradually and slowly decreases over time while the number of red cells increases until the reaching of a plateau (graph minutes 400-700). The cells in the field of view were easily tracked and counted transforming the dots in particles with imaris (D,E,F). The images and graph refers to the acquired portion of the embryos, equivalent to the upper part.*

Once reached their final position, the YSL nuclei did not move, divide or migrate anymore. Therefore, the YSL cells could be used as a reference to correct for yolk movements, that often

occurred in the embryos during the development, and allowed to precisely track the movements of all the other cells and structures (Figure 2.23).

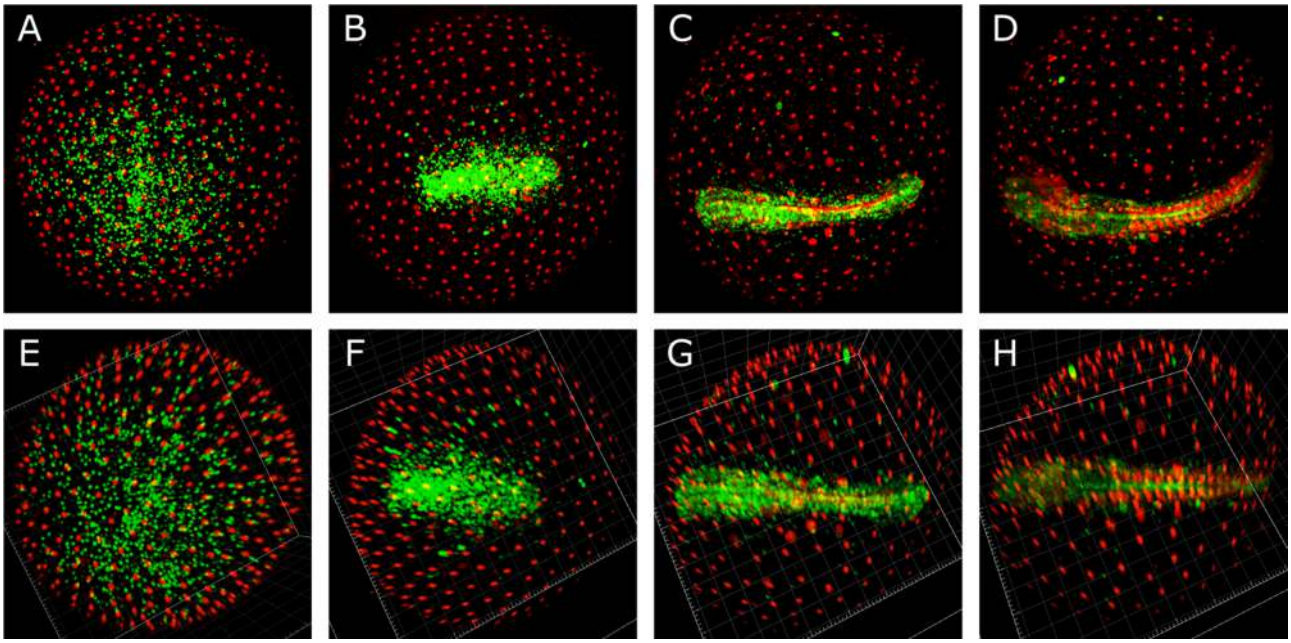

Figure 2.23. ***YSL nuclei as reference point for drift correction.*** *Embryos continuously move through all the development (A,B,C,D) but YSL nuclei once in their final position (that occurs at the end of epiboy) never move anymore. These nuclei can therefore be used as reference points and drifts and rotations that occurs during developmenta can be corrected using ther position (E,G,F,H). Correctiong the drifts allows a more precise and reiable cell tracking and data analysis.*

2.3.2 Early dispersed phase (Wourms stages 19-20) and diapause I.

When epiboly ended and the dispersed phase began, the number of detectable green cells and red cells not in the YSL was reduced from more than 200 to less than 70 for each kind, in a ratio of almost 1:1 (Figure 2.24 C). At this stage it was possible to separately count YSL red cells and epiblast red cells because their nuclei diameter greatly varied (~22 µm vs ~9 µm respectively) and could be easily and precisely distinguished by Imaris (Figure 2.24 B).The drop in number of epiblast cells was progressive, began with the start of the epiboly and slowly proceeded during all this phase (Figure 2.22). Is important to remark that this description refers to the cells that were in a S/G2/M or G1/G0 phases, and not to the total number of cells present in the embryos. FUCCI is indeed unable to mark, for example cells at the interface between the M and the G1or S phase that cannot be therefore counted.

So, the correct statement for epiboly description is that in this developmental stage the number of detectable cells (S/G2/M/G1/G0) significantly drops, but the total number of epiblast cells probably remains constant, since migrating cells are clearly visible in transmitted light throughout the dispersed phase (Figure 2.5 B and Movie S1).

In addition, is necessary to remark that all the embryos observed (N > 30), despite inevitable variations of ambient paramenters, step in this condition after the end of epiboly, where only few epiblast green or red cells were detectable, although this condition may last just a few days .

This condition, if extends its duration over time, is probably what in literature is defined as diapause I stage (DI). It starts with the beginning of the dispersed phase, and has these characteristic features:

- regularly spaced YSL big cells nuclei (19-25 μm nucleus diameter), that do not move, migrate or divide.
- presence of few (less than 80) red and green small (7-13 μm nucleus diameter) epiblast cells, cycling at a very slow rate or not cycling at all. These cells move randomly above the YSL surface during the whole diapause I process.
- this stage presents, even if in some cases just for few hours, in all the embryos, it is reached by a continuous decrease of red and green epiblast cells during epiboly, and starts with the start of the dispersed phase.
- this stage can last for variable amount of times, depending on environmental conditions.

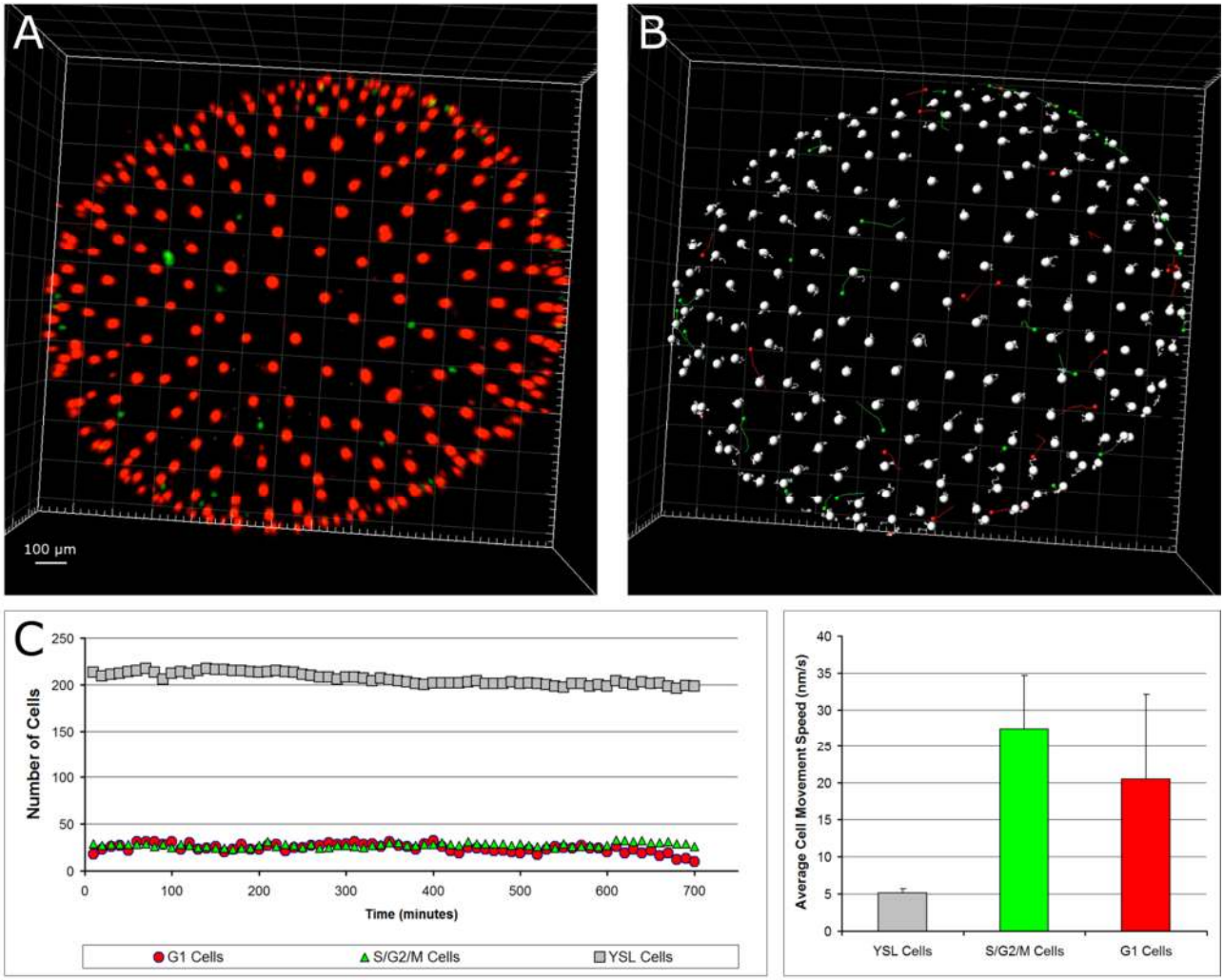

Figure 2.24. ***Cells behaviour during early dispersed phase (Worms stages 19-20).*** *The first part of the dispersed phase is charachterized by the presence of few epiblast green or red cell (A). YSL cells were converted in white big dots while epiblast green and red cells in green and red small dots (B) and the all the cells were tracked over time. The number of each type of cell resulted constant for more than 10 hours (C graph) and epiblast cells continuosly moved during the whole time (C diagram). The images and graph refers to the acquired portion of the embryos, equivalent to the upper part.*

2.3.3 Release from diapause I.

There are at present no direct data concerning which could be the activation signal that release an embryo from diapause I, even if probably temperature and oxygen levels are involved in the process. The experience collected during my time lapse experiments shows that the time of the permanence in this condition is variable (in the order of days) and there are hints that the release happens in a very short amount of time (less than 1 day). During my observations, I was indeed able to image only embryos with either few green cells or crowded with green cells. I can therefore assume that the transition step, from few to many green cells is a very fast step, difficult or impossible to acquire just performing random samples observation.

The following description, concerning the dynamics how diapause I ends and embryos development reactivates refers to only one embryo acquisition (Movie S5), because, as said before, this transition is extremely challenging to observe due to its speed and unpredictability.

The release from diapause I was characterized by a rapid appearance of a large number of green fluoresecent cells, indicating that most of the red and “invisible” dark epiblast cells, entered into S/G2/M divisions, without becoming red(Figure 2.25). These reactivated cells divided together and synchronously generating pulses of green/dark cells. The amount of cells involved in this process increased pulse after pulse, indicating that the cells that proliferated and divided (green) generated cells that in their turn proliferated. These pulses occurred every 10 hours at 26°C and the cells involved in these divisions didn't go or barely went through a G1 red phase. Most of them just step from a green to a dark phase, a pattern reminiscent of that seen during segmentation, only having S/G2/M green phases.

In addition, the proliferating cells moved in an apparently random fashion during all the division processes, in a way that was totally comparable to the movements of epiblast cells that were documented during diapause I by brightfield microscopy (Movie S1) or during early dispersed phase by confocal microscopy.

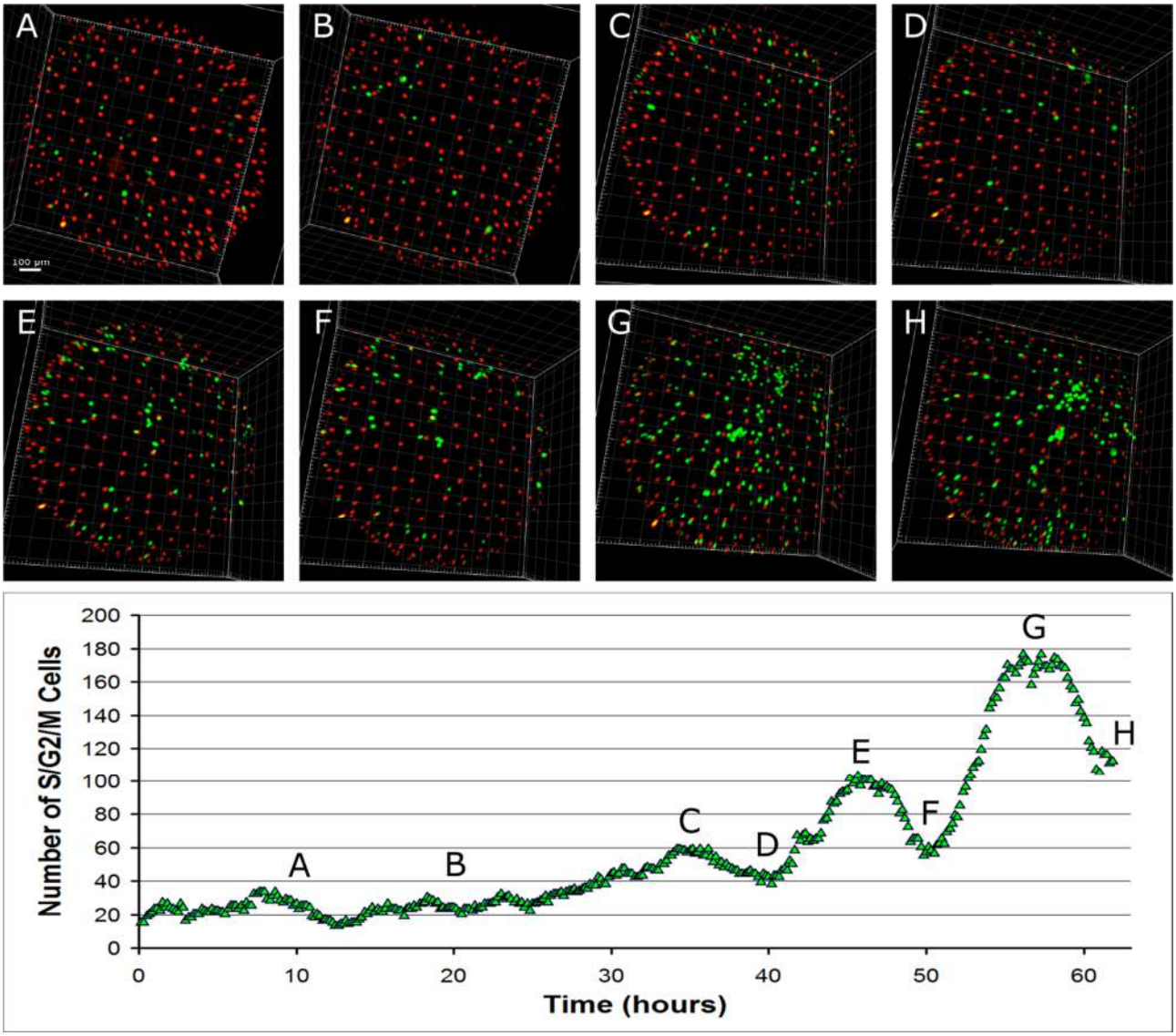

Figure 2.25. ***Transition from early to late dispersed phase.*** *From an initial codition where only few epiblast cells could be detected as green or red (A) multiple reactivation and division events bring green cell number to increase up to a final condition where their number is 4-6 times more (H). Division events happens sinchronously and are characterized by multiple peaks of proliferation in which cells grow (C,E,G) and divide (D,F,H) alltogether. The images and graph refers to the acquired portion of the embryos, equivalent to the upper part.*

2.3.4 Late dispersed phase (Wourms stage 20).

In this way the number of the epiblast cells increased dramatically in few hours and the embryo was able to prepare for axiogenesis in less than 2 days.

The increase in the amount of green cells led to the second part of the dispersed phase (Figure 2.26), that was characterized by an almost equal number of YSL, epiblast green and epiblast red cells, that was around 500 each in the whole embryo (Figure 2.26 C). Similarly to the first part of the dispersed phase, also in this second part, the epiblast cells appeared to not divide or cycle or change their average number so were probably blocked in G1 or G2 phases but they migrated randomly

over the YSL surface at a speed that was comparable to the speed that they reached during the early dispersed phase and diapause II, amounting to 61,2 ± 26,3 nm/s. The second part of dispersed phase, once the pulses of proliferation were completed, was actually similar to the diapause I stage, with the only difference that the red and green detectable cells were 4 to 5 times higher in number. The amount of time embryos spent in this second part of dispersed phase could not be determined in my experiments and is not clear if it was fixed or variable.

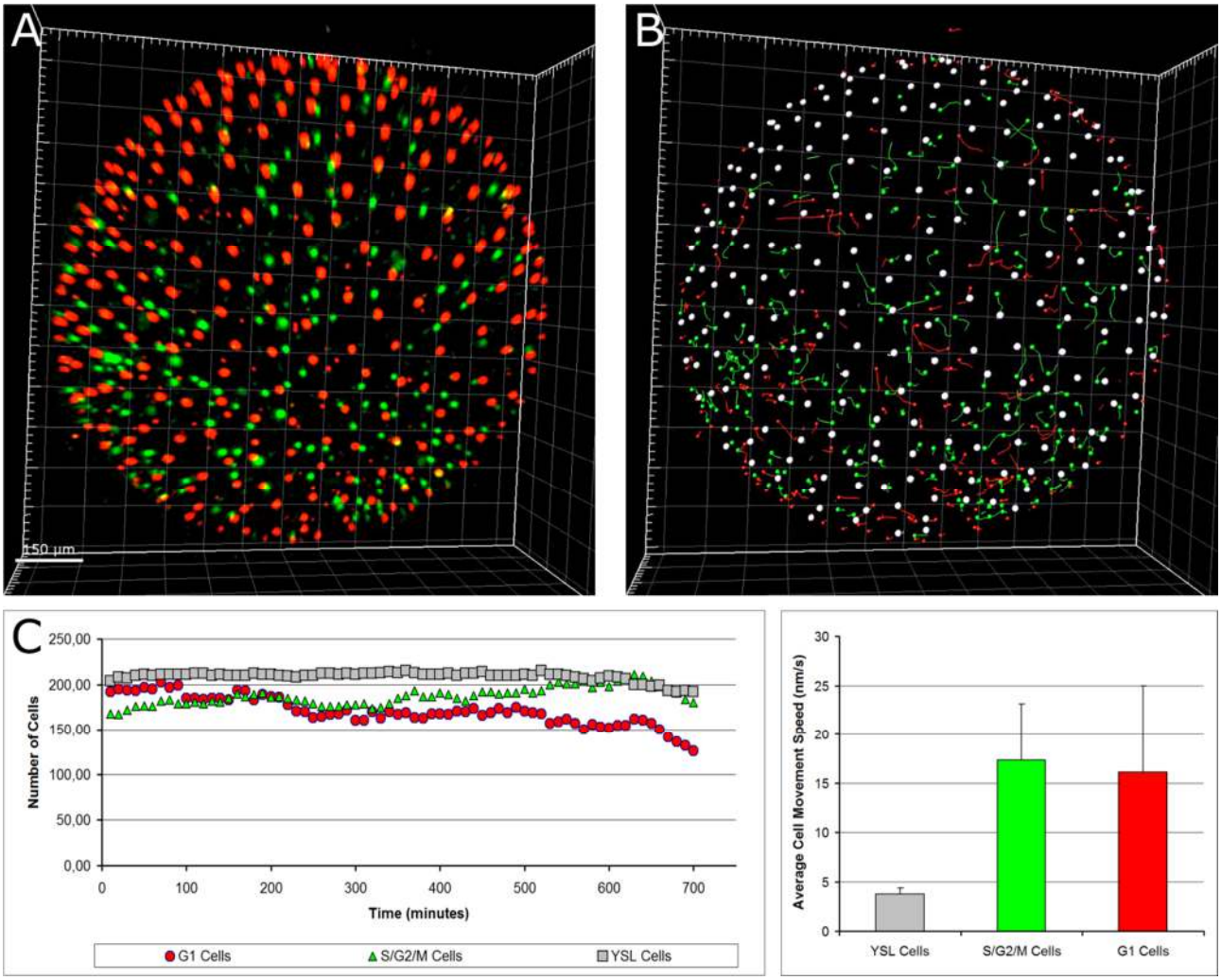

Figure 2.26. ***Cells behaviour during late dispersed phase (Wourms stage 20).*** *The second part of the dispersed phase is charachterized by the presence of many epiblast green or red cell (A), at least 4 times more compared to the initial early part. YSL cells were converted in white big dots while epiblast green and red cells in green and red small dots (B) and the all the cells were tracked over time. The number of each type of cell resulted rather constant for more than 10 hours (C graph) and epiblast cells continuosly moved during the whole time (C diagram). The images and graph refers to the acquired portion of the embryos, equivalent to the upper part.*

2.3.5 Reaggregation (Wourms stages 21-26).

When a certain number (not possible to define with my experimental datas, it could futhermore vary between different specimen) of green cells was reached, the majority of those cells migrated towards a undefined point of the embryo, forming a circular aggregate that was initially sparse and whose radius became progressively smaller (Figure 2.27 and Movie S6). I couldn't determine the point of the embryo toward wich cells migrated, but experiments performed by Wourms in the 1972 [17] suggest that it is located in the lower emisphere of the egg, opposed to the animal pole. The movements of the cells in this region were greatly reduced in speed, compared to the previous phases, and the circular formation step from an initial diameter of about 900 μm to a final one of about 470 um (radius estimation was done on a single embryo using a cell density threshold with Imaris). The whole reaggregation process required a short fraction of total developmental time and in about 15 hours the final short radius green cells circular formation was completely defined.

From this circular aggregate of proliferating cells the whole embryo evolved.

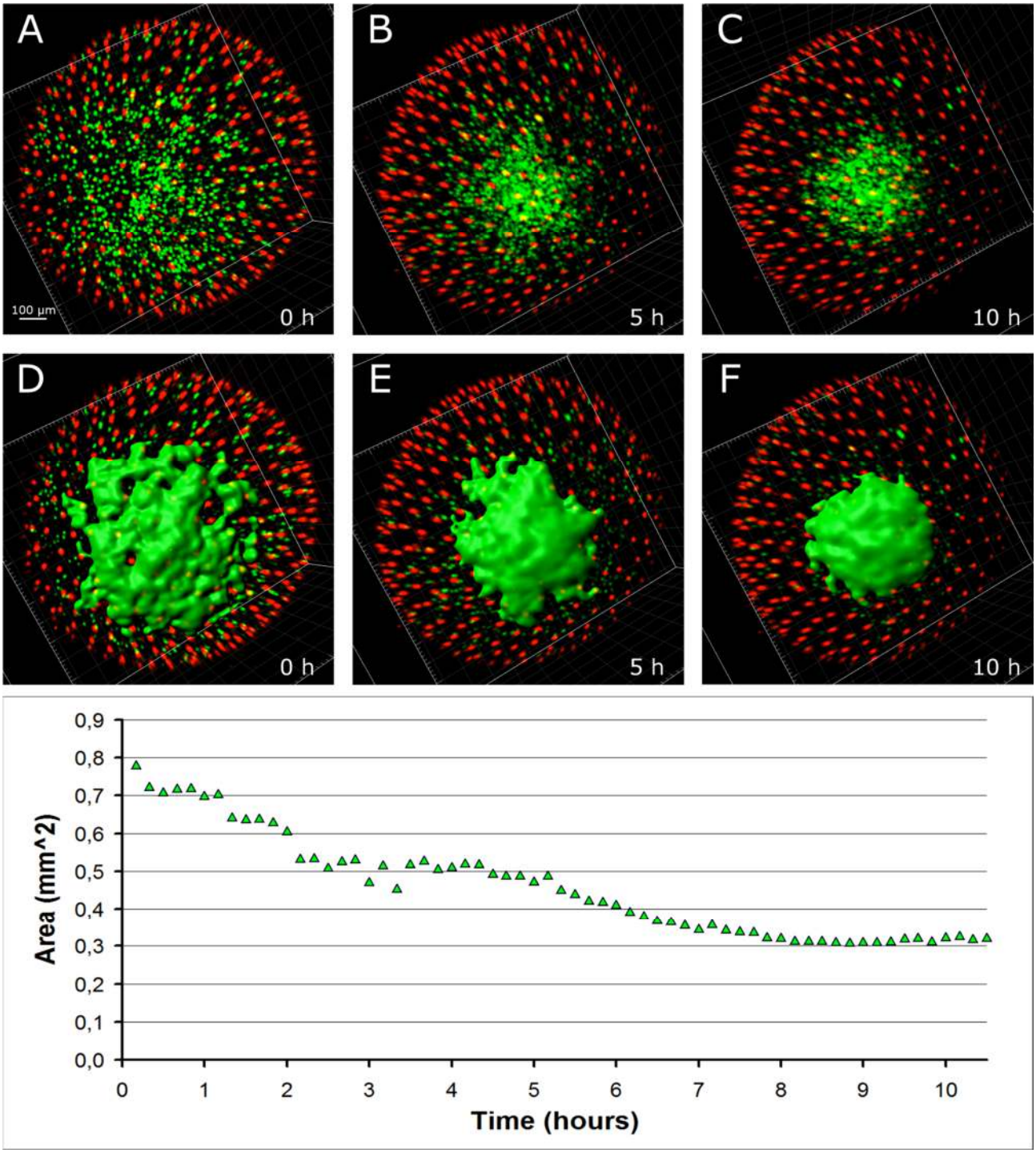

Figure 2.27. ***Reaggregation phase (Wourms stages 21-25).*** *Green cells are the ones that mostly take part in the embryonix axis formation and development. Initially they gathers in a point of the embryo (A,B,C), forming a circular structure that progressively reduce its radius. The green formation can be converted in a surface (D,E,F) that shows that the area reduction evolves with a linear dynamic over time (graph). The images and graph refers to the acquired portion of the embryos, equivalent to the upper part.*

Slowly the circular organization changed in shape, becoming an ellipsoid, lengthening, and retaining a higher density of the dividing cells in the inner part and a lower density in the borders (Figure 2.28 and Movie S6). The area of the whole structure almost remained unchanged and only its shape changed. Since the cumulative green signal intensity did not vary at this stage and the

cells mostly rearranged in the space, it can be assumed that the cell proliferation was reduced. In this phase, the number of epiblast green or red cells that did not belong to the main formation and that wandered over the YSL surface was greatly reduced, and was comparable or inferior to the number of cells that randomly moved over the YSL surface during diapause I (<80).

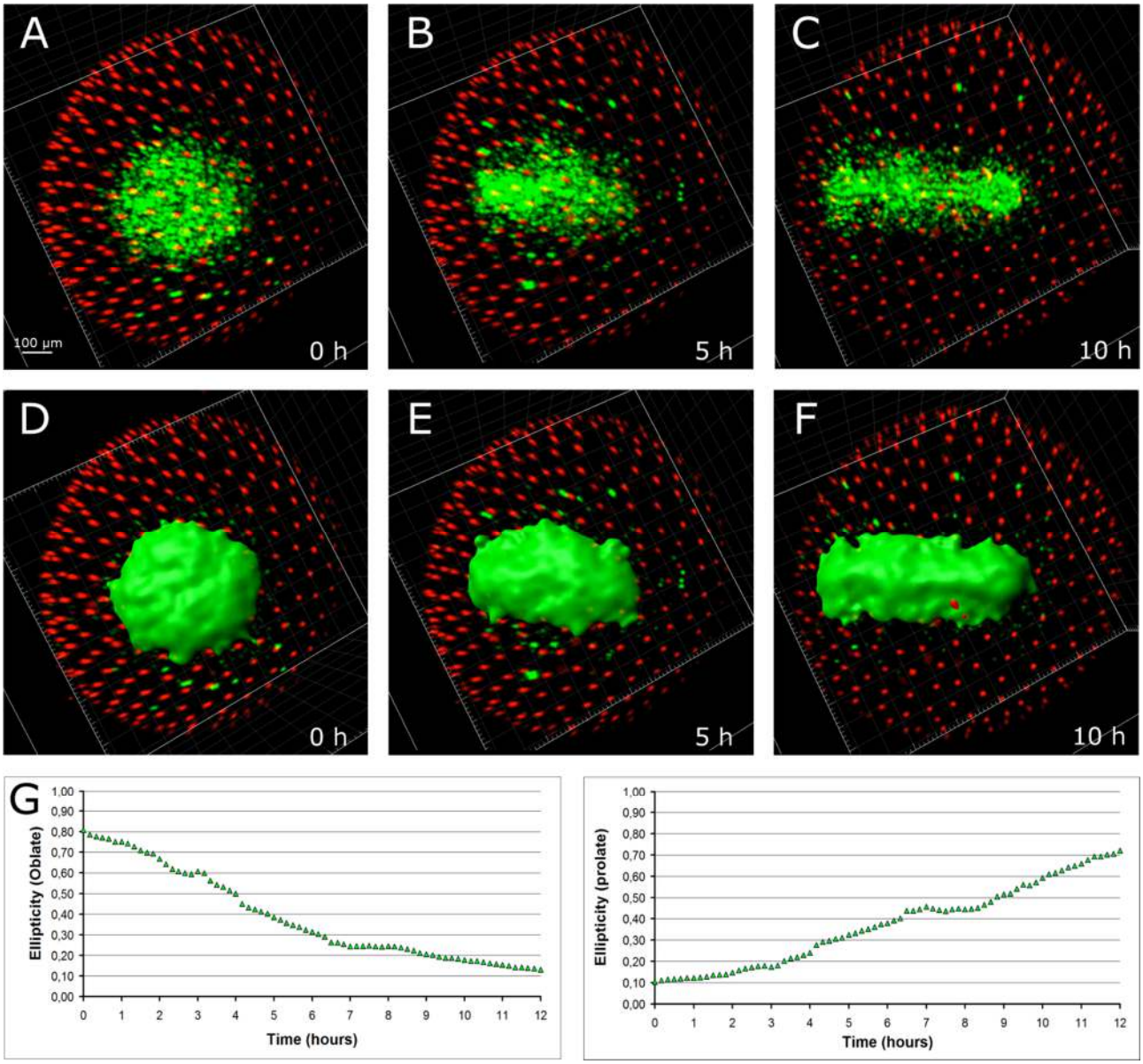

Figure 2.28. ***Axis extension phase (Wourms stage 26).*** *Green cells play a major role in this phase. The initial circular formation (A) evolves lenghtning until the formation of the primordial axis (C). The change in shape can be measured (D,E,F) and is slow, progressive and homogeneous (G). The images and graph refers to the acquired portion of the embryos, equivalent to the upper part.*

As the main structure evolved and lengthened, its shape changed, and so changed the density of the dividing cells in the different regions.

Just before the start of the somitogenesis (Wourms stages 27-28), the developing embryo appeared constituted by 2 streaks of dense proliferating green cells on the left and right side of the embryo, clearly separated by a narrow dark cell layer (Figure 2.29, detail). The cells from these 2 streaks divided and migrated toward the inside. Movements kinetics can be better appreciated in movie S6 (min 00:20 to 00:25).

At the top and the bottom of the formation were present two circular enlargements, dense with proliferating cells, that will form respectively the head and the somites of the embryo (Figure 2.29).

These cells divided and migrated in a circular way (can be appreciated better in Movie S6).

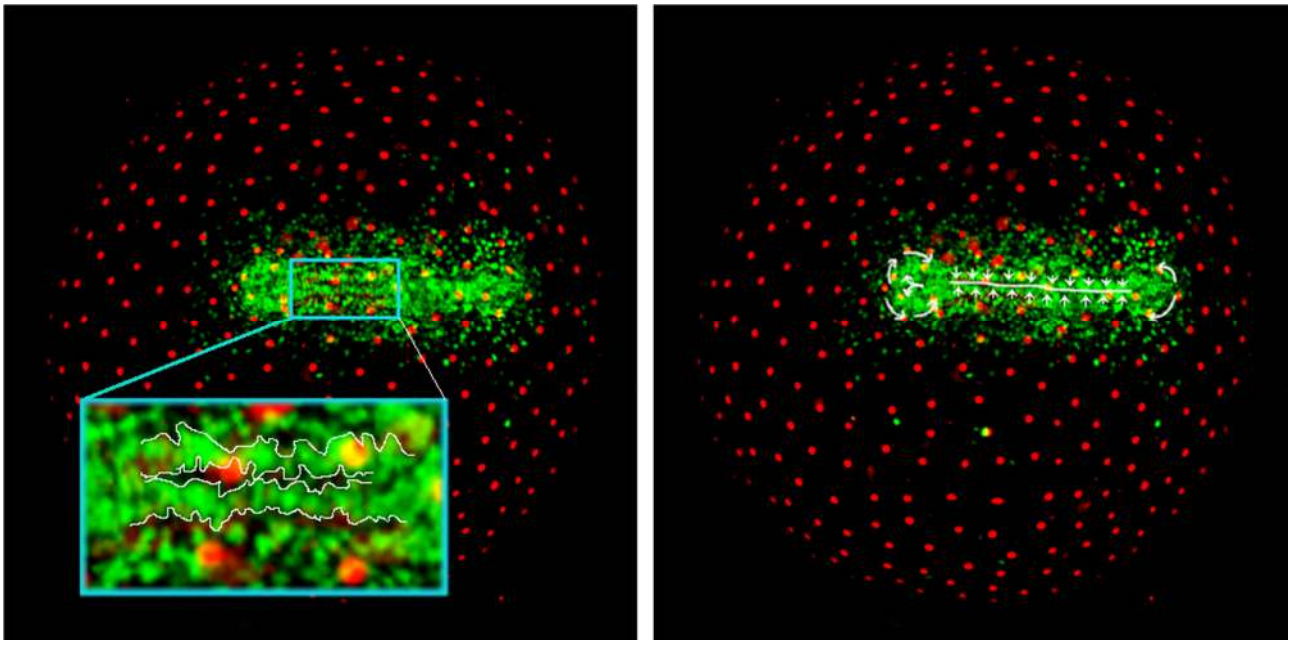

Figure 2.29. ***Axis elongation kinetics (Wourms stage 28).*** *Green cells greatly proliferate and move in the transition phase that links the end of axis definition with the beginning of somitogenesis. The cells populating the rostral and the caudal tip of the axis performs mainly circulat movements, in diraction of the axis body, while the cells belonging to the middle part of the axis are disposed in 2 streaks (detail) and move inwards towards the midline.*

2.3.6 Somitogenesis (Wourms stages 29-33+).

The first red structures that appeared, formed by clusters of red G1/G0 cells, were the somites. They started to form approximately in the 2/3 posterior part of the embryo and they increased in number as in all other fish species by addition of progressively more caudal somite pairs (Figure 2.30). The formation of somites was progressive and initial dispersed ensembles of red cells in few hours turned into defined red cell aggregates, forming the somite (Movie S6).

In the somites, only red G1/G0 cells were present and an overlap or co-existence of dividing and differentiated cells was not visible.

The somites structures were inserted among dividing cells, exactly between the green cells of the midline streak and the green cells at the border of the embryo. In a lateral view, instead, they appeared to be above the green cells of the midline streak (Figure not shown).

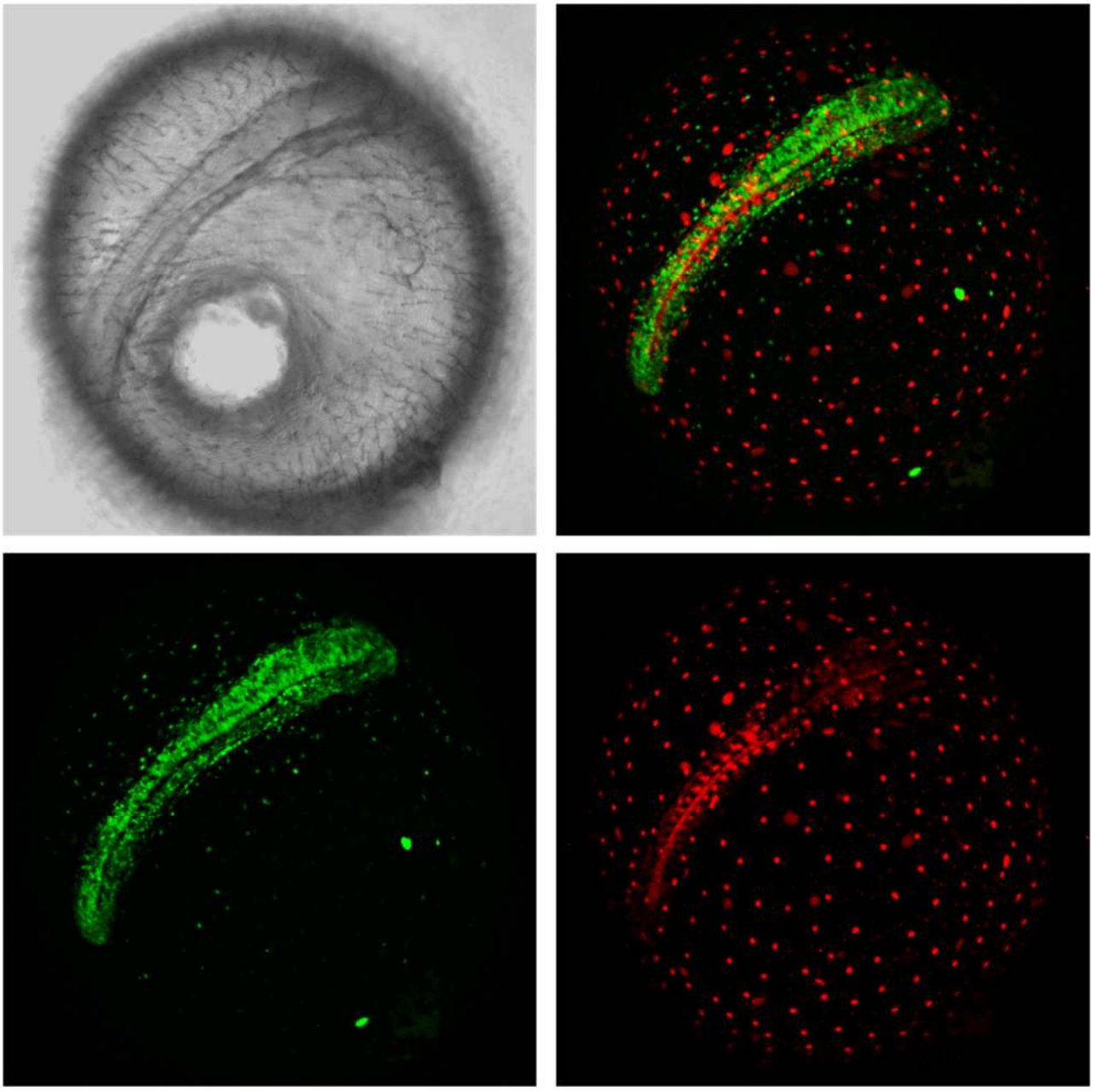

Figure 2.30. ***Somitogenesis (Wourms stage 31).*** *At mid somitogenesis green cells populate the major part of the embryos, that is in active proliferation, while red cells are mostly confined to already determined somite pairs. There is no overlap between green and red cells.*

Embryos destined to go in diapause II and embryos that would skip diapause followed different developmental paths, as already showed by Furness [30].The morphology of the forming nothochord was different between the two developmental trajectories.

The following experiments and measurements refer to only one diapause II committed embryo (DCE) and one not diapause II committed embryo (not-DCE), since only two embryos resulted correctly oriented to allow a precise measurement of body length and somites length (Figure 2.31). The data suggested a possible difference between a DCE and a not DCE already at the stage of 10 somites, but as already said this is the the suggestion derived by only one comparison, since no additional datas are available. For this particular stage description length measurements were performed by hand using Fiji. The DCE is an embryo that was imaged day after day as many other embryos, and that by chance arrested in diapause II phase at mid somitogenesis. The analysis and comparison are therefore been done in a blind way, and the commitment of the DCE specimen revealed only aftermath.

The elongation of the nothochord structure was much faster in embryos that were committed to skip diapause. The effect of temperature could be excluded since all embryos were imaged at 26°C.

The DCE imaged started to form the first somites (formed by a cloud of differentiated red cells) when they reached a total lenght of about 530 um, while not-DCE showed the first red somites when they were about 600 μm long. So, the first morphological difference in lenght between committed and not committed embryos was observed at the start of somitogenesis, before the 10-somite stage described by Furness [30].

In addition, as development proceeded not-DCE showed an elongation speed that was higher compared to DCE. In fact, the elongation speed for not-DCE was approximately 18 um/hour while for DCE only approximately 5,6 um/hours. Also the somite region elongation speed, accordingly to the reduced elongation rates between the two developmental trajectories was reduced. Not-DCE showed a somite region elongation speed (that is the speed at which the somite region extend in lenght, due to the progressive formation of the somites) of about 26,4 um/hours while DCE of about 11,5 um/hours.

The ratio between total elongation and somites elongation in DCE and not-DCE was not so different (approximately 0,68 vs approximately 0,49) and the embryos following either of the two developmental trajectories, even if developing at different rates, mostly conserved the relative proportions between their parts.

As previously described [30], [31], the width of DCE and not-DCE differed greatly. Unfortunately, since FUCCI only marks the nuclei of the cells and not the whole cells, this measurement was hard to define and absolutely not precise, so no quantitative data could be gathered regarding this measure although a difference between the width of DCE and not-DCE was clearly visible, with DCEnot-DCE being broader, particularly in the head region, possibly due to the increased proliferation in the lateral embryonic axis.

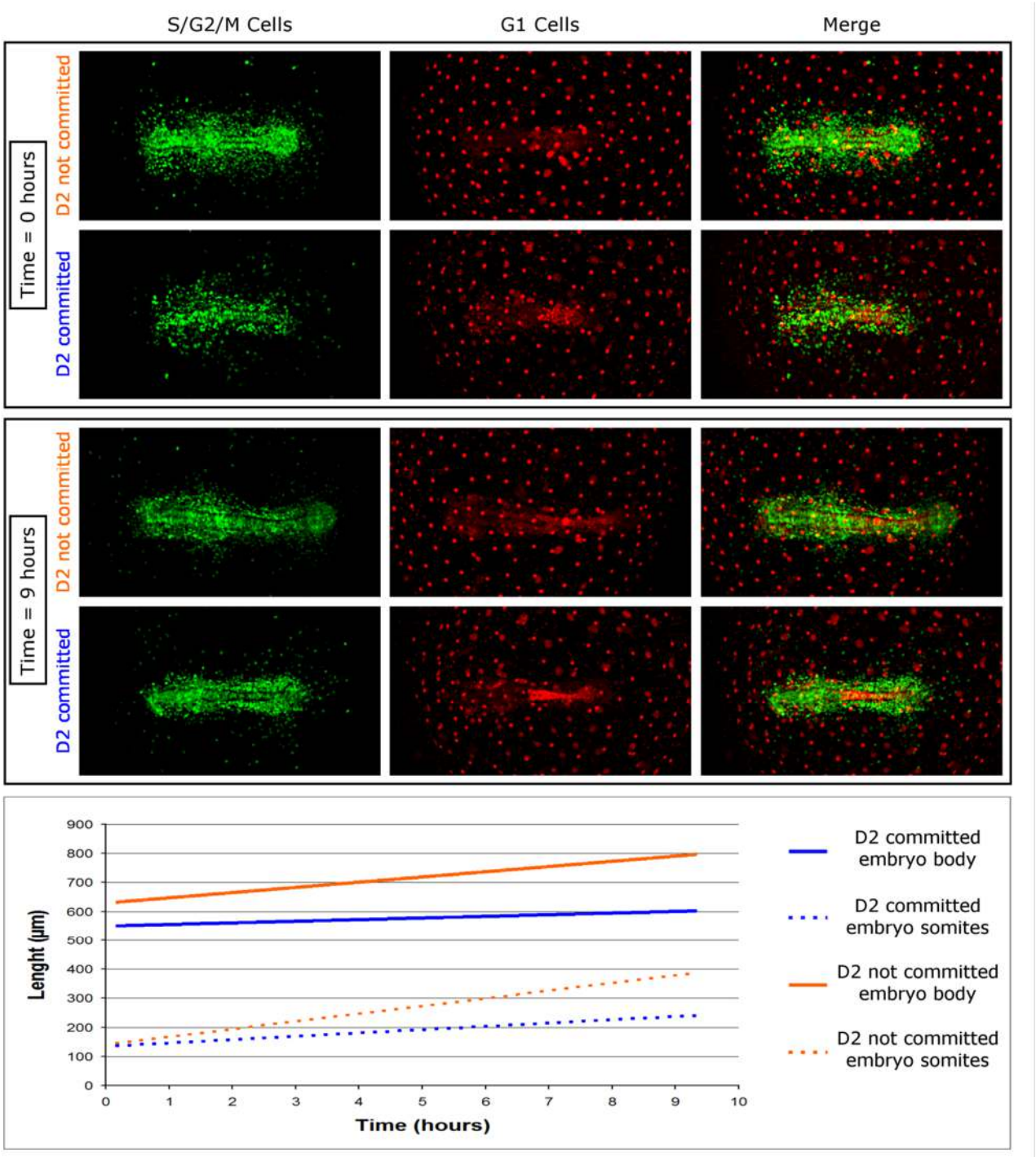

Figure 2.31. ***Differential axis elongation between diapause II committed and not committed embryos (Wourms stages 29-30).*** *Diapause II committed embryos show an axis lenght that is inferior compared to not committed embryos when somitogenesis starts. The somite region result proportionally inferior aswell. Axis and somites increase in lenght with a comparable speed both in committed and not committed embryos as development proceeds. Length measurements were performed by hand using Fiji*

2.3.7 Diapause II

The diapause II stage was charactherized by a dramatically reduction of proliferating cells. In diapause II embryos, all processes of development as proliferation or migration were suppressed. There were some green cells, spread among the somites, but their number was dramatically reduced as compared to the previous stages of development (Figure 2.32). In addition, these remaining green cells were possibly blocked in G2, since they were not dividing or moving.

Under our experimental conditions, when embryos entered diapause II somites were made by red cells and could be easily counted. All DCE entered diapause at the 30 somites stage.

Even if in the diapause II stage cell movements and dynamics were almost inexistent, sometimes muscular twitches bending the nothochord were detected. Their pattern appeared random without periodicity or being triggered by external stimuli. It was therefore impossible to estimate the number of twitch per hour.

In addition, at this stage, the length of the embryo was absolutely comparable to the length of a not-DCE, as opposed the width that was significantly lower as compared to a 30 somites not-DCE.

I documented the final stage of a diapausing embryo, when proliferation was suppressed (Figure 2.32). I could not document how this stage was reached and therefore the kinetics by which proliferation dropped (i.e. gradually or abruptly).

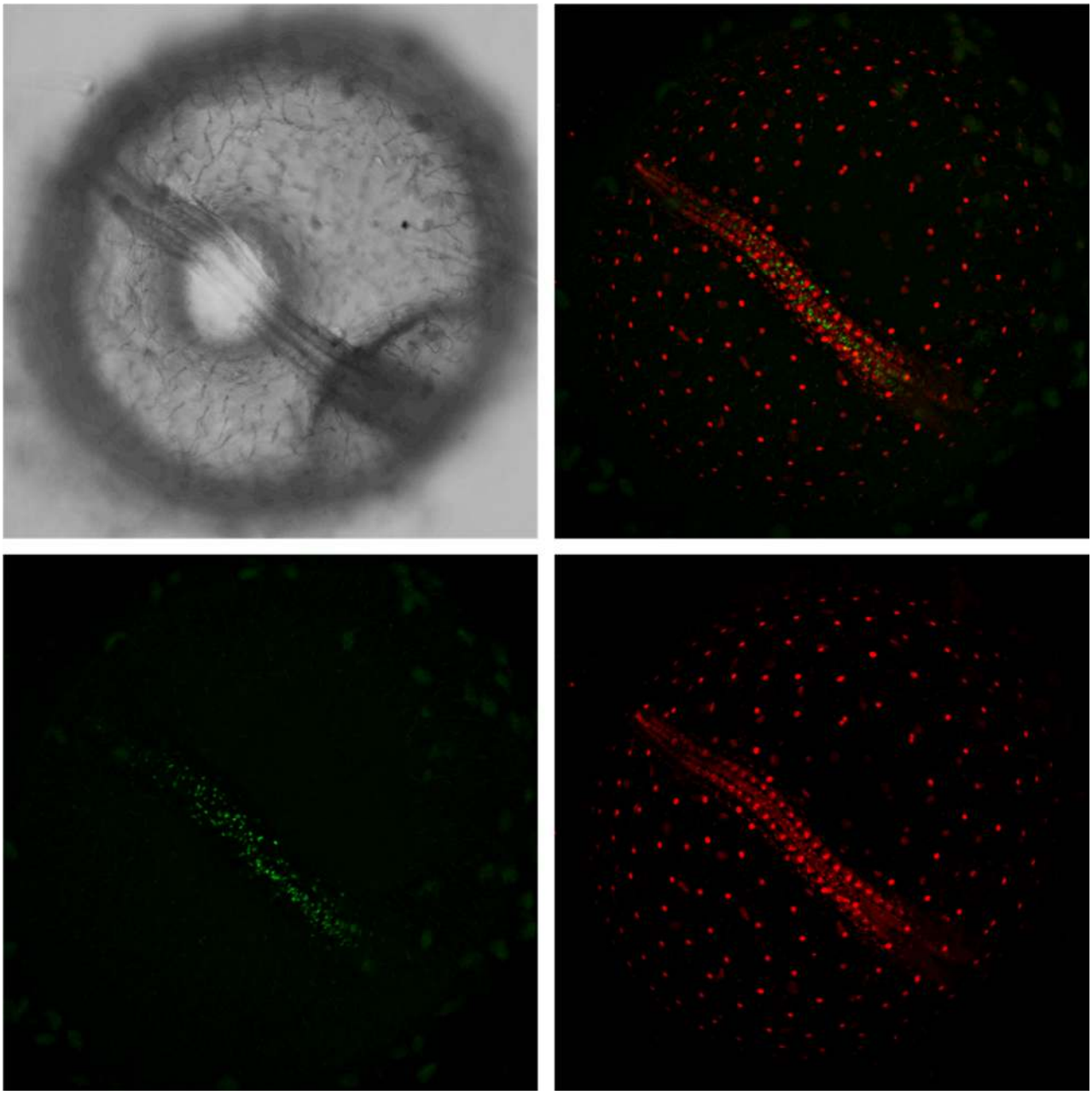

Figure 2.32. ***Diapause II arrested embryo..*** *Embryos arrested in diapause II shows an extremely reduced presence of green cells. Red cells clearly define the already formed somites and populate in a diffuse way the whole axis region. At this stage the embryos do not develop and cells do not proliferate or move, anyway sometimes muscolar contraction can be observed in the axis.*

2.3.8 Release from diapause II

The release from diapause II was documented in 3 embryos and was characterized by a rapid catch-up process by which almost all the previously red or colorless cells of the embryo (excluding the red cells forming the already complete somites) switched to green fluorescence(Figure 2.33 and Movie S7). These cells started to divide, stepping mostly through S/G2/M phases. Cell cycle reactivation happened in less than 4 hours, and started apparently simultaneously in all the cells of

the embryo. After the burst of reactivation, that lasted for at least 6 hours, it reduced to a steady state with similar kinetics (Figure 2.33 G).

During this process, red cells remained confined in the somites and in a more diffuse way in the head and in the trunk, without populating new areas of the embryo.

Anyway, what could be noticed was an increase of thickness of these regions. Red cells, that at the beginning of the reactivation delineated a long and skinny embryo (Figure 2.33 A,H), at the end of the process revealed a more wide and chubby body (Figure 2.33 F,I), much more similar to the embryos that skipped the diapause II stage.

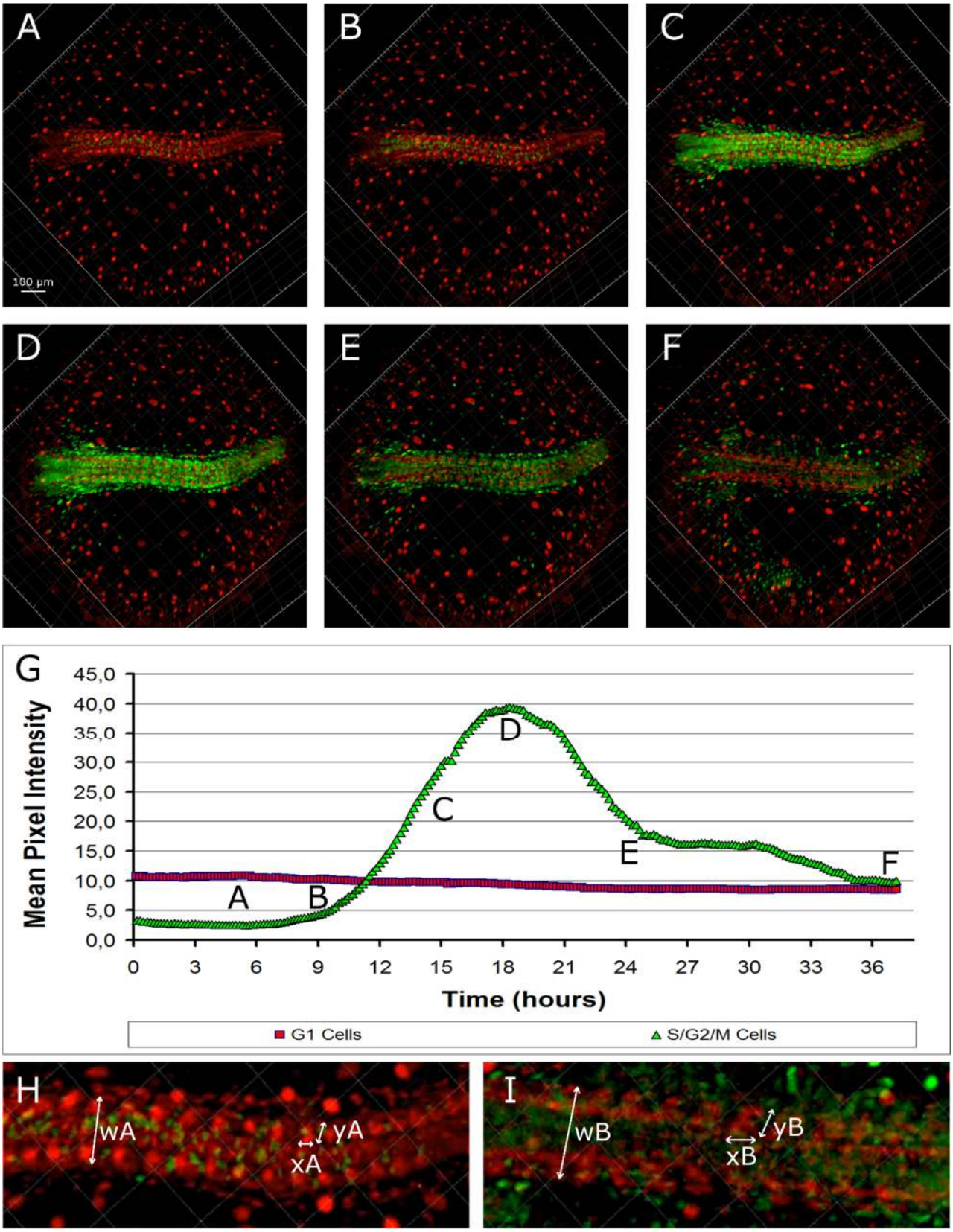

Figure 2.33. ***Release from diapause II.*** *A sudden reactivation of almost all the embryos cells determines the release from diapause II. Green cells greatly increase their number and density in less than 10 hours (B,C,D) increasing the lateral size of the embryo and reactivating the development. After the initial proliferation burst green cells slowly decrease in number and density (D,E,F), becoming comparable to embryos that did not arrested in diapause, at a comparable stage. Somites morphology changes after cells proliferation, and embryos width and each somite size become bigger (H,I). wA=70 ± 6 um; wB= 97 ± 9 um; xA= 16.5 ± 2.5 um; xB= 24.6 ± 2.8 um; yA= 16.7 ± 2.4 um; yB= 25.5 ± 3,5 um. Measurements performed with fiji. The images and graph refers to the acquired portion of the embryos, equivalent to the upper part. The bend in E is due to a slight loss of the imaging focal plane and is artifactual.*

2.3.9 DCE development past diapause II (Wourms stages 33+).

As the embryonic development approached to an end in DCE embryos, the proliferating cells density became similar to the previous phases, with a major concentration of green cells in the two midline streaks, at the border of the embryo, and in the head. In addition, as soon as cell cycle was reactivated, also cell migration started again. Similarly to the previous developmental stages, cells from the two lateral streaks appeared to migrate toward the midline, both in the somite region and in the head of the embryo.

As already said the green signal slowly faded and the proliferating cells remained in the stem cell niches and otherwise were scatterd across the embryo, generating mostly red cells that contributed to the increase on embryo width. After one day from the reactivation, DCE were comparable in morphology to not-DCE, and also the pattern of red and green cells was not visibly different.

2.3.10 Development of not-DCE

In the embryos that did not step into the diapause II arrest phase, the densitiy of green cells did not diminish, that means that in these embryos cells continued to cycle during all the development until the complete formation of the embryo. After the formation of the first 2 somites, 4 symmetrical green streaks of proliferation, that went from the base of the head to the end of the tail, could be clearly defined in the embryo. Two inner proliferation streaks, close to the midline and divided by the midline itself, and two outer streaks, one left and one right, defining the outer borders of the embryo (Figure 2.34).

If the two inner streaks had cells that migrates inwards (Movie S6), the movements of the cells of the outer streaks were less predictable, as they seemed to move in random directions. The cells belonging to the outer streak also moved outside the embryo formation region, going over the YSL cells covering the yolk surface, probably contributing in forming the blood vessels that would completely surround what remained of the yolk once the embryogenesis process was completed.

All the somites were defined by red cells while the main green proliferation event occurred in the rest of the embryo. As the development proceeded, the green signal slowly reduced in intensity and the proliferating cells became spreader and spreader in the embryo while the red cells became more and more dominant, expanding from the somites regions to the head and to the all the other parts of

the trunk. In not-DCE there is never a stage comparable to DCE where the green intensity drops nearly to zero.

The not-DCE embryos never present furthermore a stage where they look skinny, since this never-stopping proliferation lead them to the characteristic chubby morphology in each phase of their development.

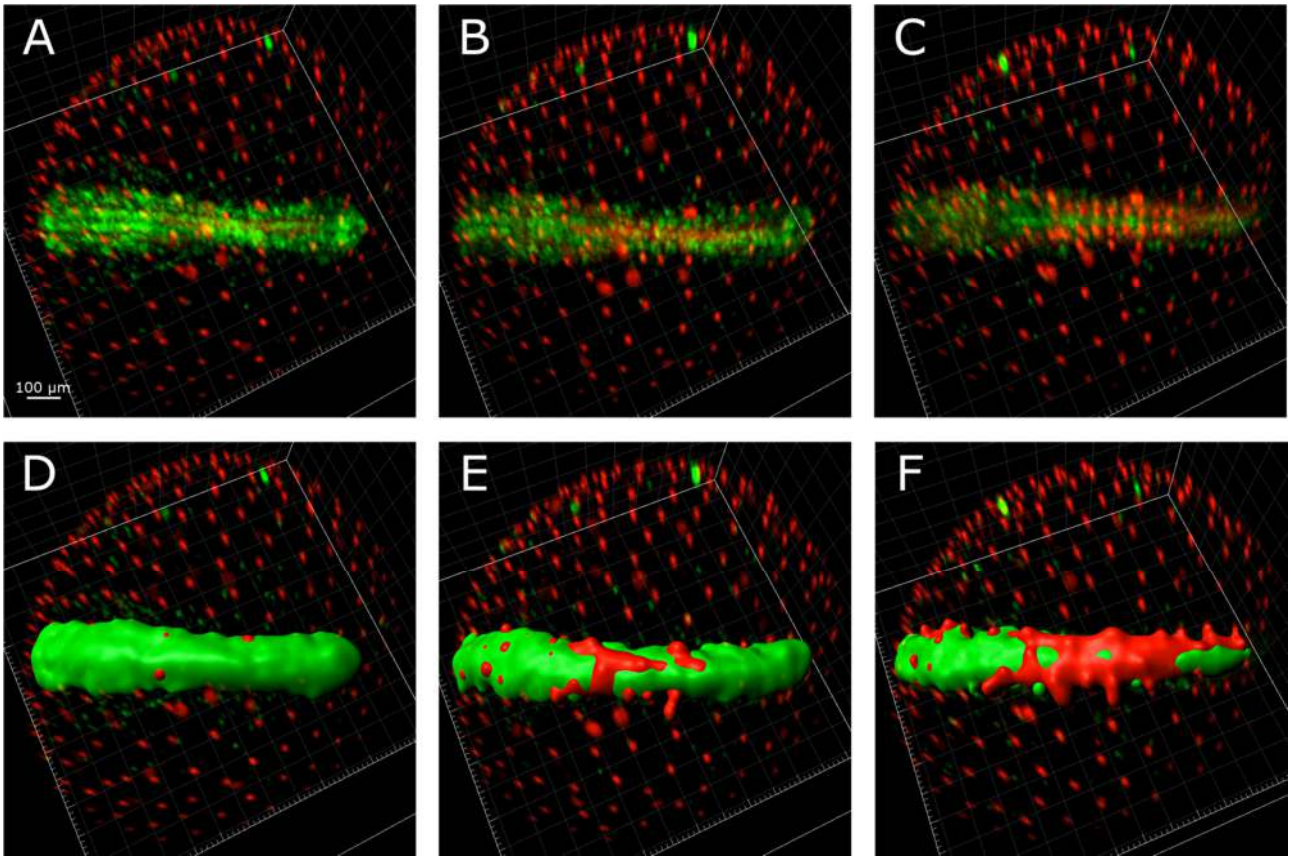

Figure 2.34. ***Not diapausing embryos end of development (Wourms stages 29-32).*** *Green cells populate the whole embryonic axis for all the somitogenesis in embryos that do not enter diapause II. Green cells number and density slowly drops as long as development proceed while red cells increase with time populating at first the somite pairs and afterwards almost every region of the axis.*

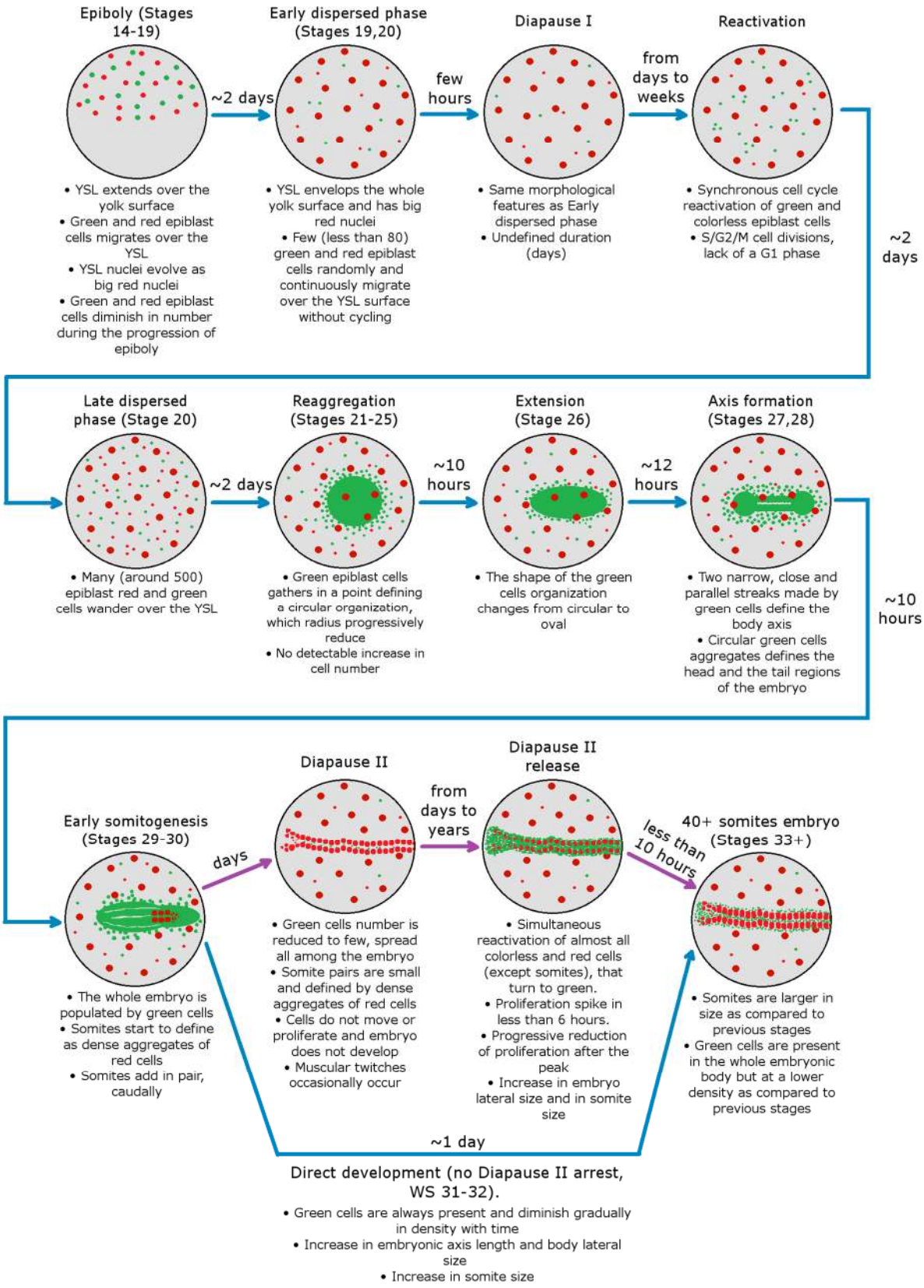

Figure 2.35. ***Graphical abstract resuming FUCCI N. furzeri fish development.*** *Images and developmental times refers to 26°C incubation conditions, except purple arrows that refers to low temperature (18°C-21°C) incubation conditions. Stages refers to developmental stages described by Wourms* [3].

2.4 Molecular analysis of diapause

2.4.1 MicroRNAs differential analysis

To begin to shed light on the molecular factors involved in the diapause process, an experiment of genome-wide expression analysis of small RNAs was performed. 7 species of killifish belonging to all of the 3 existent clades were selected (Figure 2.36). From South America, were chosen the annual species *Austrofundulus leohoignei* and the related non-annual species *Rivulus cylindraceus*. From Africa, west of Dahomey gap, the annual species *Callopanchax occidentalis* and the non-annual species *Epiplatys dageti monroviae*. From Africa, east of Dahomey gap, the annual species *Nothobranchius furzeri* (5 replicates) and the non-annual species *Aphyosemion striatum* (4 replicates).

As outgroup, *Aplocheilus lineatus* was chosen as the closest outgroup *taxon* to all annual killifish.

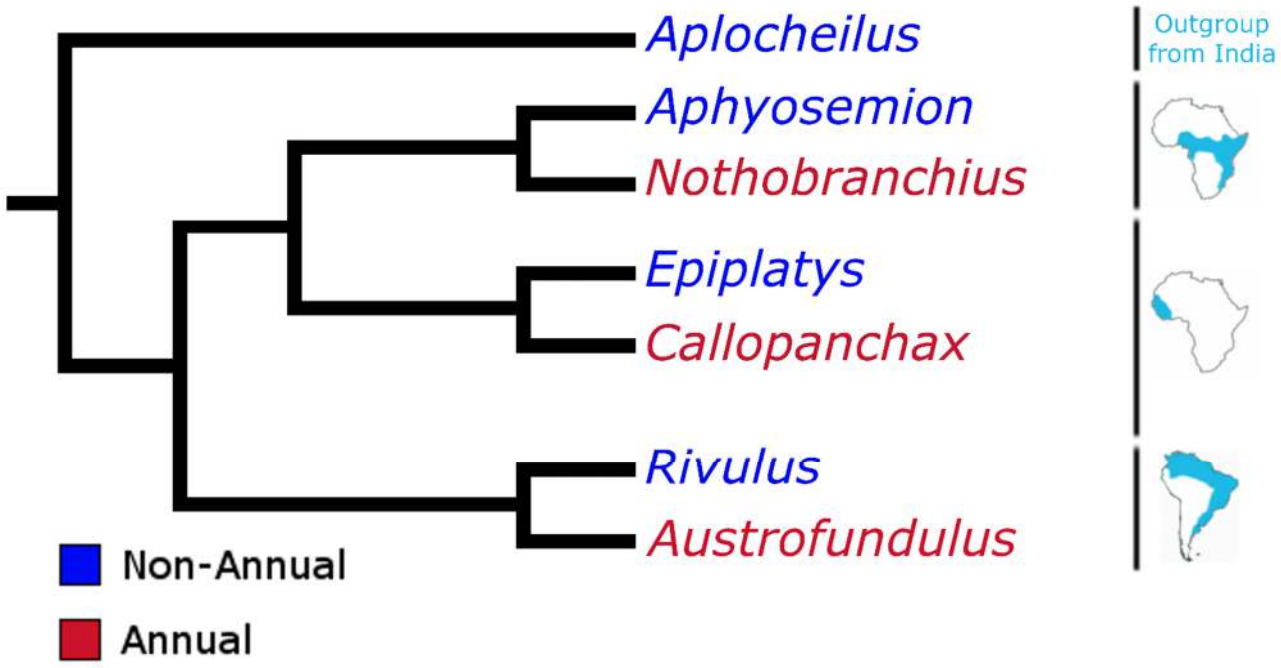

Figure 2.36: ***Phylogram of the species used for the experiments.*** *Blue indicates non-annual species, red annual species. The geographic distribution of each lineage is show on the right. The phylogram is derived from the original Murphy and Collier molecular phylogram based on cytochrome b, 12 s rRNA and 16 s rRNA genes* [2].

Fertilized embryos were collected from each species and were kept at 24°C. At this temperature, more than 50% of the annual embryos stopped their development in the diapause 2 phase.

30 to 50 embryos from each species, blocked in diapause 2 for annual species or at the equivalent developmental stage (mid somitogenesis) for non annual species, were pooled, and the RNA was extracted.

In a second experiment, two groups of *N. furzeri* embryos were kept in different conditions. One group was kept at low temperature (21°C) and the other group at high temperature (27°C), in order to induce or prevent the arrest in diapause 2, respectively. RNA was extracted from diapausing embryos belonging to the first group and from 30 somite-stage not diapausing embryos belonging to the second group. To confirm that the embryos from the second group were effectively not arresting in diapause, only 30% of the embryos were sacrificed for RNA extraction and the others left to develop as control. All the control embryos did not stop in diapause.

From total RNA extracted from each sample, the miRNA portion was isolated and the miRNAs expression was analyzed by miRNA-Seq. This analysis was performed by Mario Baumgart at the Leibniz Institute on Aging in Jena.

In total, $1.97x10^8$ sequences in the 18-33 nt size range were obtained and $2.97x10^7$ (15%) could be annotated as miRNAs based on miRBase v21.0 allowing two mismatches with *Danio rerio* reference miRNAs. Distribution of size classes was bimodal and showed two peaks: one at 22 bp, that is consistent with the size of mature miRNAs, and one at 28 bp, that is consistent with the size of piRNAs. On the other hand, size distribution of small RNAs previously obtained from *Nothobranchius furzeri* somatic tissues [67] was unimodal and centered on the expected size of mature miRNAs. Therefore, low annotation yields could be due to a prevalence of piRNAs in the small RNA population of the killifish embryos at this developmental stage. Indeed, presence of piRNAs in zebrafish embryos up to 1-day postfertilization (when somitogenesis is completd) was recently reported [121]. However, since the genomes of the species analyzed here are not available, it is not possible to annotate piRNAs in our datasets. In total, we identified 291 evolutionarily-conserved miRNAs expressed in at least one sample. In order to reveal the effects of phylogeny and physiological status on global miRNA expression, multidimensional scaling (MDS) was performed. MDS is an iterative algorithm that projects individual samples onto a plane minimizing the difference between their distance on the plane and their distance based on miRNA expression (defined a 1-ρ, where ρ is the Spearman's correlation coefficient). The result is a dimensional clustering that reveals the similarities between all the embryonic samples (Figure 2.37).

Analyzing the MDS graph, the following observations can be made:

There is a complete separation between annual and non annual killifishes species samples, regardless of their clade affiliation or phylogenesis. The two groups of killifishes, annual and non annual, form well-separated clusters.

Further, biological replicates *of Nothobranchius furzeri* and *Aphyosemion striatum* form two distinct clusters nested within the annual and non annual clusters, respectively.

Nothobranchius furzeri 30 somites not diapausing embryos cluster together and position in the graph very close to diapausing *N. furzeri* embryos samples, but shifted toward the non annual samples.

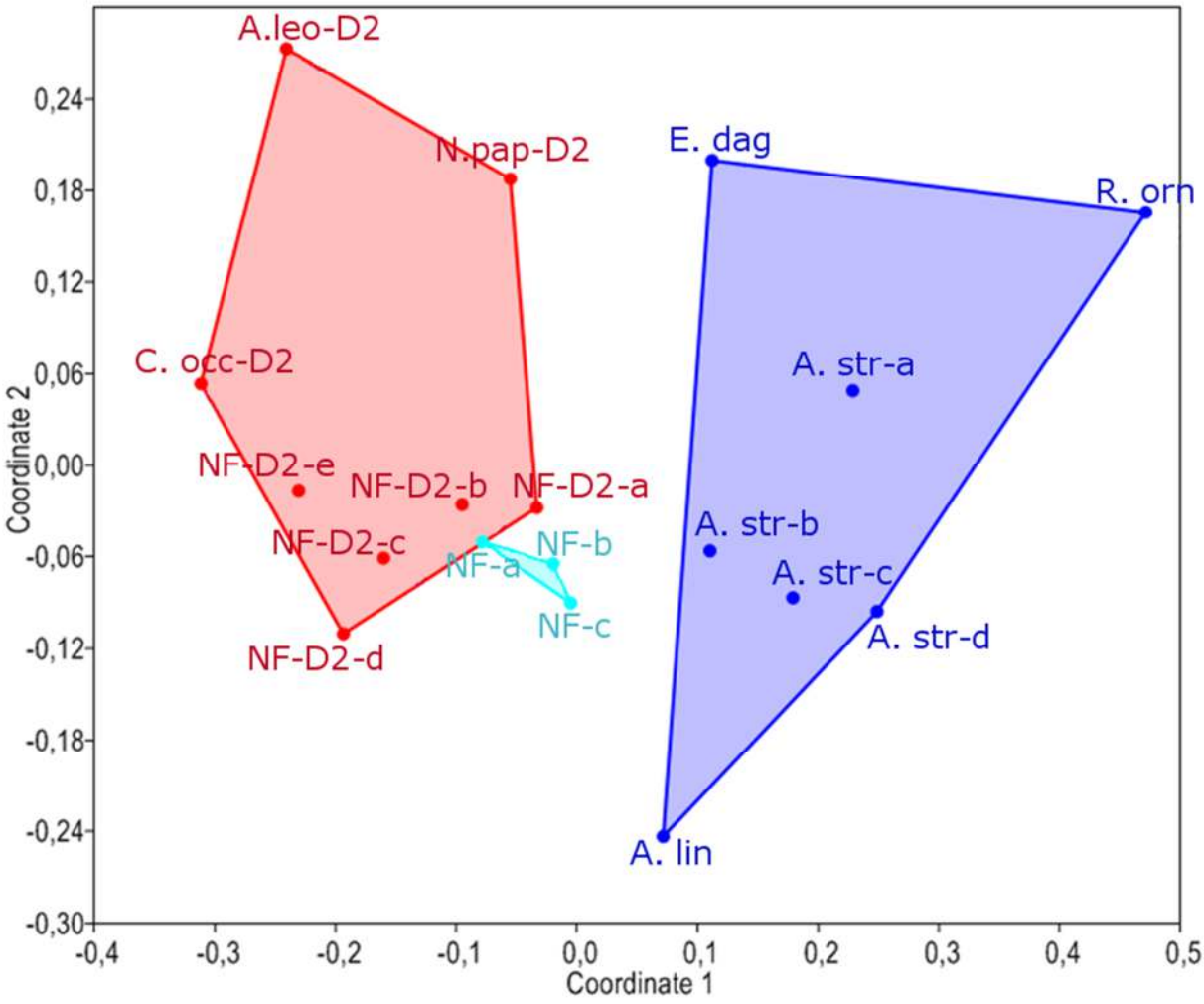

Figure 2.37: ***Mid somitogenesis killifishes miRNA MDS****. The two axis show the principal components. MicroRNAs of diapausing annual embryos (red), mid somitogenesis non annual embryos (blue), and Nothobranchius furzeri mid somitogenesis not diapausing embryos (light blue) are plotted on the graph. Annual and non annual killifishes completely separate and not diapausing N. furzeri embryos belongs to the annual group but are shifted towards non annual species.*

In a first approach, we identified DEMs common to all three lineages. For each of the three lineages, we contrasted the non-annual species with one annual species (Kal's Z-test, FDR-corrected $p<0.01$ and absolute fold change > 1.5). Venn analysis revealed six miRNAs that were up-regulated in DII embryos in all three lineages : miR-10a/b/d miR-101a, miR-146a and miR-192 (Figure 2.38 B). Seven miRNAs were down-regulated in DII embryos in all three lineages: miR-130, miR.184, miR-18a, miR-22a, miR-430a, miR-462, miR-731 (Figure 2.38 A).
Was then investigated the existence of differentially-expressed miRNAs (DEMs) linked to diapause using DESeq2 [122].

In second analysis we performed two different tests :
In test 1, we treated each species as replicate, with only one replicate each for *N. furzeri* and *A. striatum,* and contrasted annual- *vs.* non-annual samples. In Test 2, we contrasted *N. furzeri* (5 replicates) with its sister non-annual *taxon*, *A. striatum* (4 replicates). In Test 1, a total of 16 DEMs were detected with false discovery rate (FDR), $p < 0.05$. 8 were higher- and 8 lower-expressed in diapausing embryos. Out of these, 6 DEM with higher expression in the diapausing embryos were also DEM in Test 2 (miR-199-3p, miR-126a-3p, miR-153a-3p, miR-141-3p, miR-30d and miR-200a-3p) and all 8 DEMs with lower expression in the diapausing embryos (miR-18b-3p, miR-200a-5p, miR-21, miR-462, miR-731, miR-430a-3p, miR-19d-5p, miR-430c-3p) were also DEMs in test 2. It shoud be noted that miR-430a and miR-430c are the most expressed miRNAs in annaul- and non-annual embryos, respectively.

If FDR correction was omitted in Test 1, were detected 17 up-regulated DEMs (out of these, 10 were in the intersection with Test 2) (Figure 2.38 D) and 30 down-regulated DEMs (out of these, 25 were in the intersection with Test 2) (Figure 2.38 C). These down-regulated DEMs included 4 out of the 6 members of the miR-17~92 cluster (miR-19a, miR-20a, miR-92a and miR-18b) that is know as important regulator of the cell cycle [123].

MiR-430a miR-462 and miR-731 emerged as down-regulated and miR-101a as up-regulated during diapause II in both the analysis.

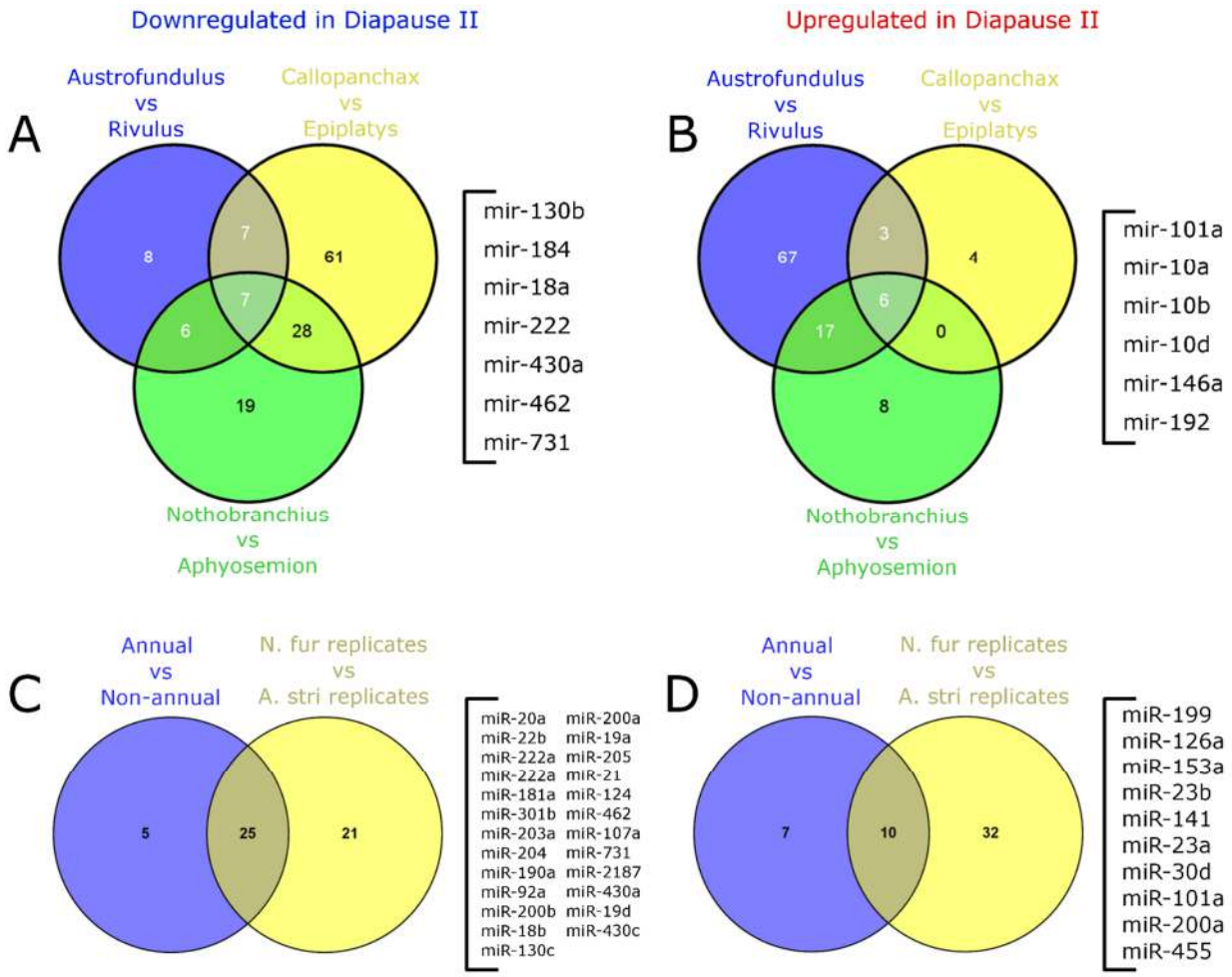

Figure 2.38: ***Differential microRNAs expression between annual and non-annual species****. A and B represent the DEMs common to all three lineages, C and D represent the DEMs common to test1 (annual vs non-annual) and test2 (5 nothobranchius furzeri replicates vs 4 aphyosemion striatum replicates). MiRNAs in A and C are less expressed in embryos arrested in diapause II while miRNAs in B and D are more expressed.*

2.4.2 MiR-430 expression in *N. furzeri*

Activity of miR-430 is linked to degradation of maternal transcripts at the mid-blastula transition [124]. This feature has been characterized in zebrafish, that as previously treated, has different developmental dynamics compared to a large part of killifish species, so I decided to investihgate whether also in *N. furzeri*, activity of miR-430 is induce at the mid-blastula transition.

Killifish 1 cell stage fertilized embryos were injected with a sensor for miR-430 (Figure 2.39).

The sensor is a GFP coding sequence fused to a 3‘-UTR containing binding sites for miR-430 (G-430). Together with the sensor, it was injected an RFP mRNA equally concentrated in order to normalize the GFP intensity level in the embryos.

A construct with a mutation in the binding sites for miR430 fused to the GFP coding sequence (G-430-mut) served as control [124]. Also in this case, the RFP mRNA was co-injected.

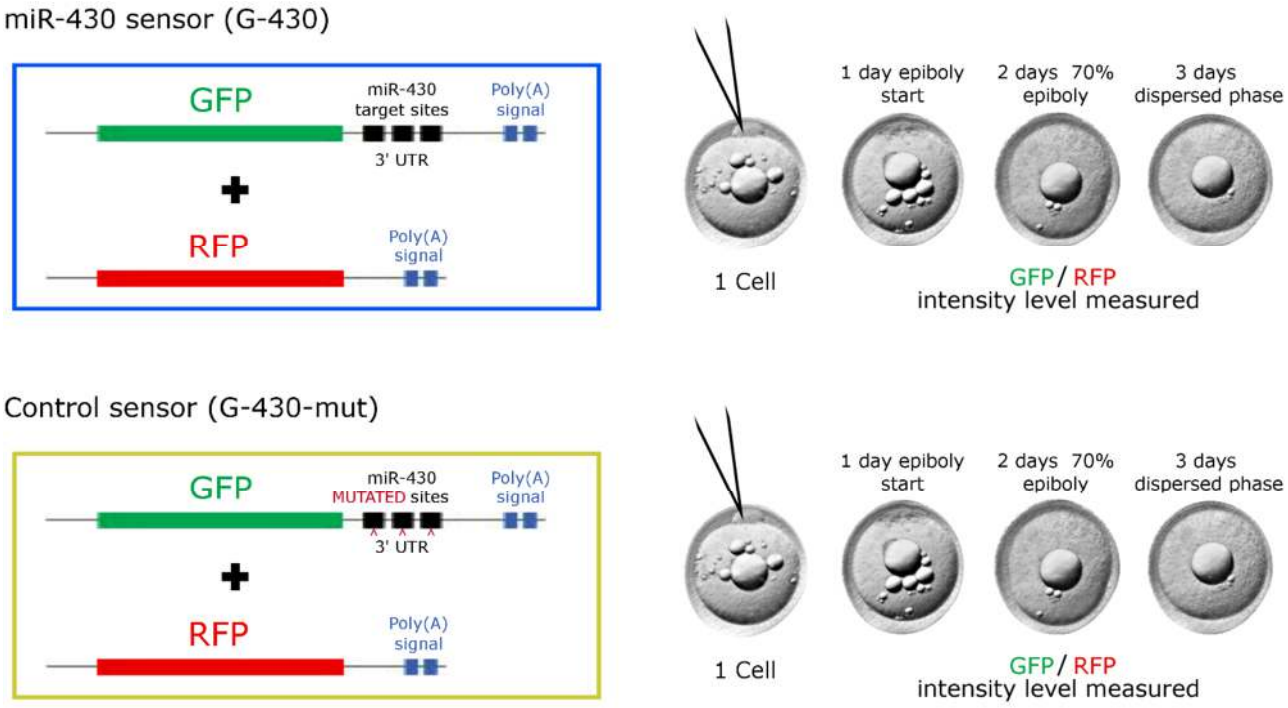

*Figure 2.39: **MiR-430 sensor**. Schematic representation of the miR-430 sensor and of the miR-430 mutated control sensor. The control sensor has point mutations in the 3'UTR sequence on miR-430 binding sites. Both the sensors were co-injected with a constitutive RFP coding RNA in 1 cell stage N. furzeri embryos. Fluorescence intensity levels were measured once a day for one week.*

Injected embryos were imaged once a day for a week and GFP and RFP intensity levels were measured (Figure 2.40).

The GFP/RFP intensity ratio showed a different behaviour in G-430 and G-430-mut injected embryos.

In G-430-mut injected embryos, both GFP and RFP were visible 24h after injection, after that the intensity ratio slowly decayed over time.

In the same way also in G430 embryos fluorescent proteins were visible at 24h after injection, but the ratio dramatically dropped in the next 24 hours, and GFP levels remained very low until the end of the imaging period.

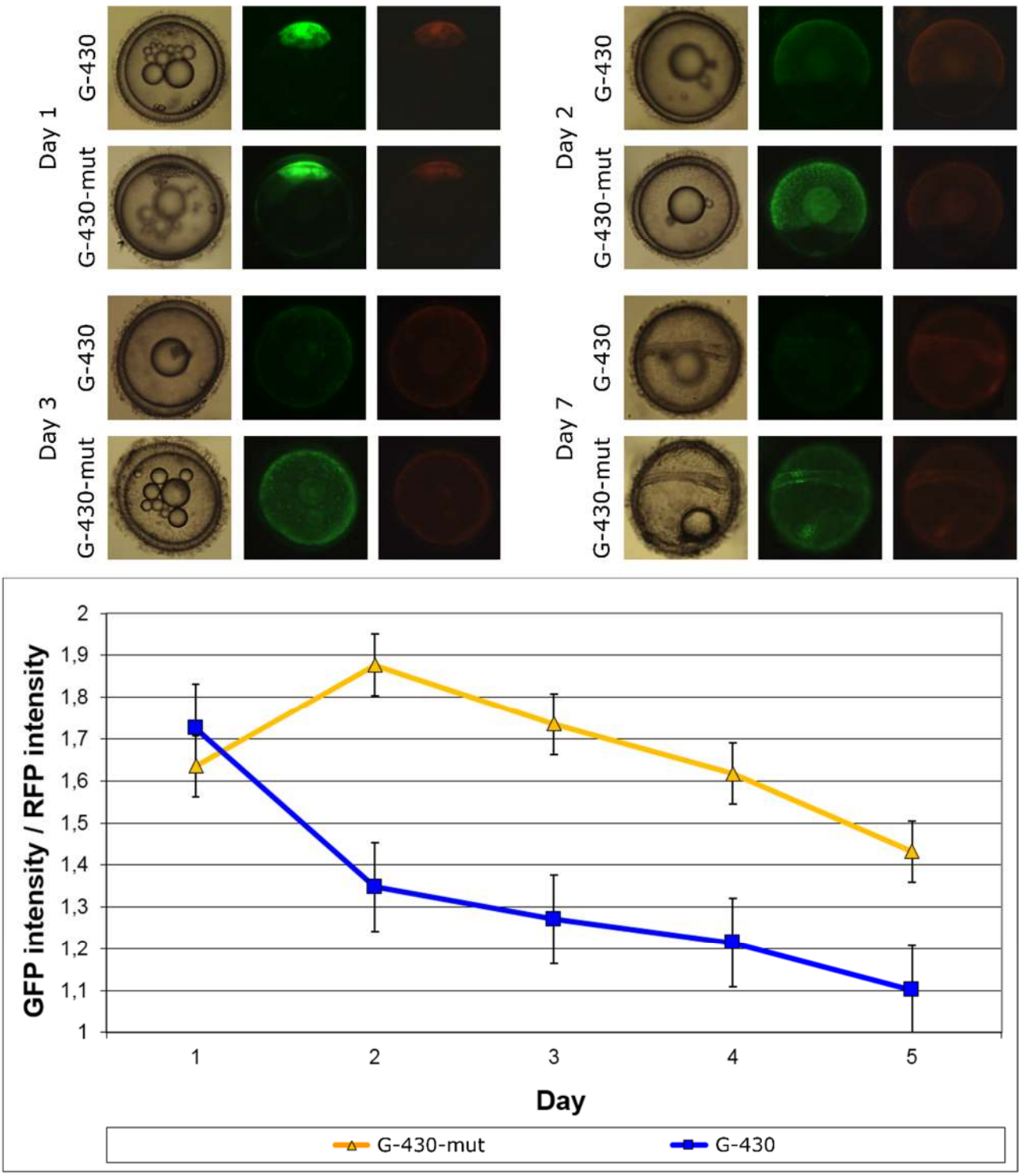

Figure 2.40: ***MiR-430 is expressed in N. furzeri between 24 and 48 hours post fertilization****. Images and the graph show a dramatic drop in GFP intensity between the first and the second day after the injection. The mutated sensor does not have this trend. RFP levels remains weak and stable for all the time of the experiment, while GFP levels gradually drops over days, at a constant rate in both the sensors.*

MiR-430 is therefore active in *N. furzeri* embryos between 24 and 48 hours after fertilization, and in embryos that will not arrest in diapause 2, its effect continues over time until the phase of mid somitogenesis.

3. Discussion

3.1 Early development in annual and non-annual killifishes

What emerges from the data presented here is a clear difference between segmentation rates of annual and non-annual embryos. Annual killifishes show cleavage rates that are on average half or less as compared to non-annual killifish.

This phenotype is conserved in all the fish analyzed, belonging to three different geographic clades separated by large geographic distance. Therefore, this developmental trait correlates with annualism, regardless of the phylogenesis of a killifish species.

This slowness in early cell division could be the result of positive selection and provide an evolutionary advantage for annual species.

Non-annual species in fact live in an relatively stable environment that is not subject to dramatic seasonal changes and is present throughout the year. For this, their development is very similar to other fish species and is under positive selection for rapid generation of a fry. The development is relatively fast and in 22 days usually the fry is able to hatch, to swim and to eat. This speed has an evolutionary meaning. Fish eggs are considered food by a large part of fish and other predators, sometimes even by their own parents. For this reason, the longer an embryo stays in its egg, the longer it is unable to escape a predator, and therefore, it can be assumed that developmental speed is under directional selection.

The evolutionary scenario of annual killifishes is totally different, since they inhabit small temporary ponds that drive evolution of completely different life-history traits.

A small pond sometimes extends for just a few tenths of meters. In addition, it is temporary, and so it is absent for a fraction of the year or sometimes, in arid habitats, not existing for several years in a row. This means that the diversity of the aquatic vertebrates that are able to populate the pond is extremely reduced, because of both its size and temporary nature. This leads to a reduced risk of predation for annual killifishes embryos.

For this reason, it is biologically convenient for an embryo to develop as slow as possible, because the chance to hatch in an environment without predators is much higher. As a result, the

evolutionary pressure on the developmental speed is relaxed in annual species and this could be a reason for the evolution of such slow early cleavages.

A second hypotesis instead postulates that the extension of early cleavages is a positively selected trait. Extending the early cleavages span implicates that the period when an embryo can respond to environmental conditions is equally extended. In fact, annual killifish embryos can skip diapause [31]. This can be interpreted as bet hedging strategy because diapause skipping embryos can hatch if the water body fills more than once during a season [125], allowing a second generation, and the commitment to this alternative developmental pathway is determined during the early development [31]. So, slowing the cleavage phase could have an effect in extending the amount of time available to embryos to respond to environmental conditions.

3.2 FUCCI transgenesis in *N. furzeri*.

FUCCI technology applied to *N. furzeri* fish proved to be a very powerful and reliable tool for cell dynamics studies and developmental analysis. Cells can be monitored from the stage of 70% epiboly to the fish adult life and their change of reporter expression in relation to the cell cycle progression is very reliable.

In this work, FUCCI was used to describe cells dynamics during the development and the diapause phases in *N. furzeri* embryos but its applications could be much wider. It is able to describe precisely how cells behave during development, and could be used to identify the environmental variables that affect the development itself. It is able to instantly detect the release from diapause I or II, and could be used in the future to perforn molecular analysis (RNA-seq, CHIP-seq, metabolomics etc...) comparing embryos that are just exiting from diapause with embryos of the same cohort that remain in diapuase, to identify the molecular mechanisms that control this process. It can monitor the proliferation or regeneration in adult fish, and could be used to follow the repair dynamics in fish at different ages, since *N. furzeri* is also a very good model of ageing. Concluding, these and other applications make FUCCI *N. furzeri* fish an innovative tool, because a highly informative techonology is applied to a very peculiar organism, that has unique developmental features and is a great model of ageing.

3.3 Diapause I

The results from FUCCI imaging describe precisely how the cells of the *N. furzeri* embryo behave during development. The initial five cell divisions are characterized by synchronous divisions, that take each the same amount of time and show only the presence of S M and possible G2 phases, without G1. Is still unclear the reason what are the molecular mechanisms responsible for extending the duration of cell divisions. Anyway, from these studies emerges that one of the phases responsible of this slowness is one among S or M or both.

Another information acquired from FUCCI imaging is the progressive decrease in the number of green colored cells during epiboly. Since green cells are in S, G2 or M phase, this means a progressive reduction of dividing cells as long as epiboly proceed. This results in a very reduced amount of green proliferating cells when epiboly ends and persists during the initial part of the dispersed phase, that can turn into diapause I.

Each embryo analyzed showed a progressive reduction of dividing cells while approaching the dispersed phase. It is therefore fair to assume that *N. furzeri* embryos are basically prone to enter the diapause I condition, and what can be modulated is only the time spent in this stage and its release.

According to the data gathered, diapause I appeared to be the default developmental program of the embryos, that can last for varying amounts of time, depending on environmental condition, but not be skipped.

According to the literature, the triggers that release an embryo from diapause I are probably the same environmental conditions that influences diapause II, like temperature, humidity, pressure and other environmental factors [8], [31], [34], [35], [38] . Anyway, contrary to diapause I, a long permanence in diapause I is difficult to observe and it seldom lasts more than a few days.

In all the life imaging experiments performed here, no embryos remained in the diapause I condition for more than 10 days and usually presented themselves in the released condition few days after the beginning of the dispersed phase.

Summing up, what emerges from the data is that diapause I is a phase in which every embryo obligatorily enters and easily leaves. This strategy is advantageous for the embryos, in fact, epiboly is one of the first step in embryos development and there is not so much time to evaluate the environmental condition and to decide if stopping in diapause I or not, even if, for what said before, slowing the initial cleavages could help in evaluating the environment.

A default programme that stops every embryo in diapause I after epiboly completion could be an economic strategy, since an embryo should just decide whether to extend this phase, if conditions are negative, or release it and continue the development, if they are not.

Concluding, the controls on diapause I are probably less strict than on diapause II because even if a wrong choice is done, the embryo can still stop on the following phase of diapause and so there is no reason and no evolutionary pressure on hard controls on diapause I.

3.4 Release from dipause I

The exit from the diapause I condition is a rapid event lasting few hours that is difficult to be documented. In the only embryo where this was possible, it was characterized by the simultaneous reactivation of many of the epiblast cells proliferated synchronously in a succession of S G2 M phases, without stepping on a G1 phase. These rounds of simultaneous cells divisions repeat several times, until the embryo reaches the amount of cells for the reaggregation phase.

Is important to say that all the cells that start to divide again on embryo reactivation start simultaneously, so, there is a mechanism of cellular communication to allow synchronization of sparse cells, rather than a domino mechanism where some cells begin to proliferate and the others follow over time.

Admittedly, this phenomenon was observed in just one embryo but there are two lines of thought that suggest that this is a general phenomenon: I) the diapause I embryos that we observed were either in the “few cells” or “many cells” stage, suggesting that the transition is rapid II) the same phenomenon is observed upon exit from diapause II.

During the ampification process and also after reaching the critical number of cells for reaggregation, epiblast cells move and migrate with a velocity that is comparable to the velocity of the cells during the diapause I stage. This continous migration is very peculiar and its biological meaning is still unknown. Since this feature is unique of annual killifishes, probably it is involved with one of the features of annualism, like the diapause I regulation.

The continuous migration of cells could in fact help in giving each cell a perception of the whole embryo rather than of a specific sector and this could lead to reactivate the epiblast cells all together rather than at different times.

3.5 Diapause II

As opposed to to diapause I, diapause II is not an obligatory developmental phase and not even a developmental block itself, but rather a more complex developmental programme. Embryos that are destined to arrest in the diapause II condition are commited to this fate much earlier and organize the axis in a different way as compared to embryos that already have decided to not stop in diapause II [30].

As already described, a DCE lengthens its axis and form somites mantaining a slim morphology, while a not DCE increases also its lateral size while lenghtening. When somitogenesis starts my datas suggests (even if observed in only one case) that a DCE is already shorter than a not DCE, and as long as the development continues the not DCE mantains much more proliferation compared to a DCE. This results in an increase in cells number also in the width of the embryo and could be the explaination for the chubby morphology.

Diapause II stage is characterized by an arrest of development and cell proliferation that happens at mid somitogenesis. FUCCI fish in diapause II condition have only few green cells along the midline of their axis, that are probably blocked in G2 since do not move or divide as far as it can be judged by eye while the other cells are in G1, G0 or in a post M phase. The dynamics of cell cycle down-regualtion in a DCE that transit from a developing embryo at 10 somite stage with the majority of cells being green and dividing cells to a totally blocked embryo in 30 somites with almost no green proliferating cells could not be documented. .

What can be theorized is either a progressive reduction of the proliferation as long as the somitogenesis proceeds, or a rapid drop after that the 30 somites stage is reached. However, considering that down-regualtion of cell cycle upon entry in diapause I is rapid and completed in a few hours, the second possibility appears more likely. All the cells kinetics are differentially modulated in diapause II and also the regulation of the cell cycle could be different or anyway delayed as compared to a normal developmental condition. Cells could for example stop to cycle at 30 somites but still appear green just because protein degradation is inhibited and fade the green signal slowly over time only due to the high GFP stability.

Unfortunately imaging the entry in diapause II is difficult due to technical limitations since the experimental conditions for imaging a developing embryo imply high temperatures that induce diapause release and inhibit diapause maintenance, induction or extension. In addition, diapause is a very long developmental process, that lasts for days and also this makes acquiring data very hard.

The release from diapause is a much more clear process and is also easier to record. It involves a large part of the cells of the embryo that synchronously, as happens for the release from diapause I, start to proliferate again. The reactivation is incredibly fast (as compared to the total duration of development) and after few hours the embryo's cells reach proliferation levels that are comparable to the levels of a not DCE at the same developmental stage. In addition, in the hours just following the reactivation, the embryo changes morphology and shapes in a way that is very similar to not DCE, becoming wider and chubby.

Concluding, in few hours the embryo reactivates the cell cycle in a large part of its cells and corrects its developmental pathway to became the same as not DCEs. Then it continues its normal development, slowing down the proliferation process, as happen also in the later embryonic stages of not DCEs and forms the complete embryo, that will be indistinguishable from a not DCE.

Why does the morphology of DCE and non-DCE embryo differ between 10- and 30-somite stages?

A theory that could explain this dynamic postulates that blocking a smaller (thinner) embryo is energetically less costly than blocking a larger (broader) one. The primordial axis of a 30 somites DCE is thinner in size compared to a not DCE. This means that to block, to maintain blocked, and mostly to reactivate its cells is less energetically demanding since the cells are smaller in number. In addition this strategy is very convenient also because in less than a day the size gap can be regained.

Thanks to these features, diapause II reveals to be the main arrest phase that can happen in a annual killifish embryo, and last even for years.

3.6 Diapause molecular factors.

The molecular factors involved in the diapause process, in killifishes, are largely unknown. Many evidences show that metabolic pathways are reduced to minimum levels but nobody knows exactly which are the key molecules that influence this change.

MiRNAs have never been investigated in vertebrate diapause. MicroRNAs act by translational inhibition and subsequent RNA degradation due to deadenylation of polyA tails. The respective contribution of these two modes of action to repression of gene expression is debated.

MicroRNAs could play a main role in diapause induction and regulation, since it is well known how a single microrna can control the expression levels of many genes belonging to the same or to different pathways.

To verify this hypothesis a microRNA expression profile was perfomed on annual and non annual killifishes species belonging to each one of the three clades, during the stage of diapause II in annual species or the equivalent morphological stage in non annual species.

Results showed how, regardless the phylogenesis, annual and non annual killifish completely separate on a MDS analysis, meaning that annuals features, in this particular stage, influence gloable miRNA expression profiles stronger than phylogenetic relationships.

This suggests that microRNAs are really involved in the diapause process and probably play a main role in diapause control during development.

Among all microRNAs found with the differential miR seq analysis, the miR 430 cluster emerges. This microRNA cluster is less expressed in annual diapausing embryos rather then in non annual or in annual developing embryos.

In zebrafish, where this cluster has been characterized, its expression rises after the mid blastula transition and its role is mainly involved with the degradation of maternal RNAs [124]. The temporal expression analysis (Figure 2.40) shows that also in N. furzeri, an annual killifish, it start to be expressed after the mid blastula transition phase.

In zebrafish, during pre-blastula stages, miRNA-430 was shown to act primarily by inhibiting protein synthesis [126]. However, after onset of zygotic transition and in adult cells mRNA degradation seems to be the predominant mechanism.

The miR-462/miR-731 cluster is induced under hypoxic stress via hypoxia-inducible factor 1α in zebrafish and functions in cellular adaptations. Overexpression of miR-462 and miR-731 represses cell proliferation through blocking cell cycle progress of DNA replication, and induces apoptosis [127]. In situ detection revealed furthermore that in zebrafish the miR-462/miR-731 cluster is highly expressed in a consistent and ubiquitous manner throughout the early developmental stages [127]. Since killifish embryos are extremely tolerant to hypoxia [128] this could be the reason why the expression of miR-462/miR-731 results lower than in developing embryos. It should be noted that hypoxia in zebrafish also up-regulates miR-430, again a finding that I observed in directly developing embryos.

Another interesting microRNA is miR-101, it acts as a highly-connected hub in gene regulatory networks transcription factors and epigenetic modulators as the first neighbors and genes involved in cell-cycle progression as second neighbors [129]. Overexpression of miR-101 is known to induce

cell-cycle arrest in different cell types [50]. So high levels of miR-101 in diapausing embryos would contribute to the G1 block that is typical of diapause [41].

Finally, down-regulation of the miR-17~92 cluster (oncomiR-1) could be linked to depression of the cell cycle. OncomiR-1 is is major regulator of cell cycle and overexpressed in several tumors cycle [123]. On the other hand, it is well-established that oncomiR-1 is downregulated during aging of human mitotically-active cells where it targets the cell-cycle inhibitor p21[130] and in different models of replicative senescence *in vitro*.

Concluding, since diapause is characterized by a prominent depression of protein synthesis, that is reduced to 10% of the pre-diapause levels, it is therefore highly likely that both proteins and mRNAs are stabilized during diapause. In this context, miRNAs could act primarily, if not exclusively, by inhibiting protein synthesis. Upon exit of diapause, release of miRNAs would allow immediate onset of translation. This concept is further supported by the observation that diapausing embryos of *N. furzeri* show paradoxical up-regulation of genes related to translational elongation, suggesting that these embryos are primed for a catch-up process upon exit from diapause.

4. Material and methods

4.1 Fish maintenance

4.1.1 Fish husbandry

Wild type fishes used were raised in 35 lt tanks (25cm x 50cm x 28cm) at these densities

Aplocheilus lineatus, Aphyosemion australe, Aphyosemion striatum, Fundulopanchax gardneri, Nothobranchius furzeri, *Nothobranchius guentheri*, *Nothobranchius korthause, Scriptaphysemion guignardi* and *Epiplatys dageti monroviae:* 3-4 couples each tank;

Nothobranchius melanospilus: 1-2 couples each tank; *Callopanchax occidentalis, Nematolebias whitei:* 1 couple each tank; *Rivulus cylindraceus, Rachovia brevis, Austrofundulus leohoignei:* 3 couples each tank;

Water parameters for all species were ph: 7-8; Kh: 3-5; T: 24-26 °C.

25% of the water in each tank was replaced with fresh tap water during every week.

Fishes were raised in 12 hours of light and 12 of darkness.

Nothobranchius furzeri transgenic fishes were raised in the same water and environmental condition of all the other fishes, but from the 3rd to the 8th week of life they were kept in smaller 3,8 lt tanks (25cm x 10cm x 15cm) at the density of 1 couple for each tank. After the 8th week they were moved in the 35 lt tank like all the other fishes.

4.1.2 Fish feeding

All the fishes were fed with “SHG microgranuli” and chironomus two times a day and “Premium Artemia Coppens®” once a day as much as they can eat except for *Nothobranchius furzeri* breeders and *Nothobranchius furzeri* transgenic lines.

Nothobranchius furzeri breeders and N*othobranchius furzeri* transgenic lines were fed instead with chironomus 2-3 times a day and “Premium Artemia Coppens®” 1-2 times a day.

4.2 Breeding

Annual and non-annual fish were bred in two different ways:

For annual ones a box (from 20cm x 15cm x 10cm to 9cm x 9cm x 4cm) half full of river sand (**ø <** 0,2mm) was put on the bottom of the tank. Lot of small boxes (0,7-1,3 for each male in the tank) worked better in tanks with 4+ males. The boxes were put in the fish tanks for 2-3 hours 3-5 days a week, and the average number of eggs layed by each female in the sand was 20-50, depending on species, fish, age and tank fish density. The sands were always put at the same hour of the day, (for example from 10 am to 13 am, or from 2 pm to 5 pm) to train the fish to breed at that hours and to maximize the egg production.

Non-annual fish were bred in a total different way. 25 cm long "breeding mops" were made using 2 mm thick green, brown or grey 100% acrylic wool and a bijou was screwed at the top of them for making them floating. One or more mops (optimum was one every two males) were put in the tanks. After a short period, fish learned to go in the mops and breed inside it, laying eggs in the on the wool filaments. Depending on species, mops were kept in the tanks from 1 hour to 1 day, allowing the fish to breed inside of them. The average number of eggs layed by each female was greatly different, from 2 to 40, depending mostly on species.

4.3 Eggs collection

Annual species eggs were collected by removing the bowl from the tank, sieving the sand with a sieve (1 mm grid width) and then trasferring the eggs from the sieve to a petri dish filled with tap water.

Non-annual species eggs were collected by removing the mops from the tanks, looking for them through the wool filaments, taking them with hands and putting them in a petri dish full of tap water.

Once collected dead and bad shaped eggs were removed from the petri dish, and the other were transferred to another petri dish in 35ml of tap water at the density of max 50 eggs per petri dish.

The eggs were then kept at 26°C.

4.4 Eggs husbandry

Non-annual fishes eggs were kept in a 50 ml petri dish with 35 ml of tap water at 26°C until the hatch (that usually required 22 days). The water in the petri dish was replaced once a day with new tap water and the embryos that died during this period were daily removed.

The hatched frys were kept for the first 4-10 weeks, depending on species, in small 4 lt tanks, in aquarium water at the density of max 5 fish in each tank, and were fed only with brine shrimps.

The water in these tanks was half replaced with aquarium water every two days, and the tanks were kept at 26 °C.

After fish reached the size of 2-3 cm they were moved in the 35 lt tanks of the aquariums.

Annual wild type fishes embryos and F1, F2 or F3 transgenic embryos were kept in 50 ml petri dish in 35 ml of tap water, at 26°C, until their eyes turned from colorless to black (that usually required around 14 days). During this period the water in the petri dish was replaced once a day with fresh tap water and the embryos that died during development were daily removed.

Once the eye of the surviving embyos turned black, they were moved to peat moss petri dishes (50 ml petri dishes with 0,5 cm of fairly humid peat moss or coconut fiber pressed on the bottom). Up to 150 embryos were put in each peat moss petri dish, and kept at 26°C in this condition until their eyes turned from black to totally golden (that usually required 14 days).

Once golden eyed, the embryos were put in a small 5 lt tank with 1 cm high 4°C aquarium water and a big spoon of peat moss. In these condition usually more than 60% of the embryos was able to hatch in 1-2 days.

The hatched frys were then kept for the first 4 weeks, depending on species, in small 4 lt tanks, in aquarium water, at the density of max 5 fish in each tank, and were fed only with brine shrimps. In these tanks was put a big spoon of peat moss, and the water level was gradually increased for the first week from 1 cm to 10 cm (+3 cm of acqaurium water every 2 days).

After the first week, the water in these tanks was half replaced with aquarium water every two days, and the tanks were kept at 26 °C.

After fish reached the size of 2-3 cm (usually after 4 weeks) they were moved in the 35 lt tanks of the aquariums.

4.5 Transgenic eggs husbandry

Nothobranchius furzeri F0 transgenic embryos (freshly injected embryos) were kept in a 50 ml petri dish in 35 ml of tap water, at 26°C for the first 2 days after injection. During this period the water in the petri dish was replaced once a day with new one and the embryos that died were daily removed.

After 2 days survived embryos were moved to peat moss petri dishes (50 ml petri dishes with 0,5 cm of fairly humid peat moss or coconut fiber pressed on the bottom). Up to 150 embryos were put in each peat moss petri dish, and kept at 26°C in this condition until their eyes fully developed turning to totally golden (this required from 20 days to several months since a lot of injected embryos entered in diapause).

Once golden eyed, the embryos were put in a small 5 lt tank with 1 cm high 4°C aquarium water and a big spoon of peat moss. In these condition usually more than 60% of the embryos was able to hatch in 1-2 days.

The hatched frys were then kept for the first 4 weeks, in small 4 lt tanks, in aquarium water, at the density of max 5 fish in each tank, and were fed only with brine shrimps. In these tanks was put a big spoon of peat moss, and the water level was gradually increased for the first week from 1 cm to 10 cm (+3 cm of acqaurium water every 2 days).

After the first week, the water in these tanks was half replaced with aquarium water every two days, and the tanks were kept at 26 °C.

After taht fish reached the 3rd week of life they were screened with a fluorescence miscroscope to check the reliability of the signal, and the embryos with an absent, too weak or not correct signal were discarded. The fish with a correct signal expression were then moved from the 3rd to the 8th week of life in smaller 3,8 lt tanks (25cm x 10cm x 15xm), in an aquarium at the density of 1 couple each tank. After the 8th week they were moved in the 35 lt tanks like all the other fishes.

4.6 Transgenic embryos screening

Transgenic embryos were screened with a fluorescence miscroscope at different stages (epiboly, dispersed phase, mid somitogenesis, hatched fry or 4 weeks old fish) depending on the injected construct.

Fish were anestetized with tricaine 0,5X for few minutes, then screened and selected.

Fish that showed the correct pattern of expression of the transgene were raised, the rest was discarded.

All the embryos belonging to all the transgenic generations were screened.

4.7 Transgenic lines generation

4.7.1 FUCCI plasmids construction

FUCCI plasmids were constructed starting from zebrafish mKO2-zCdt1(1/190) and mAG-zGem(1/100) plasmids [116], replacing the original promoter with the zebrafish ubiquitin promoter.

Original plasmids were amplified in E. coli and purified with Wizard® Plus SV Minipreps DNA Purification Promega. Then 2 µg of each plasmid were cut with Nhe1 and BamHI, ran on gel and the higher band was piurified using Wizard® SV Gel and PCR Clean-Up Promega.

Ubiquitin promoter was amplified by PCR from pENTR5'_ubi using Q5® High-Fidelity DNA Polymerase, with these primers (F: 5'-cattgaGCTAGCatggatgttttcccagtcacgacg-3', R:5'-tgactaGGATCCtgtaaacaaattcaaagtaagat-3') and the following termocicling protocol :

98°C 30"

(98°C 10", 52°C 30", 72°C 2') X35 cycles

72°C 2'

pENTR5'_ubi was a gift from Leonard Zon (Addgene plasmid # 27320) [131].

The PCR product was ran on an agarose gel and the band purified using Wizard® SV Gel and PCR Clean-Up Promega.

Vectors and the ubiquitn promoter insert were ligated over night using NEB T4 DNA Ligase, in a molar ratio of 1:3, mixing 50 ng of vectors and 73 ng of insert.

The resulting plasmid was then amplified in E. coli and purified with Wizard® Plus SV Minipreps DNA Purification Promega. This final plasmid was injected in 1 cell stage embryos together with the tol2 synthetic RNA.

4.7.2 Tol2 RNA synthesis

Tol2 synthetic RNA was synthetized using mMESSAGE mMACHINE® SP6 Transcription Kit Ambion. pCS2FA-transposase plasmid, linearized using NotI was used as template and sp6 as promoter for RNA trascription. Resulting synthetic RNA concentration was measured with a nanodrop and on an agarose gel.

4.7.3 Eggs injection

Transgenic fish were generated injecting 1 µl of a solution containing 30ng/µl of TOL2 RNA, 40ng/µl of plasmid DNA, 400 mM of KCl in 1 cell stage *N. furzeri* embryos.

Injections were performed at 26°C using a Leica M80 stereo microscope and a Tritech air injection system.

Eggs were oriented on a 2% agar framework and injected sequentially.

Once injected, eggs were put in a petri dish with 26°C aquarium water. After1.5 hours dead eggs were removed, and the others were let develop in a new petri dish with 35 ml of 26°C aquarium water.

4.8 FUCCI synthetic RNA

FUCCI synthetic RNAs were synthetized using mMESSAGE mMACHINE® SP6 Transcription Kit Ambion. Azami green-geminin and kusabira orange-Cdt1 DNA fragments were cloned in a pCS2 vector using BamH1 and Cla1. Then the resulting vectors were linearized using NotI and used as template for trascription. Sp6 promoter was used for trascription. synthetic RNA concentration was measured with a nanodrop and on an agarose gel.

Once transcribed the RNA was stored at -80 and thawed just before the injection.

The injections were performed exactly in the same way as for the transgenic line generation.

The mixture injected was 1 ul composed by 400 ng/ul of total RNA (half FUCCI green RNA and half FUCCI red RNA).

1 hour after injections, dead eggs were removed and the other ones were embedded in 1% low melting agarose following the microscope sample preparation protocol.

4.9 Mir-430 reporter RNA

Mir-430 reporters synthetic RNA were synthetized using mMESSAGE mMACHINE® SP6 Transcription Kit Ambion. The reporter plasmid and the mutated reporter plasmid, gifted by Giraldez AJ [124], were linearized using NotI and used as template. Sp6 promoter was used for RNA trascription. Resulting synthetic RNAs concentration was measured with a nanodrop and on an agarose gel.

4.10 Microscopy

4.10.1 Samples preparation

All the pre-hatching embryos acquired were prepared in this way, regardless their developmental stage:

From 3 to 40 eggs (depending on experiment) were put in a 1,5 ml falcon tube with 10 ml of liquid low melting agarose 1,5% solution, not warmer than 32°C. The falcon was left in agitation for 30 seconds to completely mix the eggs and the liquid agarose.

The non-annual species eggs, that presented a lot of hairs on the surface, were shaved with forceps before the agar embedding, in order to achieve a better quality of image during images acquisitions.

The eggs and 3 ml of the agar solution were poured in a willco dish and the eggs were put in the middle using forceps, spaced each other by more or less 2 mm. Only for the experiment of the miR-430 reporter 40 eggs were poured into a 50 ml petri dish with 30 ml of liquid low melting agar

solution. After poured into the dish, the eggs were carefully oriented in the desired way using forceps, then the agar was left solidify at room temperature for 10 to 30 minutes.

4.10.2 Brightfield acquisitions

Once ready with agarose embedded eggs, the willco dish was parafilmed, reversed upside down and put under a Leica M80 stereo microscope. Up to 6 eggs were embedded each time for brightfield acquisitions. The microscope was setted up to offer the best condition of brightness and constrast and the zoom was adjusted accordingly to the number and the size of the eggs to image.

Photos were captured every 2 to 5 minutes, depending on species, with a Nikon Digital Sight DS-Fi1 camera or with a ZEISS Axiocam ERc 5s camera. Acquisition lasted from hours to several days, depending on species.

4.10.3 Brightfield videos and images processing

All the acquired photos relative to a single acquisition session, were loaded on Fiji imagej as an image sequence and analyzed to verify sincrony between the eggs in the acquisition field.

A single egg present in the image was chosen, rotated and cropped, in order to make a new image sequence including only that embryo, and this was saved in a separated folder.

This new folder was imported in Sony Vegas, a video-make software, in order to make a smooth video from a discontinuous image sequence. Time, writings, video effects and soundtrack were added as different levels and all the levels were rendered olny once in a .avi file to mantain the best possible resolution.

Brightfield images were edited with GIMP. Contrast, brightness and sharpness were modified in order to make pictures the most possible beautiful, clear and informative.

4.10.4 Confocal acquisitions

For confacal acquisitions a Leica TCS SP5 X inverted microscope was used. 3 to 5 embryos were embedded in agar in a willko dish that was then sealed with parafilm. The position of each embryo in the dish was marked with the Leica confocal software Leica LAS X Core, and automatically, every 10 minutes, every embryo in the dish was scanned sequentially with a 488 nm and a 543 nm argon laser. Only the top half of each embryo (about 500 μm) was scanned, since the light can't well penetrate the lower half, resulting in distorted and faded lower part images. Images stacks were acquired every 7-12 μm, depending on samples and on experiments. Experimental sessions lasted from 10 to 61 hours, depeding on the developmental stage acquired. Time lapses acquisitions were performed at 26°C. Images were acquired with a 10x dry objective and with a digital zoom of 1.2x.

4.10.5 Fluorescence images processing

All the stacks relative to a single time point were projected using Fiji Z-project standard deviation algorithm, both for green and red fluorescence channels. Projected images were then adjusted in brightness and contrast with GIMP in order to optimize the "signal to noise" ratio and be more clear and informative.

4.10.6 Imaris analysis

Raw Leica datas from time lapses acquisitions were analyzed with Imaris. Whole time lapses acquisition datas were loaded on Imaris, then the red and green channel were adjusted in brightness and contrast in order to separate the cells nuclei from the background as best as possible. For the stages of epiboly, diapause I and dispersed phase the red and green nuclei were then converted in YSL cells dots, epiblast red cells and epiblast green cells with Imaris particle analysis function. It was possible to separate YSL red cells and epiblast red cells (that appeared both red) using the size recognition function of Imaris particle analysis.

For the stages of reaggregation, axis formation, segmentation and diapause II, was not possible to track separately the cells nuclei, so the aggregates of cells were converted in an unique surface with the surface analysis function of Imaris. Parameters for particle or surface recognition were adjusted

in different way for each set of images analyzed, in order to track the structures of interest getting rid of the background and of the aspecific signals.

Particles belonging to background or to artifact structures that were not filtered out by the automatic recognition process were removed manually.

4.11 Graphs productions

Annual vs non-annual developmental graphs were produced by recognizing on the time lapses image sequences the various developmental stages (1, 2, 4, 8, n cells). Then the relative photo number was multiplied by the number of minutes by which the photos were acquired, divided by 60 to convert it into hours and plotted on a graph.

Imaris related graphs, concerning FUCCI fluorescence analysis, were made with Imaris, with the particle or surface analysis feature. All datas plotted in the graphs are relative to the segmentation analysis or the track analysis done by the program.

The graph relative to the comparison between CDE and not CDE during somitogenesis was done measuring manually with Fiji the lenght of the different part of the two kind of embryos, time point by time point, and then plotting the datas in the graph.

4.12 Sequencing

4.12.1 Samples collection

Annual fishes embryos were collected for the RNA extraction during diapause II stage, after at least a week from the beginning of the diapause condition. Non-annual fishes embryos were instead collected at mid somitogenesis, in a developmental stage equivalent to the annual diapause II.

For the differential analysis on *N. furzeri* two pool of eggs were made.

200 eggs were collected from *Notobranchius furzeri* PL strain, then 100 were kept at 18°C and the other 100 at 28°C. All the 100 eggs at 18°C entered diapause II and, after one week that they were in diapause, 30 of them were grinded for RNA extraction. Concerning the 100 eggs at 28°C, at the

stage of mid somitogenesis 30 of them were grinded for RNA extraction, and the other 70 were kept as control. All the 70 control eggs didn't entered into the diapause condition.

4.12.2 RNA extraction

The RNA from killifish embryos was extracted with the following protocol:

15-30 Embryos in diapause 2 or diapause 2 equivalent stage (mid somitogenesis) were grinded together in 1 ml of QIAzol Lysis Reagent QUIAGEN and incubated for 5 minutes at RT. 200 ul of chloroform were added to the homogenate and then the samples were heavily shaked and centrifuged at 12.000 xg at 4°C for 20 minutes. The aqueous phase was transferred to a new cup and 1,1 volumes of isopropanol, 0,16 volumes of NaAc (2M; pH 4.0), and 10µg of glicogen were added to each solution. After an incubation of 2 hours at -80°C the samples were centrifuged at 12.000 xg at 4°C for 20 minutes. Supernatants were discarded and the pellet were washed twice with 1ml of 80% ethanol.

RNAs were resuspended in ultra-pure H_2O.

4.12.3 Sequencing

miRNAs new generation sequencing on annual and non-annual fishes embryos samples were performed by Mario Baumgard in the Leibniz Institute for Age Research - Fritz Lipmann Institute in Jena.

4.13 Fin cut experiment

Specimens were anesthetized with a tricaine solution (400 mg/L), wedged in a sponge, and the fin was gently cutted using sharp scissors. The operation did not required more than 30 seconds. The fish were observed once a day for 10 days using a Leica MZ10 F stereo microscope. Both fluorescence and brightfield Images were captured using fixed exposure and gain parameters. Fish were kept anesthetized in a tricaine solution (400 mg/L) for the whole acquisition procedure, that lasted no more than 5 minutes for each specimen.

4.14 Mir-430 sensor experiment

4.14.1 Sensor injection

Embryos were injected with 0,5 ul of 400 ng/µl miR-430 sensor RNA or with miR-430-Mut sensor RNA at 1 cell stage. In both case, also 0,5ul of 400ng/µl of RFP RNA were co-injected. 30 minutes after the injection dead embryos were removed and the living ones were embedded in 26°C liquid 0,7% low melting agarose, on the bottom of a 50 ml petri dish. Separated petri dishes were used for the two pool of injected embryos (miR-430 and miR-430-Mut).

After the agarose solidyfied both petri dishes were incubated at 26°C.

4.14.2 Sensor image acquisition

Sensor injected embryos were acquired every day using a Nikon Eclipse E600 straight fluorescence microscope.

Images were captured using a Nikon element NIS-Elements F. The same values of gain and exposure were used for all the pictures and for both red and green fluorescence channels. One-two embryos were captured in each image field, at a magnification of 10X.

4.14.3 Sensor graph production

Sensors injected embryos images were opened in Fiji as an image sequence, eggs were selected with the round selection tool and pixel intensity was measured inside the selection. An individual measurement was performed for the images acquired in red and green, exactly in the same selection region. Each time point in the graph represent the mean of each embryo's green-pixel-intensity/red-pixel-intesity ratio.

References

[1] D. P. Ranier Froese, “List of Nominal Species of Rivulidae (Rivulines),” *FishBase*, 2007.

[2] C. G. Murphy WJ, “A molecular phylogeny for aplocheiloid fishes (Atherinomorpha, Cyprinodontiformes): the role of vicariance and the origins of annualism.,” *Mol Biol Evol*, vol. 14, pp. 790–799, 1997.

[3] J. P. Wourms, “Developmental biology of annual fishes. I. Stages in the normal development of Austrofundulus myersi Dahl.,” *J. Exp. Zool.*, vol. 182, no. 2, pp. 143–167, 1972.

[4] T. Hrbek and A. Larson, “The evolution of diapause in the killifish family Rivulidae (Atherinomorpha, Cyprinodontiformes): a molecular phylogenetic and biogeographic perspective,” *Evolution (N. Y).*, vol. 53, no. 4, pp. 1200–1216, 1999.

[5] W. J. E. M. Costa, “No TitleAnàlise filogenètica da famìlia Rivulidae (Cyprinodontiformes, Aplocheiloidei),” *Rev. Bras. Biol.*, vol. 50, pp. 65–82, 1990.

[6] A. I. Furness, “The evolution of an annual life cycle in killifish: adaptation to ephemeral aquatic environments through embryonic diapause,” *Biol. Rev.*, p. n/a–n/a, May 2015.

[7] M. GS, “Annual fishes,” *Aquarium J.*, vol. 23, pp. 125–141, 1952.

[8] R. Blažek, M. Polačik, and M. Reichard, “Rapid growth, early maturation and short generation time in African annual fishes.,” *Evodevo*, vol. 4, no. 1, p. 24, 2013.

[9] T. Genade, M. Benedetti, E. Terzibasi, P. Roncaglia, D. R. Valenzano, A. Cattaneo, and A. Cellerino, “Annual fishes of the genus Nothobranchius as a model system for aging research.,” *Aging Cell*, vol. 4, no. 5, pp. 223–233, 2005.

[10] J. E. Podrabsky, J. F. Carpenter, and S. C. Hand, “Survival of water stress in annual fish embryos: dehydration avoidance and egg envelope amyloid fibers.,” *Am. J. Physiol. Regul. Integr. Comp. Physiol.*, vol. 280, no. 1, pp. R123–R131, 2001.

[11] J. Podrabsky and S. Hand, “The bioenergetics of embryonic diapause in an annual killifish, austrofundulus limnaeus,” *J. Exp. Biol.*, vol. 202 (Pt 19, pp. 2567–80, 1999.

[12] J. P. Wourms, “Developmental Biology of Annual Fishes,” *J. Exp. Zool.*, pp. 143–168, 1972.

[13] D. L. Denlinger, “Regulation of diapause.,” *Annu. Rev. Entomol.*, vol. 47, pp. 93–122, 2002.

[14] D. A. Hahn and D. L. Denlinger, “Energetics of insect diapause.,” *Annu. Rev. Entomol.*, vol. 56, pp. 103–121, 2011.

[15] V. Koštál, “Eco-physiological phases of insect diapause,” *Journal of Insect Physiology*, vol. 52, no. 2. pp. 113–127, 2006.

[16] J. C. Fenelon, A. Banerjee, and B. D. Murphy, “Embryonic diapause: Development on hold,” *Int. J. Dev. Biol.*, vol. 58, no. 2–4, pp. 163–174, 2014.

[17] J. P. Wourms, “The developmental biology of annual fishes. II. Naturally occurring dispersion and reaggregation of blastomers during the development of annual fish eggs.,” *J. Exp. Zool.*, vol. 182, no. 2, pp. 169–200, 1972.

[18] J. P. Wourms, “The developmental biology of annual fishes. 3. Pre-embryonic and embryonic diapause of variable duration in the eggs of annual fishes.,” *J. Exp. Zool.*, vol. 182, no. 3, pp. 389–414, 1972.

[19] J. M. Oppenheimer, “The normal stages of Fundulus heteroclitus,” *Anat. Rec.*, vol. 68, no. 1, pp. 1–15, Apr. 1937.

[20] C. B. Kimmel, W. W. Ballard, S. R. Kimmel, B. Ullmann, and T. F. Schilling, “Stages of embryonic development of the zebrafish.,” *Dev. Dyn.*, vol. 203, no. 3, pp. 253–310, 1995.

[21] T. Iwamatsu, “Stages of normal development in the medaka Oryzias latipes.,” *Mech. Dev.*, vol. 121, no. 7–8, pp. 605–618, 2004.

[22] H. SWARUP, “Stages in the development of the stickleback Gasterosteus aculeatus (L.).,” *J. Embryol. Exp. Morphol.*, vol. 6, no. 3, pp. 373–383, 1958.

[23] J. Newport and M. Kirschner, “A major developmental transition in early Xenopus embryos: II. Control of the onset of transcription.,” *Cell*, vol. 30, no. 3, pp. 687–696, 1982.

[24] G. SF, “Developmental Biology,” *Sunderl. Sinauer Assoc.*, 2000.

[25] C. F. Graham and R. W. Morgan, “Changes in the cell cycle during early amphibian development,” *Developmental Biology*, vol. 14, no. 3. pp. 439–460, 1966.

[26] M. Kraeussling, T. U. Wagner, and M. Schartl, “Highly asynchronous and asymmetric cleavage divisions accompany early transcriptional activity in pre-blastula medaka embryos.,” *PLoS One*, vol. 6, no. 7, p. e21741, 2011.

[27] S. Mathavan, S. G. P. Lee, A. Mak, L. D. Miller, K. R. K. Murthy, K. R. Govindarajan, Y. Tong, Y. L. Wu, S. H. Lam, H. Yang, Y. Ruan, V. Korzh, Z. Gong, E. T. Liu, and T. Lufkin, "Transcriptome analysis of zebrafish embryogenesis using microarrays," *PLoS Genet.*, vol. 1, no. 2, pp. 0260–0276, 2005.

[28] L. Carvalho and C. P. Heisenberg, "The yolk syncytial layer in early zebrafish development," *Trends in Cell Biology*, vol. 20, no. 10. pp. 586–592, 2010.

[29] C. Schröter, L. Herrgen, A. Cardona, G. J. Brouhard, B. Feldman, and A. C. Oates, "Dynamics of zebrafish somitogenesis," *Dev. Dyn.*, vol. 237, no. 3, pp. 545–553, 2008.

[30] A. I. Furness, D. N. Reznick, M. S. Springer, and R. W. Meredith, "Convergent evolution of alternative developmental trajectories associated with diapause in African and South American killifish," *Proc. R. Soc. B Biol. Sci.*, vol. 282, no. 1802, pp. 20142189–20142189, Jan. 2015.

[31] J. E. Podrabsky, I. D. F. Garrett, and Z. F. Kohl, "Alternative developmental pathways associated with diapause regulated by temperature and maternal influences in embryos of the annual killifish Austrofundulus limnaeus.," *J. Exp. Biol.*, vol. 213, no. Pt 19, pp. 3280–3288, 2010.

[32] C. a Carter and J. P. Wourms, "Cell behavior during early development in the South American annual fishes of the genus Cynolebias.," *J. Morphol.*, vol. 210, no. 3, pp. 247–66, 1991.

[33] L. PJ, "An experimental study of diapause in annual fishes," *Kathol. Univ. te Nijmegen*, pp. 1–179, 1988.

[34] J. Markofsky and J. R. Matias, "The effects of temperature and season of collection on the onset and duration of diapause in embryos of the annual fish Nothobranchius guentheri.," *J. Exp. Zool.*, vol. 202, no. 1, pp. 49–56, 1977.

[35] D. R. Valenzano, S. Sharp, A. Brunet, and B. J. Andrews, "Transposon-Mediated Transgenesis in the Short-Lived African Killifish Nothobranchius furzeri, a Vertebrate Model for Aging," *G3: Genes|Genomes|Genetics*, vol. 1, no. 7. pp. 531–538, 2011.

[36] B. E. Machado and J. E. Podrabsky, "Salinity tolerance in diapausing embryos of the annual killifish Austrofundulus limnaeus is supported by exceptionally low water and ion permeability," *J. Comp. Physiol. B Biochem. Syst. Environ. Physiol.*, vol. 177, no. 7, pp. 809–820, 2007.

[37] M. Polačik and M. Reichard, "Asymmetric reproductive isolation between two sympatric

annual killifish with extremely short lifespans," *PLoS One*, vol. 6, no. 8, 2011.

[38] A. I. Furness, K. Lee, and D. N. Reznick, "Adaptation in a variable environment: Phenotypic plasticity and bet-hedging during egg diapause and hatching in an annual killifish," *Evolution (N. Y).*, vol. 69, no. 6, pp. 1461–1475, Jun. 2015.

[39] J. M. Duerr and J. E. Podrabsky, "Mitochondrial physiology of diapausing and developing embryos of the annual killifish Austrofundulus limnaeus: Implications for extreme anoxia tolerance," *J. Comp. Physiol. B Biochem. Syst. Environ. Physiol.*, vol. 180, no. 7, pp. 991–1003, 2010.

[40] C. L. Meller, R. Meller, R. P. Simon, K. M. Culpepper, and J. E. Podrabsky, "Cell cycle arrest associated with anoxia-induced quiescence, anoxic preconditioning, and embryonic diapause in embryos of the annual killifish Austrofundulus limnaeus," *J. Comp. Physiol. B Biochem. Syst. Environ. Physiol.*, vol. 182, no. 7, pp. 909–920, 2012.

[41] J. E. Podrabsky and K. M. Culpepper, "Cell cycle regulation during development and dormancy in embryos of the annual killifish Austrofundulus limnaeus," *Cell Cycle*, vol. 11, no. 9. pp. 1697–1704, 2012.

[42] P. J. Levels, R. E. Gubbels, and J. M. Denucé, "Oxygen consumption during embryonic development of the annual fish Nothobranchius korthausae with special reference to diapause.," *Comp. Biochem. Physiol. A. Comp. Physiol.*, vol. 84, no. 4, pp. 767–770, 1986.

[43] E. T. Tozzini, A. Dorn, E. Ng'oma, M. Polačik, R. Blažek, K. Reichwald, A. Petzold, B. Watters, M. Reichard, and A. Cellerino, "Parallel evolution of senescence in annual fishes in response to extrinsic mortality.," *BMC Evol. Biol.*, vol. 13, p. 77, 2013.

[44] L. Fontana, L. Partridge, and V. D. Longo, "Extending healthy life span--from yeast to humans.," *Science*, vol. 328, no. 5976, pp. 321–326, 2010.

[45] C. Kenyon, "The first long-lived mutants: discovery of the insulin/IGF-1 pathway for ageing.," *Philos. Trans. R. Soc. Lond. B. Biol. Sci.*, vol. 366, no. 1561, pp. 9–16, Jan. 2011.

[46] J. J. McElwee, E. Schuster, E. Blanc, J. H. Thomas, and D. Gems, "Shared transcriptional signature in Caenorhabditis elegans Dauer larvae and long-lived daf-2 mutants implicates detoxification system in longevity assurance.," *J. Biol. Chem.*, vol. 279, no. 43, pp. 44533–43, 2004.

[47] X. Zhang, R. Zabinsky, Y. Teng, M. Cui, and M. Han, "microRNAs play critical roles in the survival and recovery of Caenorhabditis elegans from starvation-induced L1 diapause," *Proc. Natl. Acad. Sci.*, vol. 108, no. 44, pp. 17997–18002, 2011.

[48] Z. Pincus, T. Smith-Vikos, and F. J. Slack, "MicroRNA predictors of longevity in Caenorhabditis elegans," *PLoS Genet.*, vol. 7, no. 9, p. e1002306, 2011.

[49] K. Boulias and H. R. Horvitz, "The C. elegans MicroRNA mir-71 acts in neurons to promote germline-mediated longevity through regulation of DAF-16/FOXO," *Cell Metab.*, vol. 15, no. 4, pp. 439–450, 2012.

[50] A. De Lencastre, Z. Pincus, K. Zhou, M. Kato, S. S. Lee, and F. J. Slack, "MicroRNAs both promote and antagonize longevity in C. elegans," *Curr. Biol.*, vol. 20, no. 24, pp. 2159–2168, 2010.

[51] J. Kirschner, D. Weber, C. Neuschl, A. Franke, M. Böttger, L. Zielke, E. Powalsky, M. Groth, D. Shagin, A. Petzold, N. Hartmann, C. Englert, G. a. Brockmann, M. Platzer, A. Cellerino, and K. Reichwald, "Mapping of quantitative trait loci controlling lifespan in the short-lived fish Nothobranchius furzeri- a new vertebrate model for age research," *Aging Cell*, vol. 11, no. 2, pp. 252–261, 2012.

[52] S. Valdesalici and A. Cellerino, "Extremely short lifespan in the annual fish Nothobranchius furzeri.," *Proc. R. Soc. B Biol. Sci.*, vol. 270 Suppl, pp. 189–191, 2003.

[53] M. Baumgart, E. Di Cicco, G. Rossi, A. Cellerino, and E. T. Tozzini, "Comparison of captive lifespan, age-associated liver neoplasias and age-dependent gene expression between two annual fish species: nothobranchius furzeri and Nothobranchius korthause.," *Biogerontology*, vol. 16, no. 1, pp. 63–9, 2015.

[54] A. Lucas-Sánchez, P. F. Almaida-Pagán, J. A. Madrid, J. de Costa, and P. Mendiola, "Age-related changes in fatty acid profile and locomotor activity rhythms in Nothobranchius korthausae," *Exp. Gerontol.*, vol. 46, no. 12, pp. 970–978, 2011.

[55] T. Genade, M. Benedetti, E. Terzibasi, P. Roncaglia, D. R. Valenzano, A. Cattaneo, and A. Cellerino, "Annual fishes of the genus *Nothobranchius* as a model system for aging research," *Aging Cell*, vol. 4, no. 5, pp. 223–233, 2005.

[56] E. Terzibasi, D. R. Valenzano, M. Benedetti, P. Roncaglia, A. Cattaneo, L. Domenici, and A. Cellerino, "Large differences in aging phenotype between strains of the short-lived annual fish Nothobranchius furzeri," *PLoS One*, vol. 3, no. 12, 2008.

[57] D. R. Valenzano, E. Terzibasi, T. Genade, A. Cattaneo, L. Domenici, and A. Cellerino, "Resveratrol prolongs lifespan and retards the onset of age-related markers in a short-lived vertebrate," *Curr. Biol.*, vol. 16, no. 3, pp. 296–300, 2006.

[58] E. Di Cicco, E. T. Tozzini, G. Rossi, and A. Cellerino, "The short-lived annual fish Nothobranchius furzeri shows a typical teleost aging process reinforced by high incidence of age-dependent neoplasias," *Exp. Gerontol.*, vol. 46, no. 4, pp. 249–256, Apr. 2011.

[59] N. Hartmann, K. Reichwald, A. Lechel, M. Graf, J. Kirschner, A. Dorn, E. Terzibasi, J. Wellner, M. Platzer, K. L. Rudolph, A. Cellerino, and C. Englert, "Telomeres shorten while Tert expression increases during ageing of the short-lived fish Nothobranchius furzeri," *Mech. Ageing Dev.*, vol. 130, no. 5, pp. 290–296, 2009.

[60] C.-Y. Hsu, Y.-C. Chiu, W.-L. Hsu, and Y.-P. Chan, "Age-related markers assayed at different developmental stages of the annual fish Nothobranchius rachovii.," *J. Gerontol. A. Biol. Sci. Med. Sci.*, vol. 63, no. 12, pp. 1267–1276, 2008.

[61] C. Liu, X. Wang, W. Feng, G. Li, F. Su, and S. Zhang, "Differential expression of aging biomarkers at different life stages of the annual fish Nothobranchius guentheri," *Biogerontology*, vol. 13, no. 5, pp. 501–510, 2012.

[62] N. Hartmann, K. Reichwald, I. Wittig, S. Dröse, S. Schmeisser, C. Lück, C. Hahn, M. Graf, U. Gausmann, E. Terzibasi, A. Cellerino, M. Ristow, U. Brandt, M. Platzer, and C. Englert, "Mitochondrial DNA copy number and function decrease with age in the short-lived fish Nothobranchius furzeri," *Aging Cell*, vol. 10, no. 5, pp. 824–831, 2011.

[63] E. Ng'oma, K. Reichwald, A. Dorn, M. Wittig, T. Balschun, A. Franke, M. Platzer, and A. Cellerino, "The age related markers lipofuscin and apoptosis show different genetic architecture by QTL mapping in short-lived Nothobranchius fish," *Aging (Albany. NY).*, vol. 6, no. 6, pp. 468–480, 2014.

[64] D. R. Valenzano, E. Terzibasi, A. Cattaneo, L. Domenici, and A. Cellerino, "Temperature affects longevity and age-related locomotor and cognitive decay in the short-lived fish: Nothobranchius furzeri," *Aging Cell*, vol. 5, no. 3, pp. 275–278, 2006.

[65] E. T. Tozzini, M. Baumgart, G. Battistoni, and A. Cellerino, "Adult neurogenesis in the short-lived teleost Nothobranchius furzeri: Localization of neurogenic niches, molecular characterization and effects of aging," *Aging Cell*, vol. 11, no. 2, pp. 241–251, 2012.

[66] E. Terzibasi Tozzini, A. Savino, R. Ripa, G. Battistoni, M. Baumgart, and A. Cellerino, "Regulation of microRNA expression in the neuronal stem cell niches during aging of the short-lived annual fish Nothobranchius furzeri.," *Front. Cell. Neurosci.*, vol. 8, no. February, p. 51, 2014.

[67] M. Baumgart, M. Groth, S. Priebe, J. Appelt, R. Guthke, M. Platzer, and A. Cellerino, "Age-dependent regulation of tumor-related microRNAs in the brain of the annual fish Nothobranchius furzeri," *Mech. Ageing Dev.*, vol. 133, no. 5, pp. 226–233, 2012.

[68] M. Vrtílek and M. Reichard, "Highly plastic resource allocation to growth and reproduction in females of an African annual fish," *Ecol. Freshw. Fish*, p. n/a–n/a, Aug. 2014.

[69] I. Harel, B. A. Benayoun, B. Machado, P. P. Singh, C.-K. Hu, M. F. Pech, D. R. Valenzano, E. Zhang, S. C. Sharp, S. E. Artandi, and A. Brunet, "A platform for rapid exploration of aging and diseases in a naturally short-lived vertebrate.," *Cell*, vol. 160, no. 5, pp. 1013–26, 2015.

[70] R. Van Haarlem, R. Van Wijk, and J. G. Konings, "Analysis of the variability and of the lengthening of intercleavage times during the cleavage stages of Nothobranchius guentheri.," *Cell Tissue Kinet.*, vol. 16, no. 2, pp. 177–187, 1983.

[71] R. Van Haarlem, J. G. Konings, and R. Van Wijk, "Analysis of the relationship between the variation in intercleavage times and cell diversification during the cleavage stages of the teleost fish Nothobranchius guentheri.," *Cell Tissue Kinet.*, vol. 16, no. 2, pp. 167–176, 1983.

[72] R. Van Haarlem, R. Van Wijk, and A. H. Fikkert, "Analysis of the variability in cleavage times and demonstration of a mitotic gradient during the cleavage stages of Nothobranchius guentheri.," *Cell Tissue Kinet.*, vol. 14, no. 3, pp. 285–300, 1981.

[73] H. Wada, M. Iwasaki, T. Sato, I. Masai, Y. Nishiwaki, H. Tanaka, A. Sato, Y. Nojima, and H. Okamoto, "Dual roles of zygotic and maternal Scribble1 in neural migration and convergent extension movements in zebrafish embryos.," *Development*, vol. 132, no. 10, pp. 2273–2285, 2005.

[74] T. Xiao, T. Roeser, W. Staub, and H. Baier, "A GFP-based genetic screen reveals mutations that disrupt the architecture of the zebrafish retinotectal projection.," *Development*, vol. 132, no. 13, pp. 2955–2967, 2005.

[75] G. W. Stuart, J. V McMurray, and M. Westerfield, "Replication, integration and stable germ-line transmission of foreign sequences injected into early zebrafish embryos.," *Development*, vol. 103, no. 2, pp. 403–412, 1988.

[76] A. Amsterdam, S. Lin, and N. Hopkins, "The Aequorea victoria green fluorescent protein can be used as a reporter in live zebrafish embryos.," *Dev. Biol.*, vol. 171, no. 1, pp. 123–129, 1995.

[77] S. Higashijima, H. Okamoto, N. Ueno, Y. Hotta, and G. Eguchi, "High-frequency generation of transgenic zebrafish which reliably express GFP in whole muscles or the whole body by using promoters of zebrafish origin.," *Dev. Biol.*, vol. 192, no. 2, pp. 289–299, 1997.

[78] Q. Long, A. Meng, H. Wang, J. R. Jessen, M. J. Farrell, and S. Lin, "GATA-1 expression pattern can be recapitulated in living transgenic zebrafish using GFP reporter gene.," *Development*, vol. 124, no. 20, pp. 4105–4111, 1997.

[79] N. Gaiano, M. Allende, A. Amsterdam, K. Kawakami, and N. Hopkins, "Highly efficient germ-line transmission of proviral insertions in zebrafish.," *Proc. Natl. Acad. Sci. U. S. A.*,

vol. 93, no. 15, pp. 7777–7782, 1996.

[80] S. Lin, N. Gaiano, P. Culp, J. C. Burns, T. Friedmann, J. K. Yee, and N. Hopkins, "Integration and germ-line transmission of a pseudotyped retroviral vector in zebrafish.," *Science*, vol. 265, no. 5172, pp. 666–669, 1994.

[81] S. Ellingsen, M. A. Laplante, M. König, H. Kikuta, T. Furmanek, E. A. Hoivik, and T. S. Becker, "Large-scale enhancer detection in the zebrafish genome.," *Development*, vol. 132, no. 17, pp. 3799–3811, 2005.

[82] A. E. Davidson, D. Balciunas, D. Mohn, J. Shaffer, S. Hermanson, S. Sivasubbu, M. P. Cliff, P. B. Hackett, and S. C. Ekker, "Efficient gene delivery and gene expression in zebrafish using the Sleeping Beauty transposon," *Dev. Biol.*, vol. 263, no. 2, pp. 191–202, 2003.

[83] J. M. Fadool, D. L. Hartl, and J. E. Dowling, "Transposition of the mariner element from Drosophila mauritiana in zebrafish.," *Proc. Natl. Acad. Sci. U. S. A.*, vol. 95, no. 9, pp. 5182–5186, 1998.

[84] K. Kawakami, A. Koga, H. Hori, and A. Shima, "Excision of the Tol2 transposable element of the medaka fish, Oryzias latipes, in zebrafish, Danio rerio," *Gene*, vol. 225, no. 1–2, pp. 17–22, Dec. 1998.

[85] E. Raz, H. G. van Luenen, B. Schaerringer, R. H. Plasterk, and W. Driever, "Transposition of the nematode Caenorhabditis elegans Tc3 element in the zebrafish Danio rerio.," *Curr. Biol.*, vol. 8, no. 2, pp. 82–88, 1998.

[86] K. Kawakami, "Transposon tools and methods in zebrafish," *Developmental Dynamics*, vol. 234, no. 2. pp. 244–254, 2005.

[87] K. Kawakami, "Tol2: a versatile gene transfer vector in vertebrates.," *Genome Biol.*, vol. 8 Suppl 1, p. S7, 2007.

[88] K. Kawakami, A. Shima, and N. Kawakami, "Identification of a functional transposase of the Tol2 element, an Ac-like element from the Japanese medaka fish, and its transposition in the zebrafish germ lineage.," *Proc. Natl. Acad. Sci. U. S. A.*, vol. 97, no. 21, pp. 11403–11408, 2000.

[89] K. Kawakami, "Transgenesis and Gene Trap Methods in Zebrafish by Using the Tol2 Transposable Element," *Methods Cell Biol.*, vol. 77, pp. 201–222, 2004.

[90] J. Ni, K. J. Clark, S. C. Fahrenkrug, and S. C. Ekker, "Transposon tools hopping in vertebrates," *Briefings Funct. Genomics Proteomics*, vol. 7, no. 6, pp. 444–453, 2008.

[91] D. Balciunas, K. J. Wangensteen, A. Wilber, J. Bell, A. Geurts, S. Sivasubbu, X. Wang, P. B. Hackett, D. A. Largaespada, R. S. McIvor, and S. C. Ekker, "Harnessing a high cargo-capacity transposon for genetic applications in vertebrates," *PLoS Genet.*, vol. 2, no. 11, pp. 1715–1724, 2006.

[92] A. Urasaki, G. Morvan, and K. Kawakami, "Functional dissection of the Tol2 transposable element identified the minimal cis-sequence and a highly repetitive sequence in the subterminal region essential for transposition," *Genetics*, vol. 174, no. 2, pp. 639–649, 2006.

[93] S. Fisher, E. A. Grice, R. M. Vinton, S. L. Bessling, A. Urasaki, K. Kawakami, and A. S. McCallion, "Evaluating the biological relevance of putative enhancers using Tol2 transposon-mediated transgenesis in zebrafish.," *Nat. Protoc.*, vol. 1, no. 3, pp. 1297–1305, 2006.

[94] K. M. Kwan, E. Fujimoto, C. Grabher, B. D. Mangum, M. E. Hardy, D. S. Campbell, J. M. Parant, H. J. Yost, J. P. Kanki, and C. Bin Chien, "The Tol2kit: A multisite gateway-based construction Kit for Tol2 transposon transgenesis constructs," *Dev. Dyn.*, vol. 236, no. 11, pp. 3088–3099, 2007.

[95] J. A. Villefranc, J. Amigo, and N. D. Lawson, "Gateway compatible vectors for analysis of gene function in the zebrafish," *Dev. Dyn.*, vol. 236, no. 11, pp. 3077–3087, 2007.

[96] K. Kawakami, H. Takeda, N. Kawakami, M. Kobayashi, N. Matsuda, and M. Mishina, "A transposon-mediated gene trap approach identifies developmentally regulated genes in zebrafish," *Dev. Cell*, vol. 7, no. 1, pp. 133–144, 2004.

[97] S. Nagayoshi, E. Hayashi, G. Abe, N. Osato, K. Asakawa, A. Urasaki, K. Horikawa, K. Ikeo, H. Takeda, and K. Kawakami, "Insertional mutagenesis by the Tol2 transposon-mediated enhancer trap approach generated mutations in two developmental genes: tcf7 and synembryn-like.," *Development*, vol. 135, no. 1, pp. 159–169, 2008.

[98] S. Parinov, I. Kondrichin, V. Korzh, and A. Emelyanov, "Tol2 transposon-mediated enhancer trap to identify developmentally regulated zebrafish genes in vivo," *Dev. Dyn.*, vol. 231, no. 2, pp. 449–459, 2004.

[99] S. a. Juntti, C. K. Hu, and R. D. Fernald, "Tol2-Mediated Generation of a Transgenic Haplochromine Cichlid, Astatotilapia burtoni," *PLoS One*, vol. 8, no. 10, pp. 1–6, 2013.

[100] R. Guyomard, D. Chourrout, C. Leroux, L. M. Houdebine, and F. Pourrain, "Integration and germ line transmission of foreign genes microinjected into fertilized trout eggs.," *Biochimie*, vol. 71, no. 7, pp. 857–863, 1989.

[101] E. S. Yaskowiak, M. A. Shears, A. Agarwal-Mawal, and G. L. Fletcher, "Characterization and multi-generational stability of the growth hormone transgene (EO-1a) responsible for

enhanced growth rates in Atlantic Salmon," *Transgenic Res.*, vol. 15, pp. 465–480, 2006.

[102] N. Hartmann and C. Englert, "A microinjection protocol for the generation of transgenic killifish (Species: Nothobranchius furzeri)," *Dev. Dyn.*, vol. 241, no. April, pp. 1133–1141, 2012.

[103] K. A. Schafer, "The cell cycle: a review.," *Vet. Pathol.*, vol. 35, no. 6, pp. 461–478, 1998.

[104] B. Alberts, A. Johnson, J. Lewis, M. Raff, K. Roberts, and P. And Walter, *Molecular Biology of the Cell*, vol. 54. 2008.

[105] M. B. Kastan and J. Bartek, "Cell-cycle checkpoints and cancer.," *Nature*, vol. 432, no. 7015, pp. 316–323, 2004.

[106] G. H. Williams and K. Stoeber, "The cell cycle and cancer," *Journal of Pathology*, vol. 226, no. 2. pp. 352–364, 2012.

[107] J. A. Pietenpol and Z. A. Stewart, "Cell cycle checkpoint signaling: Cell cycle arrest versus apoptosis," *Toxicology*, vol. 181–182, pp. 475–481, 2002.

[108] N. C. Walworth, "Cell-cycle checkpoint kinases: Checking in on the cell cycle," *Current Opinion in Cell Biology*, vol. 12, no. 6. pp. 697–704, 2000.

[109] A. Sakaue-Sawano, H. Kurokawa, T. Morimura, A. Hanyu, H. Hama, H. Osawa, S. Kashiwagi, K. Fukami, T. Miyata, H. Miyoshi, T. Imamura, M. Ogawa, H. Masai, and A. Miyawaki, "Visualizing Spatiotemporal Dynamics of Multicellular Cell-Cycle Progression," *Cell*, vol. 132, no. 3, pp. 487–498, 2008.

[110] R. H. Newman and J. Zhang, "Fucci: Street Lights on the Road to Mitosis," *Chemistry and Biology*, vol. 15, no. 2. pp. 97–98, 2008.

[111] H. C. Vodermaier, "APC/C and SCF: Controlling each other and the cell cycle," *Current Biology*, vol. 14, no. 18. 2004.

[112] R. Benmaamar and M. Pagano, "Involvement of the SCF complex in the control of Cdh1 degradation in S-phase," *Cell Cycle*, vol. 4, no. 9, pp. 1230–1232, 2005.

[113] W. Wei, N. G. Ayad, Y. Wan, G.-J. Zhang, M. W. Kirschner, and W. G. Kaelin, "Degradation of the SCF component Skp2 in cell-cycle phase G1 by the anaphase-promoting complex.," *Nature*, vol. 428, no. 6979, pp. 194–198, 2004.

[114] H. Nishitani, Z. Lygerou, T. Nishimoto, and P. Nurse, "The Cdt1 protein is required to

license DNA for replication in fission yeast.," *Nature*, vol. 404, no. 6778, pp. 625–628, 2000.

[115] H. Nishitani, Z. Lygerou, and T. Nishimoto, "Proteolysis of DNA replication licensing factor Cdt1 in S-phase is performed independently of Geminin through its N-terminal region," *J. Biol. Chem.*, vol. 279, no. 29, pp. 30807–30816, 2004.

[116] M. Sugiyama, A. Sakaue-Sawano, T. Iimura, K. Fukami, T. Kitaguchi, K. Kawakami, H. Okamoto, S. Higashijima, and A. Miyawaki, "Illuminating cell-cycle progression in the developing zebrafish embryo.," *Proc. Natl. Acad. Sci. U. S. A.*, vol. 106, no. 49, pp. 20812–20817, 2009.

[117] R. H. Webb, "Confocal optical microscopy," *Reports on Progress in Physics*, vol. 59, no. 3. pp. 427–471, 1999.

[118] J. Huisken, J. Swoger, F. Del Bene, J. Wittbrodt, and E. H. K. Stelzer, "Optical sectioning deep inside live embryos by selective plane illumination microscopy.," *Science*, vol. 305, no. 5686, pp. 1007–1009, 2004.

[119] P. J. Keller, A. D. Schmidt, J. Wittbrodt, and E. H. K. Stelzer, "Reconstruction of zebrafish early embryonic development by scanned light sheet microscopy.," *Science*, vol. 322, no. 5904, pp. 1065–1069, 2008.

[120] R. J. Lesseps, A. H. van Kessel, and J. M. Denucé, "Cell patterns and cell movements during early development of an annual fish, Nothobranchius neumanni.," *J. Exp. Zool.*, vol. 193, pp. 137–146, 1975.

[121] C. Wei, L. Salichos, C. M. Wittgrove, A. Rokas, and J. G. Patton, "Transcriptome-wide analysis of small RNA expression in early zebrafish development.," *RNA*, vol. 18, no. 5, pp. 915–29, 2012.

[122] M. I. Love, W. Huber, and S. Anders, "Moderated estimation of fold change and dispersion for RNA-seq data with DESeq2.," *Genome Biol.*, vol. 15, no. 12, p. 550, 2014.

[123] V. Olive, I. Jiang, and L. He, "Mir-17-92, a cluster of miRNAs in the midst of the cancer network," *Int. J. Biochem. Cell Biol.*, vol. 42, no. 8, pp. 1348–1354, 2010.

[124] A. J. Giraldez, Y. Mishima, J. Rihel, R. J. Grocock, S. Van Dongen, K. Inoue, A. J. Enright, and A. F. Schier, "Zebrafish MiR-430 promotes deadenylation and clearance of maternal mRNAs.," *Science*, vol. 312, no. 5770, pp. 75–79, 2006.

[125] M. Polačik, R. Blažek, R. Řežucha, M. Vrtílek, E. Terzibasi Tozzini, and M. Reichard, "Alternative intrapopulation life-history strategies and their trade-offs in an African annual fish," *J. Evol. Biol.*, vol. 27, no. 5, pp. 854–865, 2014.

[126] A. A. Bazzini, M. T. Lee, and A. J. Giraldez, “Ribosome Profiling Shows That miR-430 Reduces Translation Before Causing mRNA Decay in Zebrafish,” *Science*, vol. 336, no. 6078. pp. 233–237, 2012.

[127] C.-X. Huang, N. Chen, X.-J. Wu, C.-H. Huang, Y. He, R. Tang, W.-M. Wang, and H.-L. Wang, “The zebrafish miR-462/miR-731 cluster is induced under hypoxic stress via hypoxia-inducible factor 1α and functions in cellular adaptations.,” *FASEB J.*, Aug. 2015.

[128] J. E. Podrabsky, J. P. Lopez, T. W. M. Fan, R. Higashi, and G. N. Somero, “Extreme anoxia tolerance in embryos of the annual killifish Austrofundulus limnaeus: insights from a metabolomics analysis.,” *J. Exp. Biol.*, vol. 210, no. Pt 13, pp. 2253–2266, 2007.

[129] Y. Huang, H.-C. Chen, C.-W. Chiang, C.-T. Yeh, S.-J. Chen, and C.-K. Chou, “Identification of a two-layer regulatory network of proliferation-related microRNAs in hepatoma cells.,” *Nucleic Acids Res.*, vol. 40, no. 20, pp. 10478–93, 2012.

[130] M. Hackl, S. Brunner, K. Fortschegger, C. Schreiner, L. Micutkova, C. Mück, G. T. Laschober, G. Lepperdinger, N. Sampson, P. Berger, D. Herndler-Brandstetter, M. Wieser, H. Kühnel, A. Strasser, M. Rinnerthaler, M. Breitenbach, M. Mildner, L. Eckhart, E. Tschachler, A. Trost, J. W. Bauer, C. Papak, Z. Trajanoski, M. Scheideler, R. Grillari-Voglauer, B. Grubeck-Loebenstein, P. Jansen-Dürr, and J. Grillari, “miR-17, miR-19b, miR-20a, and miR-106a are down-regulated in human aging.,” *Aging Cell*, vol. 9, no. 2, pp. 291–6, 2010.

[131] C. Mosimann, C. K. Kaufman, P. Li, E. K. Pugach, O. J. Tamplin, and L. I. Zon, “Ubiquitous transgene expression and Cre-based recombination driven by the ubiquitin promoter in zebrafish.,” *Development*, vol. 138, no. 1, pp. 169–177, 2011.